FUNDAÇÃO OSWALDO CRUZ
CENTRO DE PESQUISAS GONÇALO MONIZ

FIOCRUZ

Curso de Pós-Graduação em Biotecnologia em Saúde e Medicina Investigativa

DISSERTAÇÃO DE MESTRADO

TERAPIA COM CÉLULAS DA MEDULA ÓSSEA EM MODELO EXPERIMENTAL DE INSUFICIÊNCIA HEPÁTICA AGUDA INDUZIDA POR ACETAMINOFEN

BRUNO SOLANO DE FREITAS SOUZA

Salvador – Brasil
2012

FUNDAÇÃO OSWALDO CRUZ

CENTRO DE PESQUISAS GONÇALO MONIZ

Curso de Pós-Graduação em Biotecnologia em Saúde e Medicina Investigativa

TERAPIA COM CÉLULAS DA MEDULA ÓSSEA EM MODELO EXPERIMENTAL DE INSUFICIÊNCIA HEPÁTICA AGUDA INDUZIDA POR ACETAMINOFEN

BRUNO SOLANO DE FREITAS SOUZA

Orientador: Prof° Dr° Ricardo Ribeiro dos Santos
Co-orientadora: Dra. Milena Botelho Pereira Soares

Dissertação apresentada ao Curso de Pós-Graduação em Biotecnologia em Saúde e Medicina Investigativa para a obtenção do grau de Mestre.
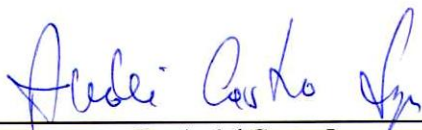
Salvador – Brasil
2012

"TERAPIA COM CÉLULAS MONONUCLEARES DA MEDULA ÓSSEA EM MODELO EXPERIMENTAL DE HEPATITE FULMINANTE INDUZIDA POR ACETAMINOFEN"
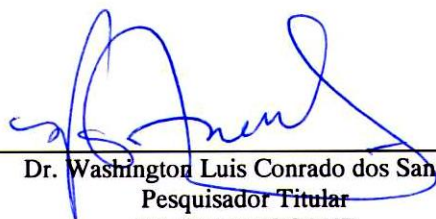

BRUNO SOLANO DE FREITAS SOUZA
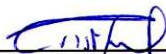

FOLHA DE APROVAÇÃO

COMISSÃO EXAMINADORA

_____
Dr. André Castro Lyra
Professor Adjunto
UFBA

_____
Dr. Washington Luis Conrado dos Santos
Pesquisador Titular
CPqGM / FIOCRUZ

_____
Drª Cristiane Flora Villarreal
Professor Adjunto
UFBA

SOUZA, Bruno Solano de Freitas. Terapia com células da medula óssea em modelo experimental de insuficiência hepática aguda induzida por acetaminofen. 53 f. il. Dissertação (Mestrado) – Fundação Oswaldo Cruz, Instituto de Pesquisas Gonçalo Moniz, Salvador, 2012.

RESUMO

Introdução e objetivos: A insuficiência hepática aguda (IHA), apesar de rara, permanece como uma condição rapidamente progressiva e frequentemente fatal. A intoxicação por acetaminofen (APAP) induz necrose hepática maciça e frequentemente leva à morte por edema cerebral. Terapias celulares são de grande interesse como potenciais tratamentos para IHA. Neste projeto foi avaliado o potencial terapêutico das células mononucleares da medula óssea (CMMO) em um modelo experimental de IHA induzida por APAP em camundongos. Métodos: A IHA foi induzida em camundongos C57Bl/6, previamente submetidos à dieta alcoólica por três semanas, através da administração de APAP na dose de 300 mg/kg por via intraperitoneal. Após a indução da IHA, os camundongos foram transplantados, por via endovenosa, com 10^7 CMMO obtidas de doadores transgênicos para a proteína verde fluorescente (GFP) ou injetados com salina. As curvas de sobrevivência, os níveis plasmáticos de aminotransferases, amônia, uréia e creatinina, a extensão da necrose hepática, o infiltrado inflamatório e a expressão de citocinas e metaloproteinases foram avaliados. A microscopia confocal foi utilizada para estudar a migração das células transplantadas para o fígado. A permeabilidade da barreira hemato-encefálica foi avaliada pela injeção do corante azul de Evans (AE) por via endovenosa. Resultados: Observou-se que os camundongos tratados com CMMO apresentaram uma redução significativa da mortalidade, com uma taxa de 60% de sobrevivência quando comparados a 20% de sobrevivência do grupo controle. As células transplantadas migraram para o fígado, mas não foi observada a diferenciação destas em células hepáticas ou fusão celular. Não foram encontradas diferenças estatisticamente significativas na extensão de necrose hepática no fígado, nos níveis plasmáticos de transaminases e amônia, na intensidade do infiltrado inflamatório no fígado entre os dois grupos com IHA, bem como nos níveis hepáticos das citocinas TNF-a e IL-10 e de transcritos para adrenomedula e endotelina 1 no cérebro, assim como na atividade da metaloproteinase 9 no soro. No entanto, observou-se uma redução dos níveis séricos de TNF-a no grupo tratado com CMMO quando comparado ao grupo injetado com salina. Esta redução está correlacionada ao aumento do mRNA para IL-10 na medula óssea e no baço dos animais tratados com CMMO. A avaliação do extravasamento do corante azul de Evans para o cérebro demonstrou que o grupo tratado com células mononucleares da medula óssea apresentou uma redução da permeabilidade da barreira hemato-encefálica quando comparado ao grupo injetado com salina. Conclusão: As CMMO exercem um efeito protetor em camundongos com IHA induzida por APAP, sem alterar o dano hepático, provavelmente através da modulação da resposta inflamatória sistêmica e da diminuição da permeabilidade da barreira hemato-encefálica.

Palavras chave: Insuficiência hepática aguda; Terapia celular; Células mononucleares da medula óssea; Acetaminofen; Citocinas; Barreira hemato-encefálica.

SOUZA, Bruno Solano de Freitas. Therapy with bone marrow cells in an experimental model of acute liver failure induced with acetaminophen. 53 f. il. Dissertação (Mestrado) – Fundação Oswaldo Cruz, Instituto de Pesquisas Gonçalo Moniz, Salvador, 2012.

ABSTRACT

Introduction and objectives: Acute liver failure (IHA), although rare, remains a rapidly progressive and often fatal condition. Poisoning by acetaminophen (APAP) induces a massive hepatic necrosis and often leads to death by cerebral edema. Cell therapies are of great interest as potential treatments for IHA. In this project we evaluated the therapeutic potential of bone marrow mononuclear cells (BMC) in an experimental model of IHA induced by APAP in mice. Methods: The IHA was induced in C57BL/6 mice previously submitted to the alcohol diet for three weeks by the administration of APAP at a dose of 300 mg / kg, intraperitoneally. After induction of IHA, the mice were transplanted intravenously with 107 BMC obtained from donors transgenic for green fluorescent protein (GFP) or injected with saline. The survival curves, plasma levels of aminotransferases, ammonia, urea and creatinine, the extent of hepatic necrosis, inflammatory infiltrate and the expression of cytokines and metalloproteinases were evaluated. Confocal microscopy was used to study the migration of transplanted cells to the liver. The permeability of the blood-brain barrier was assessed by injection of Evans blue dye (AE) intravenously. Results: We found that mice treated with BMC showed a significant reduction in mortality, with a rate of 60% survival compared to 20% survival in the control group. The transplanted cells migrated to the liver, but we did not observe the differentiation of these cells or fusion with liver cells. There were no statistically significant differences in the extent of hepatic necrosis in the liver, plasma levels of transaminases and ammonia, and in the intensity of the inflammatory infiltrate in the liver between the two groups with IHA, as well as in hepatic levels of TNF-α and IL-10, transcripts for endothelin 1 and adrenomedullin in the brain and serum metalloproteinase 9 activity. However, there was a reduction of serum TNF-α in BMC-treated group compared to the group injected with saline. This decrease correlated with the increase in IL-10 mRNA expression in the bone marrow and spleen of BMC-treated mice. The assessment of Evans blue extravasation into the brain showed that the group treated with BMC had a reduced permeability of the blood-brain barrier compared to the group injected with saline. Conclusion: Bone marrow mononuclear cells exert a protective effect in mice with APAP-induced IHA, without changing the liver injury, probably through modulation of systemic inflammatory response and decrease the permeability of the blood-brain barrier.

Keywords: Acute liver failure, cell therapy, bone marrow mononuclear cells; Acetaminophen; Cytokines; blood-brain barrier.

LISTA DE ILUSTRAÇÕES

LISTA DE ABREVIATURAS E SIGLAS

AE	Aloficocianina
APAP	N-acetil-p-aminofenol
BHE	Barreira hemato-encefálica
CMMO	Células mononucleares da medula óssea
CYP	Citocromo P450
DAMP	Padrão molecular associado ao dano (*Damage-associated molecular pattern*)
DNA	Ácido desoxirribonucléico (*Deoxyribonucleic acid*)
ESC	Células-tronco embrionárias (*Embryonic stem cells*)
GFP	Proteína fluorescente verde (*Green fluorescent protein*)
HGF	Fator de crescimento de hepatócitos (*Hepatocyte growth factor*)
HSP	Proteína de choque térmico *(Heat shock proteín)*
IHA	Insuficiência hepática aguda
IL	Interleucina
mRNA	Ácido ribonucleico mensageiro (*Messenger ribonucleic acid*)
NAPQI	N-acetil-parabenzoquinoimida
SDF-1	Fator derivado de célula estromal-1 (*Stromal cell-derived factor-1*)
TLR	Receptor semelhante ao Toll (*Toll-like receptor*)
TNF	Fator de necrose tumoral (*Tumor necrosis factor*)

SUMÁRIO

1 INTRODUÇÃO

O fígado é um órgão responsável por grande número de funções, sendo o seu funcionamento regular de fundamental importância para a homeostasia do organismo. Apesar de ser um órgão privilegiado por possuir grande reserva funcional e elevada capacidade de regeneração tecidual, diversos fatores e agentes de lesão podem levar à perda maciça da função hepática uma vez que os mecanismos de agravo sejam capazes de suplantar os mecanismos de defesa do tecido.

A insuficiência hepática aguda (IHA) é uma síndrome clínica decorrente de necrose hepatocelular maciça ou submaciça, sendo caracterizada pela perda rápida da função hepática e desenvolvimento de alterações do estado mental e coagulopatia em indivíduo sem doença hepática pré-existente. As principais causas da IHA são as hepatites virais, assim como diversas drogas e toxinas. Dentre elas destaca-se o analgésico acetaminofen, que, quando utilizado em doses excessivas pode levar à necrose hepática maciça. Entretanto, vários outros medicamentos utilizados freqüentemente, podem, potencialmente, levar à necrose maciça do fígado. Além disso, doenças metabólicas e autoimunes hepáticas fígado também são fatores etiológicos importantes da IHA.

Dentre as alterações clínicas que se desenvolvem em decorrência da necrose massiva do fígado, o edema cerebral é freqüente, sendo uma causa importante de mortalidade. A maioria dos pacientes desenvolve disfunção pulmonar, insuficiência renal, coagulopatia, infecções e complicações metabólicas, como hipoglicemia, distúrbio hidro-eletrolítico e ácido-básico. A história natural da doença demonstra que o paciente evoluiu ou para a cura com recuperação total da função hepática, ou para a morte em poucos dias.

O transplante hepático é o único tratamento eficaz para os pacientes com insuficiência hepática crônica ou aguda (em casos em que não há recuperação espontânea). Embora o fígado seja um órgão de baixa rejeição imunológica, todo transplante de órgão é um procedimento de risco que acarreta o uso de drogas imunossupressoras para o resto da vida dos indivíduos transplantados. No entanto, a disponibilidade de órgãos para a realização do transplante pode ser um fator limitante para o tratamento de pacientes com insuficiência hepática, sobretudo em países onde a captação de órgãos não é eficaz o suficiente para suprir a demanda, como o Brasil, além de ser um procedimento de alto custo. Deste modo, o desenvolvimento de novas estratégias terapêuticas para melhorar a função hepática e a qualidade de vida dos indivíduos é de grande relevância.

A utilização de terapia celular vem sendo investigada nos últimos anos, utilizando diversos modelos de doenças hepáticas. De um modo geral, observou-se aceleração do processo de regeneração tecidual, resultando em melhora da função hepática e aumento da sobrevida dos animais após o tratamento com diversos tipos de células-tronco. No entanto, a grande maioria dos estudos utilizou modelos de doenças crônicas do fígado. Assim, é de grande relevância a realização de estudos que visem investigar o potencial terapêutico de células-tronco e progenitoras em modelos de IHA.

O transplante de células de medula óssea autólogas apresenta-se como uma opção na medicina regenerativa, pois é um procedimento já bem estabelecido na prática médica, sendo estas células de relativa facilidade de obtenção e baixo custo. Vários modelos animais, incluindo os de doenças hepáticas, têm sido utilizados para investigar o potencial terapêutico das células de medula óssea. Em estudos prévios realizados pelo nosso grupo, demonstramos efeitos terapêuticos das células mononucleares de medula óssea em modelos de cardiomiopatia chagásica crônica (SOARES et al., 2011, ANEXO II), epilepsia (COSTA-FERRO et al., 2012, ANEXO III) e doenças crônicas do fígado (OLIVEIRA et al., 2012, ANEXO III).

No presente estudo investigamos os efeitos da terapia com células mononucleares de medula óssea em um modelo de IHA induzida por acetaminofen em camundongos previamente sensibilizados com etanol.

2 REVISÃO DA LITERATURA

2.1 A INSUFICIÊNCIA HEPÁTICA AGUDA

A IHA é uma síndrome clínica decorrente de necrose hepatocelular maciça ou submaciça, sendo caracterizada pela perda rápida da função hepática e desenvolvimento de alterações do estado mental e coagulopatia em indivíduo sem doença hepática pré-existente (LEE WM *et al.*, 2011). Devido à gravidade do quadro, é também conhecida pelos termos insuficiência hepática fulminante e hepatite fulminante. Felizmente, apesar da elevada gravidade desta síndrome clínica, trata-se de um evento raro, com incidência anual estimada em aproximadamente 2000 casos nos EUA e um a oito casos para cada milhão de pessoas no Reino Unido (HOOFNAGLE JH *et al.*, 1995; LEE WM *et al.*, 2008; BERNAL W *et al.*, 2010).

A etiologia da IHA varia geograficamente e, principalmente, de acordo com o nível de desenvolvimento econômico e social. A hepatite aguda fulminante viral é uma das principais causas na maioria das regiões em todo o mundo (WRIGHT *et al.*, 1992; SCHIODT *et al.*, 1999). Os vírus A e B são os agentes responsáveis mais importantes, embora os vírus das hepatites C, D e E e vírus não A-E também possam desencadear o quadro. Doenças metabólicas e auto-imunes hepáticas também são fatores etiológicos importantes. Diversas drogas e toxinas, da mesma forma, podem provocar um quadro de hepatite fulminante, seja por toxicidade dose-dependente ou por reações idiossincráticas (DUFFY *et al.*, 1989; NEUBERGER *et al.*, 1990). Nos países ocidentais desenvolvidos, as causas mais comuns são as relacionadas à toxicidade induzida por drogas, perfazendo até 50% dos casos. Outras causas incluem hepatites virais, doenças autoimunes do fígado e choque ou hipoperfusão (GILL, *et al.* 2001). Além das etiologias conhecidas, estima-se ainda que em até 15% dos casos não é possível identificar nenhuma causa conhecida de IHA (OSTAPOWICZ *et al.*, 2002).

2.2 A IHA CAUSADA POR ACETAMINOFEN

Uma das medicações mais associadas ao desenvolvimento de IHA é o analgésico e antipirético acetaminofen, também conhecido como paracetamol e N-acetil-p-aminofenol (APAP). Trata-se de uma toxina dose-dependente, que pode levar ao quadro de IHA quando ingerida em doses superiores a 150 mg/kg por dia, seja inadvertidamente, ou mesmo

intencionalmente em casos de tentativa de suicídio (LEE *et al.*, 2011). Casos de IHA também já foram descritos após ingestão de doses menores, em indivíduos com susceptibilidade aumentada à droga (BONKOVSKY *et al.*, 1994). Dentre os fatores que podem levar a um aumento na susceptibilidade à hepatoxicidade por APAP está o uso crônico de álcool, que leva à depleção dos estoques de substâncias redutoras como a glutationa, levando a um aumento do estresse oxidativo (ZIMMERMAN *et al.*, 1995; WHITCOMB *et al.*, 1994).

Do ponto de vista bioquímico, o acetaminofen é convertido no fígado pelo citocromo P450 (CYP2E1) a N-acetil-parabenzoquinoimida (NAPQI), um metabólito reativo que se liga covalentemente a proteínas. Em doses usuais não tóxicas, este metabólito consegue ser inteiramente detoxificado pela ligação com a glutationa (JOLLOW *et al.,* 1974). Entretanto, em situações de sobredosagem, indução enzimática do sistema P-450 (frequentemente causadas por uso de álcool ou anticonvulsivantes, etc) ou depleção das reservas de glutationa (álcool, desnutrição) a capacidade de defesa do fígado pode ser superada, levando a um quadro de necrose celular maciça, predominantemente na zona centrolobular (ZIMMERMAN *et al.*, 1995; WHITCOMB *et al.*, 1994). Isso ocorre uma vez que, quando a capacidade de ligação da glutationa é completamente saturada, o NAPQI passa a se ligar a proteínas e causar estresse oxidativo, levando a alterações no metabolismo do cálcio, na transdução de sinais e na função mitocondrial (HINSON *et al.*, 2010). As alterações mitocondriais levam à perda da capacidade de síntese de ATP, levando à morte celular por necrose (MASUBUCHI *et al.*, 2005) (Figura 1).
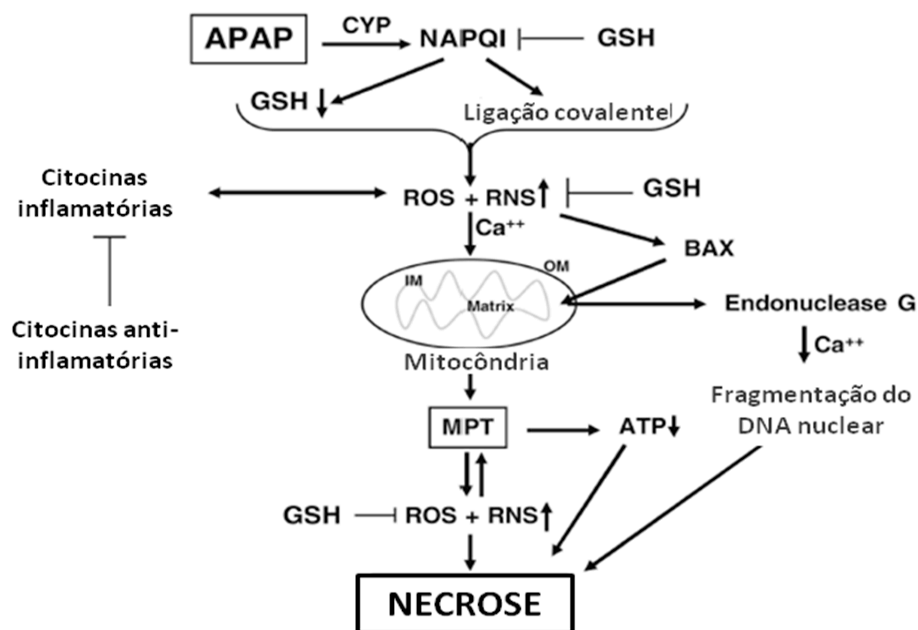
Figura 1: Mecanismos envolvidos na hepatotoxicidade induzida por APAP. APAP: Acetaminofen, NAPQI: N-acetil-parabenzoquinoimida, CYP: citocromo P-450, GSH glutationa reduzida, ROS: espécies reativas de oxigênio, RNS: espécies reativas de nitrogênio, OM: membrana externa, IM: membrana interna, MPT: transição de permeabilidade da mitocôndria,, BAX: proteína X associada a Bcl-2. Fonte: HINSON *et al.*, 2010.

2.3 A RESPOSTA INFLAMATÓRIA NA IHA

O papel da resposta inflamatória na gravidade da lesão hepática tem sido investigado nos últimos anos. Um grande número de moléculas liberadas pelas células necróticas é capaz de, a partir do reconhecimento por receptores *toll-like* (TLR), induzir uma resposta inflamatória inicialmente local, mas que pode se tornar sistêmica. Estas moléculas são conhecidas como DAMPs, do inglês *damage-associated molecular patterns*, ou padrões moleculares associados ao dano, Dentro desta categoria de moléculas encontramos *high mobility group box-1* (HMGB1), *heat-shock proteins* (HSPs) e fragmentos de DNA (LOTZE *et al.*, 2005; MARTIN-MURPHY *et al.*, 2010; SCAFFIDI *et al.*, 2002). Através deste mecanismo, a morte celular disseminada que ocorre no fígado leva à ativação de células de Kupffer (macrófagos residentes do fígado), ao aumento de diversos mediadores inflamatórios, incluindo fatores do complemento (JAESCHKE *et al.*, 1993), citocinas e quimiocinas

(OKAYA *et al.*, 2003), além do recrutamento de células inflamatórias para o fígado (SCAFFIDI *et al.*, 2002) (Figura 2).
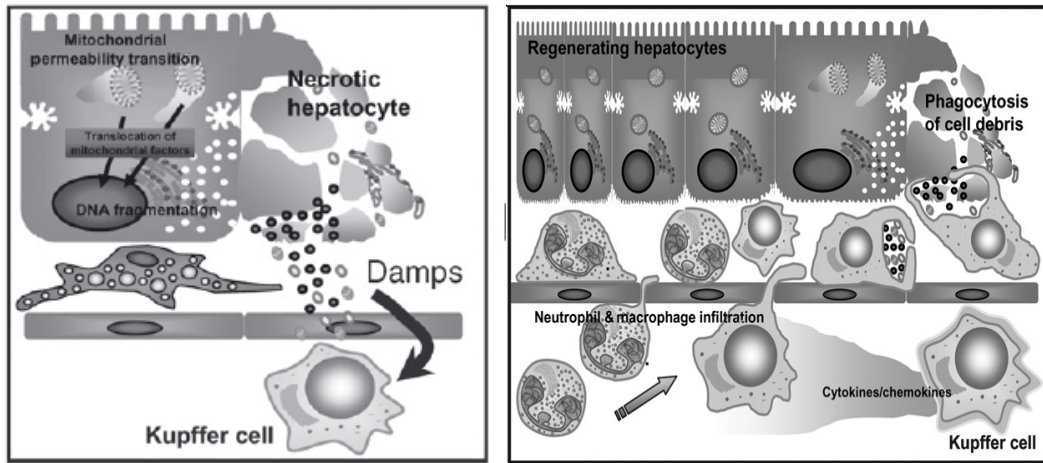

Figura 2. Ativação e recrutamento de células imunes após o dano induzido por APAP.
Após o estabelecimento do dano hepático por APAP, ocorre a transição da permeabilidade mitocondrial, com translocação de proteínas mitocondriais como fator indutor de apoptose e endonuclease G para o núcleo, levando à fragmentação do DNA e morte celular por necrose. Vários componentes celulares são liberados após a necrose, incluindo fragmentos de DNA e HMGB1, atuando como DAMPs para ativação de macrófagos residentes (células de Kupffer) e atraindo leucócitos para o tecido lesionado para facilitar a remoção de células mortas. Fonte: JAESCHKE, 2012.

Experimentalmente, foi demonstrado que camundongos *knockout* para IFN-γ apresentam uma proteção relativa à toxicidade pelo acetaminofen e redução na expressão de outras citocinas pró-inflamatórias (ISHIDA *et al.*, 2002). Camunodngos *knockout* para IL-10, por sua vez apresentam aumento da toxicidade induzida por APAP, além de elevações nos níveis de mediadores pró-inflamatórios e no estresse oxidativo (BOURDI *et al.*, 2002). Ainda é controverso se estes fatores contribuem para a perpetuação da lesão hepática, mas seu envolvimento na patogênese das complicações sistêmicas associadas à IHA, que muitas vezes são as grandes responsáveis pela letalidade, tem sido demonstrado (JAESCHKE *et al.*, 2012; ROLANDO *et al.*, 2000).

O TNF-α é uma citocina pró-inflamatória com papel central em uma série de processos imunológicos, sendo secretada, em resposta ao dano tecidual, por diversas células, incluindo macrófagos, monócitos, neutrófilos, linfócitos, células NK, astrócitos, microglia e células de Kupffer no fígado (ODEH, 2007). O TNF-α é encontrado elevado no soro dos pacientes em diversas doenças agudas e crônicas do fígado (STREETZ *et al.*, 2000; TILG *et*

al., 1992). Na IHA, os níveis de TNF-α se correlacionam com a gravidade da doença e com a progressão da encefalopatia hepática, retornando a níveis reduzidos quando há resposta ao tratamento (Figura 3). Além disso, níveis circulantes aumentados de TNF-α estão significativamente relacionados ao risco de morte tanto em pacientes quanto em animais (STREETZ et al., 2000; NAGAKI et al., 2000).
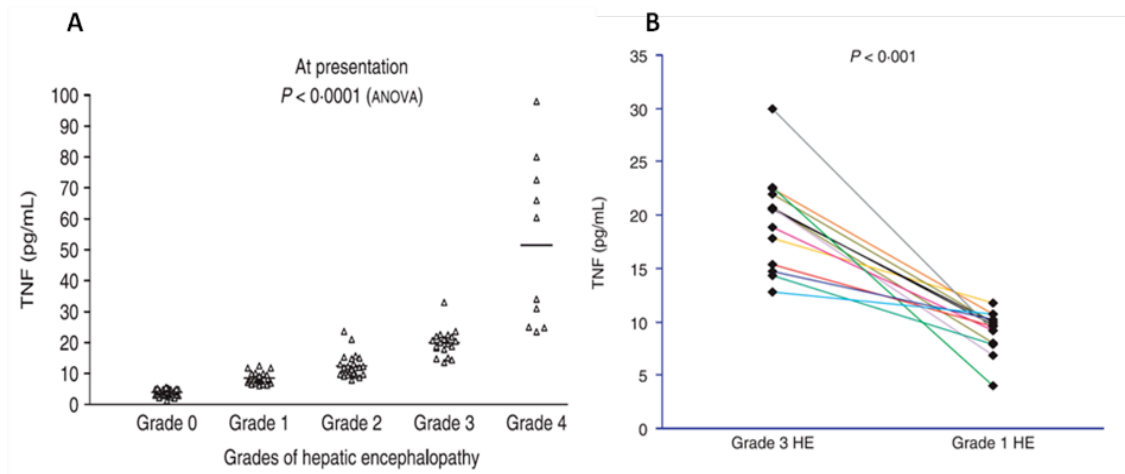
Figura 3. Correlação entre os níveis séricos de TNF-α e a gravidade da encefalopatia hepática na IHA. Observa-se que os níveis de TNF-α aumentam significativamente durante a evolução da encefalopatia na IHA, classificada de grau 0 a grau 4 **(A)**. Inversamente, há uma redução estatisticamente significativa dos níveis séricos de TNF-α quando os pacientes respondem à terapia, regredindo o grau de encefalopatia hepática. Fonte: ODEH, 2007.

A história natural da doença demonstra que o paciente evolui ou para a cura com recuperação total da função hepática ou para morte em poucos dias (MEERMAN et al., 1997). A maioria dos pacientes com IHA desenvolve complicações sistêmicas como disfunção pulmonar, insuficiência renal, coagulopatia, infecções e distúrbios metabólicos, como hipoglicemia, distúrbio hidro-eletrolítico e ácido-básico. Além destas complicações, o edema cerebral é freqüente, ocorrendo em até 80% dos pacientes com IHA e representando uma causa importante de mortalidade (OSTAPOWICZ et al., 2002).

2.4 A ENCEFALOPATIA NA IHA

O edema cerebral associado com IHA parece ter origem multifatorial, possuindo componentes citotóxico e vasogênico (BJERRING et al., 2009). O componente citotóxico já foi bem estudado e decorre dos efeitos osmóticos exercidos pela amônia, glutamina e citocinas inflamatórias sobre o tecido cerebral. A hiperamonemia observada na IHA resulta da

incapacidade de coversão hepática em uréia no ciclo da ornitina e parece ter um papel central neste componente citotóxico do edema cerebral (BJERRING et al., 2009; ALBRECHT et al., 2006). O edema de astrócitos é uma consequência da desregulação da osmolaridade celular no cérebro, como resultado da hiperamonemia. A amônia, uma vez que entra no cérebro, é detoxificada em glutamina através de uma reação de amidação do glutamato pela enzima glutamina sintetase. O acúmulo da glutamina nos astrócitos leva ao edema. Portanto, já é bastante conhecido que a hiperamonemia causa um distúrbio na função cerebral e é um componente importante do edema cerebral associado à IHA (NORENBERG *et al.*, 2004).

Apesar do envolvimento central da hiperamonemia na patogênese do edema cerebral associado com IHA, é sabido que isoladamente ela não é suficiente para o desenvolvimento de edema cerebral, e, portanto a co-existência de outros mecanismos atuando no aumento da permeabilidade da barreira hemato-encefálica ainda é atualmente alvo de debate. Em condições normais, é sabido que o cérebro mantém um controle estreito da entrada de moléculas, devido à separação entre o sangue proveniente da circulação sistêmica e o tecido cerebral, pela presença de especialização endotelial que forma a barreira hemato-encefálica (Figura 3). Estas células endoteliais possuem junções de oclusão que são compostas de proteínas como claudinas, ocludinas e zona occludens (ZO). A presença de projeções de astrócitos sobre as células endoteliais reforça a seletividade da barreira hemato-encefálica em condições normais (BRADBURY *et al.*, 1993).

As células endoteliais cérebrais apresentam, além da presença de junções de oclusão que limitam o transplante paracelular de moléculas, pequeno número de vesículas pinocitóticas, o que rstringe o tráfego de moléculas e células por via transendotelial e ainda contam com a atividade de transportadores de efluxo, que restringem ainda mais o tráfego de moléculas (KIS *et al.*, 2006). São ainda capazes de controlar a permeabilidade vascular e o fluxo sanguíneo através da atuação de uma série de peptídeos secretados pelo próprio endotélio vascular cerebral, com função autócrina e parácrina, dentre os quais merece destaque a adrenomedulina e a endotelina-1. O endotélio cerebral secreta elevados níveis de adrenomedulina em resposta a fatores secretados pelos astrócitos. Este peptídeo possui ação vasodilatadora, aumentando assim a perfusão, ao passo que estimula a síntese e organização de proteínas das junções de oclusão, reforçando a função de barreira hemato-encefálica. A infusão de adrenomedulina é ainda capaz de reduzir o dano cerebral em modelo experimental de acidente vascular cerebral (WATANABE *et al.*, 2001). Por outro lado, a endotelina-1 é capaz de estimular a vasoconstricção e, quando liberada em excesso em condições de lesão,

estimula a formação do edema cerebral, uma vez que leva à inibição de bombas de efluxo e ao aumento da permeabilidade vascular (KIS *et al.*, 2006).
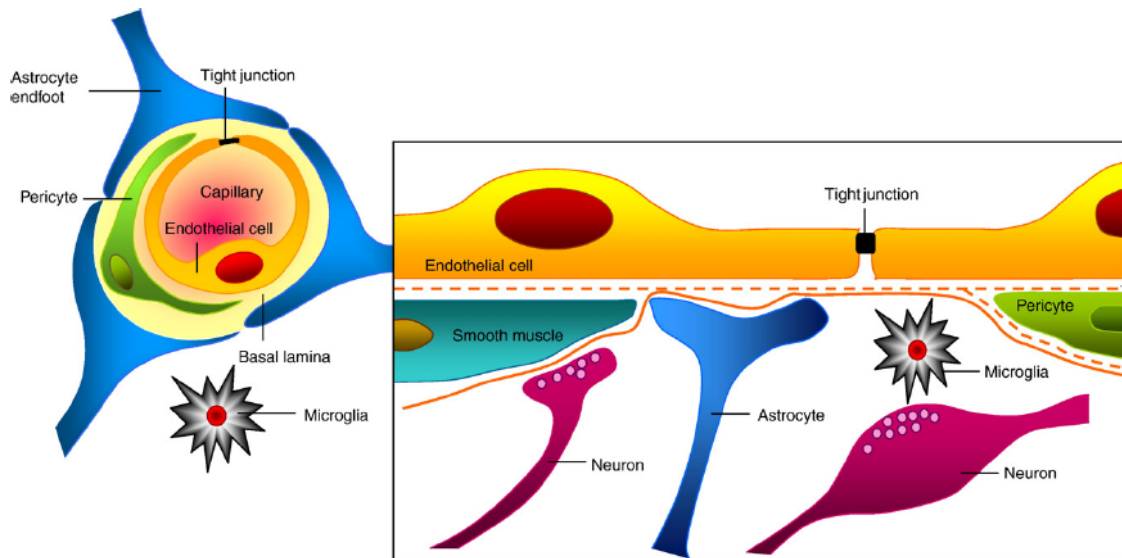

Figura 4. Representação gráfica dos componentes da barreira hemato-encefálica. As células endoteliais cerebrais formam junções de oclusão nas suas margens, impedindo a difusão paracelular de moléculas. Pericitos se distribuem descontinuamente ao longo dos capilares cerebrais, circundando parcialmente o endotélio. Processos emitidos pelos astrócitos formam uma rede complexa que envolve os capilares e contribuem para a função da barreira. Fonte: ABOT, 2010.

Mediadores inflamatórios atuando sistemicamente podem aumentar o fluxo sanguíneo cerebral e modular as junções de oclusão, levando à redução da expressão das suas proteínas constituintes e aumentando a permeabilidade da BHE, contribuindo assim para o edema cerebral (GAILLARD *et al.*, 2006). Estudos experimentais em modelos de IHA tem revelado que o aumento da liberação hepática de metaloproteinase-9, leva à degradação de proteínas de junção intercelular no endotélio cerebral, principalmente claudina-5 e ocludina (CHEN *et al.*, 2009; SHIMOJIMA *et al.*, 2008; NGUYEN *et al.*, 2006). A supressão da expressão gênica da claudina-5 também foi demonstrada em resposta a níveis elevados de de TNF-α (ASLAM *et al.*, 2012). Como consequência, as junções de oclusão perdem a sua função, levando à disfunção da barreira hemato-encefálica, e edema cerebral (WANG *et al.*, 2011).

Apesar de não haver pleno conhecimento sobre as causas do edema cerebral, é sabido que suas consequências clinicamente se manifestam como aumento da pressão intracraniana e herniação cerebral, perfazendo grande parte das causas de morte em pacientes com hepatite fulminante (WARE *et al.*, 1971).

2.5 TRATAMENTO DA IHA

O transplante hepático é o único tratamento definitivo eficaz para os pacientes com IHA existente até o momento capaz de reduzir mortalidade (LIDOFSKY et al., 1993). Embora o fígado seja um órgão de baixa rejeição imunológica, todo transplante de órgão é um procedimento de risco que acarreta o uso de drogas imunossupressoras para o resto da vida dos indivíduos transplantados. No entanto, a disponibilidade de órgãos para a realização do transplante pode ser um fator limitante para o tratamento de pacientes com insuficiência hepática, sobretudo em países onde a captação de órgãos não é eficaz o suficiente para suprir a demanda, como o Brasil, além de ser um procedimento de alto custo e de elevados riscos associados. Deste modo, o desenvolvimento de novas estratégias terapêuticas para melhorar a função hepática e a sobrevida dos indivíduos é de grande relevância. Tendo em vista que a regeneração completa do órgão sem seqüelas teciduais é a regra nos casos que sobrevivem mesmo sem transplante, novas estratégias terapêuticas vem sendo buscadas para dar suporte aos pacientes, atuando sobre os determinantes de mortalidade.

A busca por novas terapias para insuficiência hepática aguda levou a um grande interesse pelo desenvolvimento de dispositivos de assistência hepática artificial, que idealmente funcionariam baseados no mesmo princípio da hemodiálise para a insuficiência renal (CARPENTIER et al., 2009). No entanto, em se tratando de um órgão com tantas e variadas funções vitais como é o caso do fígado, a perspectiva do desenvolvimento de uma máquina capaz de substituir todas estas funções é basante remota. No entanto, a utilização combinada de hepatócitos de origem humana ou xenogênica em dispositivos extracorpóreos poderia resolver esta questão, estratégia conhecida como fígado bioartificial, que seria capaz de remover toxinas por filtração e absorção ao mesmo tempo que realiza funções sintéticas pela presença de hepatócitos. Estes dispositivos vêm sendo testados clinicamente em diferentes configurações com diferentes configurações e ainda se encontra em fase de desenvolvimento (ROGER et al., 1998; YU et al., 2012).

Outros estudos demonstraram que o transplante de hepatócitos pode ajudar no manejo de pacientes com IHA. Existem evidências, partindo de estudos pré-clínicos em modelos experimentais de IHA, de que o transplante de hepatócitos leva ao aumento das taxas de sobrevivência em mais de 60% (MAKOWKA et al., 1980; BAUMGARTNER et al., 1983). Estudos clínicos demonstraram que os hepatócitos transplantados são capazes de dar suporte e aumentar a sobrevida dos pacientes que estão aguardando transplante de fígado ou recuperação espontânea ou ainda podem em alguns casos substituir a necessidade de

transplante do órgão (STROM *et al.*, 1997; HABIBULLAH *et al.*, 1994; BACCARANI *et al.*, 2005). Por outro lado, a disponibilidade de hepatócitos humanos possui a limitação da necessidade de suficientes doadores. Neste sentido, grande interesse tem surgido na utilização de substitutos celulares, particularmente células-tronco, no desenvolvimento de novas terapias para IHA.

2.6 TERAPIA COM CÉLULAS-TRONCO NA IHA

A terapia celular é uma ferramenta da medicina regenerativa que envolve o conjunto de métodos e abordagens tecnológicas com a utilização de células no tratamento de diversas doenças. A terapia celular com células-tronco tem despertado maior interesse na comunidade científica devido à capacidade que essas células indiferenciadas possuem de preservar sua própria população e de se diferenciar em células dos diversos tecidos (ZAGO *et al.*, 2005). As células-tronco, por definição, são células indiferenciadas capazes de divisão assimétrica, processo pelo qual podem gerar células-filhas igualmente indiferenciadas, deste modo mantendo um reservatório de células não-especializadas (auto-renovação), ou ainda dar origem a células diferenciadas (ZAGO *et al.*, 2005) (Figura 4).

As células-tronco podem ser obtidas de diferentes fontes, que incluem o embrião, tecidos fetais e organismos adultos (DAN *et al.*, 2008). Dependendo do seu potencial de diferenciação em diferentes linhagens, as células-tronco podem ser classificadas em totipotentes, pluripotentes ou multipotentes. Uma célula multipotente pode dar origem a múltiplos tipos celulares dentro de um mesmo folheto embrionário. Uma célula pluripotente, por sua vez, deve ser capaz de dar origem a todos os tipos celulares encontrados em um organismo adulto. Já a célula totipotente é capaz de produzir um organismo por inteiro, incluindo tecidos extra-embrionários (ZAGO *et al.*, 2005).
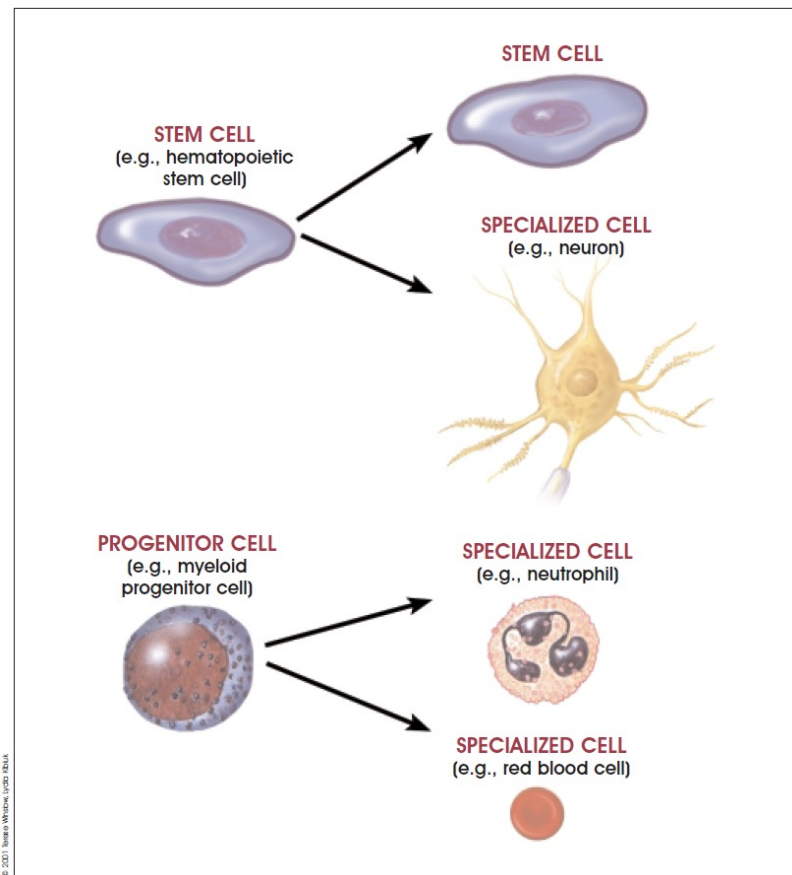
Figura 5. Diferenças entre células-tronco e células progenitoras / precursoras. Exemplo de uma célula-tronco hematopoética produzindo uma segunda geração de células-tronco e um neurônio. A célula progenitora (também conhecida como célula precursora) não-especializada dá origem a duas células especializadas. A figura exemplifica um progenitor mielóide produzindo duas células especializadas (neutrófilos e hemácias). Fonte: WINSLOW, 2001.

De um modo geral, dois tipos de células-tronco têm sido apontados como candidatos à utilização na regeneração hepatica: as células-tronco embrionárias (ESCs) e as células-tronco adultas. As ESCs são derivadas da massa interna do blastocisto, enquanto que as células-tronco adultas podem ser isoladas de tecidos pós-natais, incluindo a medula óssea (LEROU *et al.,* 2008).

A medula óssea foi identificada primariamente como um órgão hematopoiético e, portanto, a sua utilização terapêutica vem sendo direcionada em terapia celular foi direcionada ao longo dos anos para o tratamento de doenças hematológicas. Em 1945 iniciaram-se os estudos experimentais com células-tronco da medula óssea, buscando a reconstituição medular em camundongos irradiados. Poucos anos depois, foi demonstrado que o transplante de medula óssea protegia esses animais contra os efeitos da radiação (LORENZ *et al.*, 1952).

Somente nos últimos anos, a potencial utilização de células da medula óssea para outras patologias tem sido estudada. Diversos outros estudos foram desenvolvidos

aumentando as perspectivas de uso dos diferentes tipos celulares presentes na medula óssea para fins terapêuticos (SOUZA *et al.*, 2009). Esta nova perspectiva partiu da observação de que células da medula óssea poderiam ser estimuladas a se diferenciar *in vitro* em diferentes tipos celulares, incluindo hepatócitos (LAGASSE *et al.*, 2000). Além disso, os hepatócitos derivados da medula óssea foram detectados pela presença do cromossomo Y nos fígados de receptoras femininas de transplantes de medula óssea de doadores masculinos (THEISE *et al.*, 2000). Posteriormente foi comprovado que a transdiferenciação de células da medula óssea em hepatócitos é um evento raro, sendo que a fusão entre estas células seria o maior responsável pelos achados de hepatócitos derivados da medula óssea (WANG *et al.*, 2003). No entanto, diversos estudos experimentais têm demonstrado efeitos benéficos após o transplante de células da medula óssea em diversos modelos experimentais, justificando os resultados por uma ação parácrina exercida por estas células através da secreção de diversas citocinas, fatores de crescimento e mediadores envolvidos na sobrevivência celular, regeneração tecidual e regulação da resposta imune (RATAJCZAK *et al.*, 2011; VAN POLL *et al.*, 2008).

A imunorregulação ocorre fisiologicamente no microambiente da medula óssea, seja através de contato celular, bem como através da secreção de fatores solúveis incluindo citocinas e parece ser importante para criar um ambiente favorável a hematopoiese, estimulando a sobrevivência celular e inibindo a apoptose. A medula óssea contém diversas populações celulares que estão envolvidas na regulação da imunidade, incluindo células-tronco mesenquimais, perfazendo de 0,01% a 0,1% do total de células, e uma presença marcante de células T regulatórias (Treg), que funcionalmente podem chegar a 30% das células T CD4 da medula óssea (ZHAO *et al.*, 2012).

O potencial terapêutico do transplante de células-tronco em hepatite fulminante tem sido avaliado em alguns estudos experimentais, com efeitos benéficos descritos para o uso de células-tronco mesenquimais, células-tronco pluripotentes induzidas, células-tronco embrionárias e células derivadas da medula óssea (PAREKKADAN *et al.*, 2007; CHIANG *et al.*, 2011; JIN *et al.*, 2011; ZHANG et al., 2009; BELARDINELLI *et al.*, 2008; KUAI et al., 2006). A mobilização de células CD34^{+} a partir da administração de G-CSF levou ao aumento das taxas de sobrevivência, redução na lesão hepática e aumento na proliferação de hepatócitos em modelo experimental de IHA induzida por d-galactosamina (ZHANG *et al.*, 2011).O transplante de células da medula óssea e hepatócitos levou à melhora da função hepática após hepatectomia parcial. O transplante de células da medula óssea levou a um pequeno aumento no número de hepatócitos no fígado, enquanto que o transplante de

hepatócitos levou a um repovoamento hepático extenso e levando a uma melhora prolongada da função hepática. (ZHANG *et al.*, 2009). Um estudo recente demonstrou em modelo experimental de insuficiência hepática aguda que o transplante de células mononucleares da medula óssea era capaz de aumentar a regeneração do fígado e a recuperação da função hepática, agindo de modo sinérgica com HGF (JIN *et al.*, 2011). Resultados positivos sobre a mortalidade foram encontrados após injeção de meio condicionado de células-tronco mesenquimais em modelo experimental de IHA. Esses resultados sugerem que as células-tronco, atuando através de um mecanismo parácrino, podem ter valor terapêutico para IHA (PARAKKEDAN *et al.*, 2007).

3 OBJETIVOS

3.1 Objetivo geral

Investigar os efeitos da terapia com células mononucleares da medula óssea em um modelo experimental de insuficiência hepática aguda induzida por acetaminofen.

3.2 Objetivos específicos

- Avaliar o efeito da terapia celular sobre a sobrevivência dos animais;
- Determinar o impacto da terapia sobre a lesão no fígado;
- Investigar a presença das células transplantadas no fígado;
- Investigar os efeitos da terapia celular sobre a resposta inflamatória no fígado e da produção de mediadores inflamatórios no fígado, cérebro, baço, medula óssea e sangue;
- Avaliar os efeitos da terapia celular sobre a permeabilidade da barreira hemato-encefálica.

4 ARTIGO

O artigo descreve os resultados obtidos neste projeto de mestrado, buscando atender a todos os objetivos levantados. Este artigo foi publicado na revista internacional indexada *Cytotherapy*.

Transplantation of bone marrow cells decreases TNF-α production, blood-brain barrier permeability and improves survival in a mouse model of acetaminophen-induced acute liver disease
Bruno Solano de Freitas Souza, Ramon Campos Nascimento, Sheilla Andrade de Oliveira, Juliana Fraga Vasconcelos, Carla Martins Kaneto, Lian Felipe Paiva Pontes de Carvalho, Ricardo Ribeiro-dos-Santos, Milena Botelho Pereira Soares, Luiz Antonio Rodrigues de Freitas.

informa
healthcare

Transplantation of bone marrow cells decreases tumor necrosis factor-α production and blood–brain barrier permeability and improves survival in a mouse model of acetaminophen-induced acute liver disease

BRUNO SOLANO DE FREITAS SOUZA[1,2], RAMON CAMPOS NASCIMENTO[3,4], SHEILLA ANDRADE DE OLIVEIRA[1,5], JULIANA FRAGA VASCONCELOS[1,2], CARLA MARTINS KANETO[2], LIAN FELIPE PAIVA PONTES DE CARVALHO[2], RICARDO RIBEIRO-DOS-SANTOS[1,2], MILENA BOTELHO PEREIRA SOARES[1,2] & LUIZ ANTONIO RODRIGUES DE FREITAS[3,4]

[1]*Laboratório de Engenharia Tecidual e Imunofarmacologia, Centro de Pesquisas Gonçalo Moniz, Fundação Oswaldo Cruz, Salvador, BA, Brazil,* [2]*Centro de Biotecnologia e Terapia Celular, Hospital São Rafael, Salvador, BA, Brazil,* [3]*Laboratório de Patologia e Biointervenção, Centro de Pesquisas Gonçalo Moniz, Fundação Oswaldo Cruz, Salvador, BA, Brazil,* [4]*Faculdade de Medicina, Universidade Federal da Bahia, Salvador, BA, Brazil, and* [5]*Laboratório de Imunopatologia e Biologia Molecular, Centro de Pesquisas Aggeu Magalhães, Fundação Oswaldo Cruz, Recife, PE, Brazil*

Abstract

Background aims. Acute liver failure (ALF), although rare, remains a rapidly progressive and frequently fatal condition. Acetaminophen (APAP) poisoning induces a massive hepatic necrosis and often leads to death as a result of cerebral edema. Cell-based therapies are currently being investigated for liver injuries. We evaluated the therapeutic potential of transplantation of bone marrow mononuclear cells (BMC) in a mouse model of acute liver injury. *Methods.* ALF was induced in C57Bl/6 mice submitted to an alcoholic diet followed by fasting and injection of APAP. Mice were transplanted with 10^7 BMC obtained from enhanced green fluorescent protein (GFP) transgenic mice. *Results.* BMC transplantation caused a significant reduction in APAP-induced mortality. However, no significant differences in serum aminotransferase concentrations, extension of liver necrosis, number of inflammatory cells and levels of cytokines in the liver were found when BMC- and saline-injected groups were compared. Moreover, recruitment of transplanted cells to the liver was very low and no donor-derived hepatocytes were observed. Mice submitted to BMC therapy had some protection against disruption of the blood–brain barrier, despite their hyperammonemia, and serum metalloproteinase (MMP)-9 activity similar to the saline-injected group. Tumor necrosis factor (TNF)-α concentrations were decreased in the serum of BMC-treated mice. This reduction was associated with an early increase in interleukin (IL)-10 mRNA expression in the spleen and bone marrow after BMC treatment. *Conclusions.* BMC transplantation protects mice submitted to high doses of APAP and is a potential candidate for ALF treatment, probably via an immunomodulatory effect on TNF-α production.

Key Words: *acetaminophen, acute liver failure, bone marrow mononuclear cells, brain edema, cell therapy, tumor necrosis factor*

Introduction

Acute liver failure (ALF) is caused by liver cell dysfunction, leading to coagulopathy, hepatic encephalopathy and death in previously healthy patients. The main cause of this illness is poisoning with acetaminophen (*N*-acetyl-paraaminophen; APAP) through unintentional overdoses or suicide attempts (1). This drug induces severe centrolobular hepatocellular necrosis and increases serum transaminase levels, in a dose-dependent manner. The extent of APAP-induced hepatic lesions is increased by fasting and alcohol consumption, both in animals and humans (2,3).

APAP is metabolized by cytochrome P450 to form *N*-acetyl-*p*-benzoquinone imine (NAPQI). This reactive metabolite depletes glutathione and covalently binds to cysteine groups on proteins, leading to inhibition of mitochondrial respiration, mitochondrial permeability transition, hepatic necrosis and inflammatory response (4,5). The consequent massive death of hepatocytes is followed by disturbances in the hepatic cycle of urea and an increase in serum

RIGHTSLINK()

ammonia levels. In the brain, the ammonia excess is incorporated as glutamate by astrocytes to form glutamine, an organic osmolyte, which leads to oxidative/nitrosative stress, blood–brain barrier (BBB) disruption and increased cerebral blood flow (6,7). All of these features induce encephalopathy and brain edema, the main cause of death in humans after an APAP overdose. Furthermore, the systemic production of the pro-inflammatory cytokine tumor necrosis factor (TNF)-α is increased in patients with acute liver failure, and a growing body of evidence indicates this cytokine to be a central mediator promoting the development of encephalopathy in this condition (8).

The definitive treatment for APAP-induced acute liver failure is liver transplantation, limited by the shortage of donors and surgical risks (9). Research for therapeutic approaches has focused on the prevention of liver damage with anti-oxidants, control of brain edema and hepatic support with bio-artificial livers or hepatocyte transplantation (10). Cell-based therapies have also been investigated as treatments for liver lesions. Transplantation of bone marrow mononuclear cells (BMC) has been shown to ameliorate dysfunction in different organs, such as the heart, brain and liver. BMC are easy to isolate and comprise different cell populations that can produce anti-inflammatory molecules related with hepatic protection in acute liver failure (11,12). In this study we evaluated the therapeutic potential of BMC transplantation in a model of APAP-induced hepatotoxicity potentiated by alcohol consumption.

Methods

Animals and acute liver failure induction

Animals were handled according to the Fundação Oswaldo Cruz (FIOCRUZ) guidelines for animal experimentation and the experimental protocols were approved by local animal ethics committees. Four to 6-week-old male C57Bl/6 mice weighing approximately 20 g were raised and maintained at the Gonçalo Moniz Research Center/Oswaldo Cruz Foundation (Salvador, Brazil) in rooms with controlled temperature ($22 \pm 2°C$) and humidity ($55 \pm 10\%$) and continuous air renovation. Animals were maintained with 10% alcohol solution in water for 3 weeks. Before APAP administration, they were fasted for approximately 12 h with free access to pure water. Fresh suspensions of 16 mL/kg APAP (All Chemistry, São Paulo, Brazil) were prepared in warm saline (40°C) and given at 300 mg/kg intraperitoneally (corresponding to a lethal dose of 70%). Control mice received the same volume of saline solution.

Transplantation of BMC

Bone marrow cells were obtained from femurs and tibiae of 4–6-week-old enhanced green fluorescent protein (EGFP)-transgenic C57Bl/6 mice. The mononuclear cell fraction was purified by centrifugation in a Histopaque gradient at 1000 *g* for 25 min at 25°C (Histopaque 1119 and 1077, 1:1; Sigma-Aldrich, St Louis, MO, USA). The mononuclear cell fraction was collected and washed three times in Dulbecco's modified Eagle medium (Sigma-Aldrich). Cell suspensions were filtered over nylon wool and diluted in saline (5×10^7 cells/mL), and their viability was evaluated by trypan blue exclusion (Sigma-Aldrich). The cells were injected into the peripheral circulation 3 h after APAP injection (1×10^7 cells/mouse). In addition, BMC samples were analyzed by flow cytometry in a FACScalibur flow cytometer using conjugated antibodies (Becton Dickinson, San Diego, CA, USA), showing that $96.5 \pm 1.3\%$ expressed green fluorescent protein (GFP) and $96.3 \pm 3.1\%$ expressed CD45. Hematopoietic progenitor markers Sca-1, CD34 and CD117 were expressed by $0.11 \pm 0.03\%$, $0.20 \pm 0.05\%$ and $0.17 \pm 0.04\%$ of the cells, respectively.

Tissue preparation and evaluation of liver injury

Mice from BMC- and saline-treated groups were anesthetized with ketamine (115 mg/kg) and xylazine (10–15 mg/kg) at different time-points after APAP injection. The animals were immediately perfused transcardially with 50 mL cold 0.9% saline, followed by 100 mL cold 4% paraformaldehyde (Merk, Darmstadt, Germany) in phosphate-buffered saline (PBS), pH 7.2. Livers were excised and left lobes were fixed in 10% formalin and paraffin-embedded. Four micrometer-thick paraffin-embedded sections were stained with hematoxylin-eosin (H&E). Analyses were performed on whole liver sections after slide scanning using an Aperio ScanScope system (Aperio Technologies, Vista, CA, USA). The images were analyzed using the Image Pro program (version 7.0; Media Cybernetics, San Diego, CA, USA). Hepatic injury was determined as a percentage of necrotic tissue, and a mean area of 24 676 428 μm^2/mouse was analyzed.

Quantification of EGFP cells in the liver by immunofluorescence

After transcardiac perfusion with paraformaldehyde, non-left hepatic lobes were additionally fixed in 4% paraformaldehyde at 4°C for 24 h. These samples were then incubated overnight in 30% sucrose solution in PBS at 4%, embedded in medium for congeal tissue and frozen at −70°C. Four-micrometer thick

sections were stained using a rabbit anti-human albumin (DAKO, Glostrup, Denmark) followed by anti-rabbit IgG conjugated with Alexa Fluor 568 (Invitrogen, Carlsbad, CA, USA), and mounted with VectaShield Hard Set medium with 4′,6-Diamidino-2-Phenylindole (DAPI) for nuclear staining (Vector, Burlingame, CA, USA). GFP$^+$ cells were quantified in five randomly selected areas per animal at a magnification of 200 ×.

Biochemical analyses

Blood was carefully collected in lithium heparinized tubes at different time-points immediately before killing, to avoid hemolysis. Plasma was obtained by centrifugation of blood for 10 min at 9000 **g** and stored at 4°C. Ammonia, Aspartate transaminase (AST) and ALT were evaluated within 2 h of plasma isolation using commercial kits (Vitros, New Jersey, USA, and Roche/Hitachi, Tokyo, Japan).

Quantification of inflammation

Quantification of infiltration of inflammatory cells was performed in 5-mm thick liver sections frozen in Optimal Cutting Temperature Compound (OCT). The analysis was performed in sections obtained from the left hepatic lobe. For microscopic analysis, an Olympus FluoView 1000 confocal laser scanning microscope (Olympus, Tokyo, Japan) was used for image acquisition. Sections were immunostained with primary antibody against mouse CD45, diluted 1:100 (Caltag, Buckingham, UK) overnight at 4°C. The next day sections were washed in PBS and incubated for 1 h at room temperature with the secondary antibody against rat IgG conjugated with Alexa Fluor 568. A total of five images per mouse was obtained in random fields. A magnification of 200 × was used in order to cover an area of 1 mm^2. Numbers of CD45$^+$ cells were counted manually using Image-Pro Plus v.7.0 software (Media Cybernetics). In order to avoid overestimation because of counting partial cells that appeared within the section, only cells with intact morphology and a visible nucleus were counted.

Analysis of cytokine production

TNF-α, interleukin (IL)-6 and IL-10 levels were measured in total liver extracts and serum. Liver proteins were extracted from 100 mg tissue/mL PBS to which 0.4 M NaCl, 0.05% Tween-20 and protease inhibitors (0.1 mM phenylmethanesulfonyl fluoride; (PMSF), 0.1 mM benzethonium chloride, 10 mM Ethylenediamine tetraacetic acid (EDTA) and 20 Kallikrein Inhibitor Unit (KIU) aprotinin A/100 mL) were added. The samples were centrifuged for

10 min at 3000 **g** and the supernatant was frozen at –70°C for later quantification. Cytokine levels were estimated using commercially available immunoassay enzyme-linked immunosorbent assay (ELISA) kits for mouse TNF-α, IL-6 and IL-10 (BD, Franklin Lakes, NJ, USA), according to the manufacturer's instructions. Briefly, 96-well plates were blocked and incubated at room temperature for 1 h. Samples were added in duplicates and incubated overnight at 4°C. Biotinylated antibodies were added and plates were incubated for 2 h at room temperature. A half-hour incubation with streptavidin–horseradish peroxidase conjugate at a dilution of 1:200 was followed by detection using 3,3′,5,5′- tetramethylbenzidine (TMB) peroxidase substrate and reading at 450 nm.

Real-time polymerase chain reaction data

RNA was harvested and isolated with TRIzol reagent (Invitrogen) and the concentration was determined by photometric measurement. The RNA quality was analyzed in a 1.2% agarose gel. A high-capacity cDNA reverse transcription kit (Applied Biosystems, Carlsbad, CA, USA) was used to synthesize cDNA of 2 μg RNA following the manufacturer's recommendations.

Real-time reverse transcription (RT)-polymerase chain reaction (PCR) assays were performed to detect the expression levels of TNF-α (Mm 00443258_m1), IL-10 (Mm 00439616_m1), endothelin-1 (EDN-1; Mm 00438656_m1), adrenomedullin (ADM) (Mm00437438_g1) and GFP (assay by design) using hydrolysis probes from Applied Biosystems. Quantitative (q)RT-PCR amplification mixtures were made with Universal master mix (Applied Biosystems) and a 7500 real-time PCR system (Applied Biosystems). The cycling
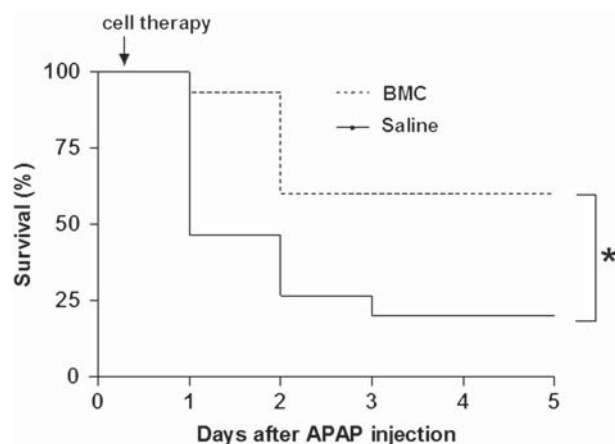

Figure 1. Effects of BMC therapy in APAP-induced lethality. Mice received saline or BMC 3 h after APAP injection. Survival was followed for 5 days. Results shown are from one experiment of four performed, each one with 15 mice/group. *$P < 0.05$.
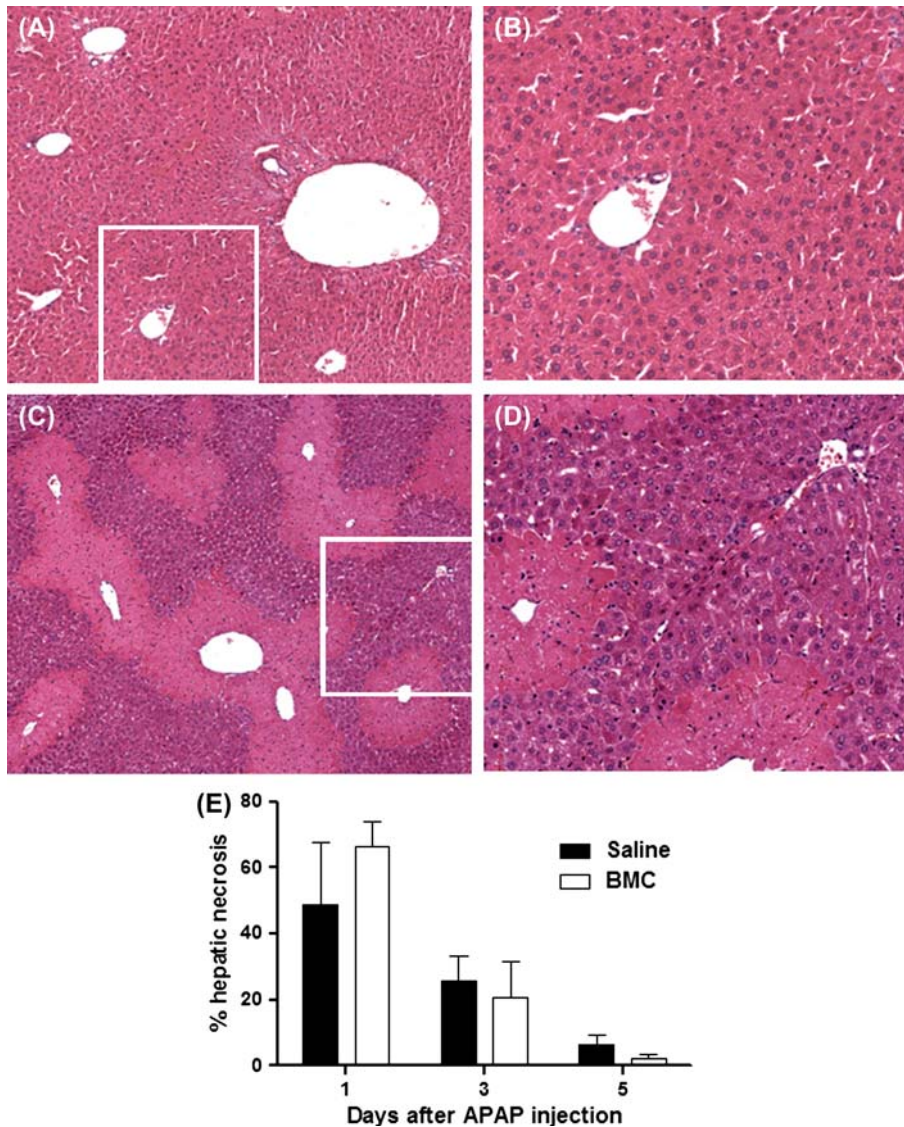
Figure 2. Liver necrosis after APAP injection and BMC transplantation. (A, B) Liver section of a mouse killed after 3 weeks of an alcoholic diet without APAP treatment, showing an absence of significant alteration of hepatic parenchyma. (C, D) Extensive centrolobular necrosis 24 h after APAP injection in the liver of saline-injected mice. (E) Quantification of the percentage of necrotic area in the liver parenchyma of saline-treated or BMC-treated mice. Results shown are from one of three experiments performed, each one with 3–5 mice/group/time-point.

conditions comprised 10 min polymerase activation at 95°C and 40 cycles at 95°C for 15 s and 60°C for 60 s. Normalization was made with the target internal control glyceraldehyde-3-phosphate dehydrogenase (GAPDH) using the cycle threshold method, and analysis of variance followed by the Tukey test.

Evaluation of BBB integrity

Evans blue (EB) has been used widely to assess brain edema (13). Mice were injected intravenously with 4 mL/kg 2% (w/v) EB solution. Thirty minutes later, the animals were killed with a ketamine overdose and brains were dissected away from the brainstem, cerebellum and meninges. Brain samples were embedded

in medium for congeal tissue (Tissue-Tek) and frozen at −70°C. Five-micrometer thick sections were prepared, fixed in paraformaldehyde 4%, and nuclei stained with DAPI. EB+ cells were quantified in five randomly selected areas per animal at a magnification of 20×.

Metalloproteinase zymogram

Serum samples diluted 1:150 in non-reducing sample buffer (Tris–HCl buffer 500 mM/L, 10% glycerol, 4% Sodium Dodecyl Sulfate (SDS) w/v, 0.04% bromophenol blue w/v, pH 6.8) were loaded onto 7.5% SDS polyacrylamide gels containing type A gelatin from porcine skin 0.2% w/v (Sigma, St. Louis, MO, USA) and electrophoresis was performed at 100 V for
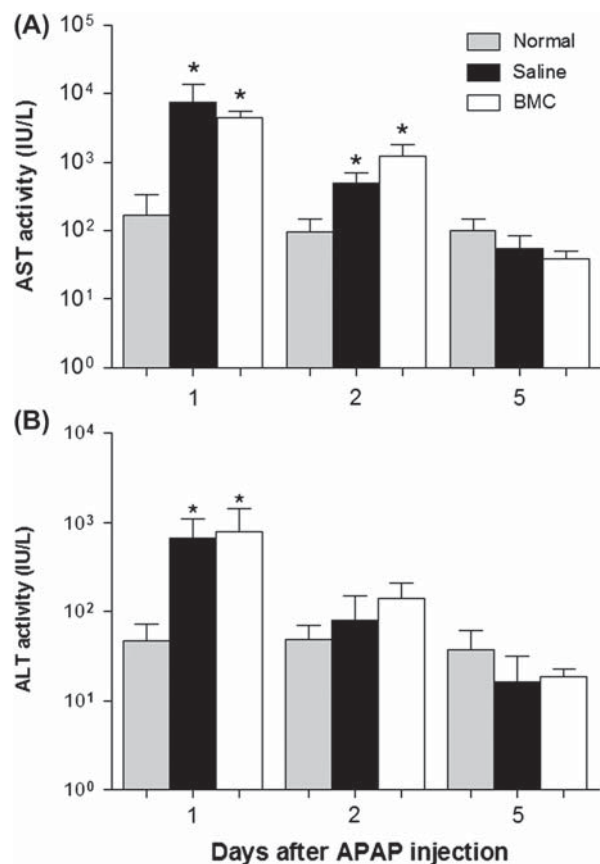
Figure 3. Measurement of serum levels of transaminases. (A) AST and (B) ALT serum levels of BMC- and saline-treated mice were determined at different time-points after APAP injection. Data obtained from one of two experiments performed represent the means $\pm$ SEM of 3–5 mice/group/time-point. $^*P < 0.05$.

3 h under cooling conditions (FB300 eletrophoresis power supply; Fisher Scientific, Waltham, MA, USA). Gels were then washed twice in 2.5% Triton X-100 solution for 30 min at room temperature with gentle agitation to remove SDS, and incubated at 37°C for 24 h in substrate buffer (Tris–HCl buffer 10 mM/L, 1.25% Triton X-100, $CaCl_2$ 5 mM/L, $ZnCl_2$ 1 μM/L, pH 7.5). Thereafter, gels were stained with a 0.5% w/v Coomassie blue R250 (Sigma-Aldrich) solution in 50% methanol, 10% acetic acid for 18 h and then unstained with the same solution without dye. Gelatinase activity was detected as unstained bands in a blue background, representing areas of proteolysis of the gelatin. After lamination and image acquisition, densitometric semi-quantitative analysis was performed using Scion image software (Image Program, National Institutes of Health, Scion Corporation, Frederick, MD, USA).

Statistical analyses

Results were expressed as mean $\pm$ SEM. Statistical comparisons were performed using Mann–Whitney or Kruskal–Wallis tests for non-parametric data. Parametric data were analyzed with *t*-test or ANOVA. Survival curves were evaluated by log-rank (Mantel–Cox) test, using Prism Software (version 5.0; GraphPad Software, San Diego, CA, USA). A *P*-value less than 0.05 was considered statistically significant.

Results

Transplantation of BMC reduces APAP-induced mortality without affecting hepatic necrosis

To evaluate the effect of BMC therapy in APAP-induced mortality, animals were injected with saline or BMC suspensions by an intravenous route 3 h after APAP injection. Five days later, the survival rate of the BMC-treated group was 60%, significantly higher than the 20% observed in the saline-injected group (Figure 1). On the other hand, when the same dose of BMC was given 9 h after APAP injection, this protective effect was not observed (data not shown).

Alcoholic diet alone did not result in any morphologic alterations visible by optic microscopy (Figure 2A, B). However, APAP administration after an alcoholic diet resulted in extensive necrosis in the centrolobular liver zone (Figure 2C, D). We did not observe any differences in necrosis extension (Figure 2E) and serum transaminase levels (Figure 3A, B) between BMC- and saline-treated groups at different time-points after APAP injection. To correct a possible selection bias in necrosis analysis as a result of mortality, an experiment was performed in which mice were organized in pairs containing one BMC- and one saline-treated mouse. Mortality was evaluated every 3 h after APAP injection. Livers from paired animals were immediately harvested after the death of any animal from each pair, and even then we did not observe differences in hepatic damage between BMC-treated and saline-injected mice (data not shown).

Transplanted BMC migrate to the liver but do not differentiate into hepatocytes or reduce local inflammation

Liver sections from BMC-treated mice were processed for analysis by immunofluorescence microscopy in order to track the presence of GFP$^+$ cells. Despite the inflammatory cell infiltrate in centrolobular areas observed in H&E sections, there was little recruitment of transplanted cells to hepatic parenchyma. The maximum engraftment occurred 24 h after APAP injection, when about 13 cells/mm^2 were found in liver sections (Figure 4B). Moreover, GFP$^+$ cells did not express albumin and did not show hepatocyte-like polygonal morphology at the time-points evaluated (Figure 4A). GFP$^+$ cell were also found in the spleens of BMC-transplanted mice (Figure 4C). The analysis of GFP mRNA expression in the bone marrow, spleens and livers of BMC-transplanted mice demonstrated that
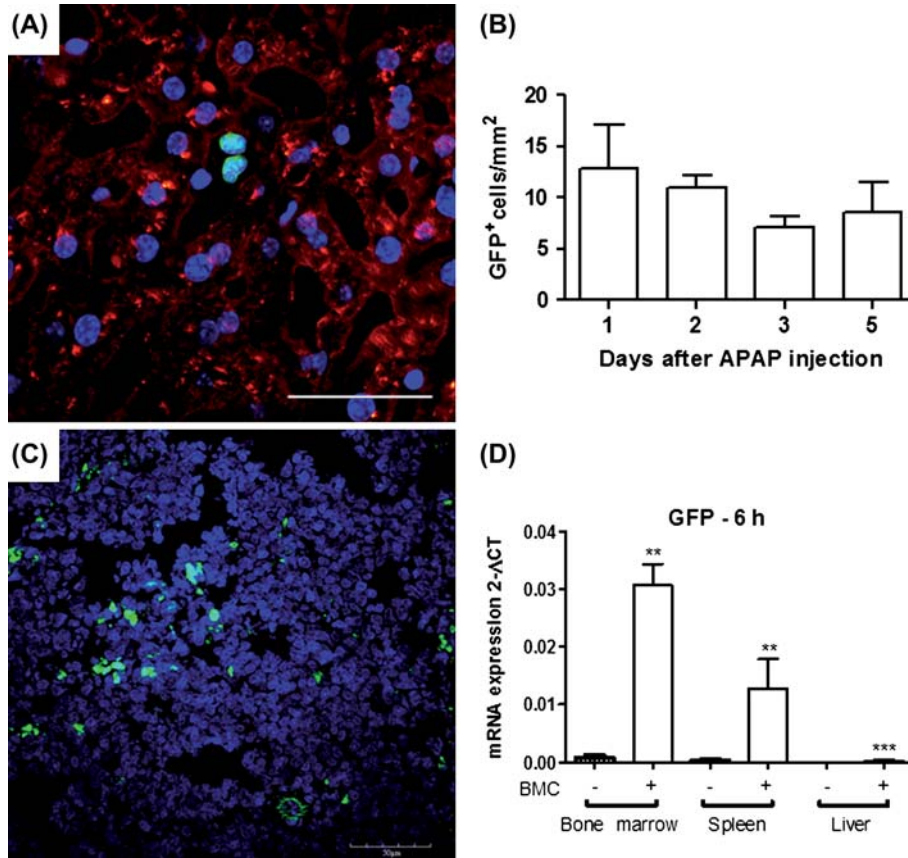
Figure 4. Migration of BMC to different organs with low recruitment to the injured liver. (A) Immunofluorescence of liver section showing a centrolobular zone from a BMC-treated mouse 5 days after APAP injection. Presence of GFP$^+$ cells (green) in sections stained with DAPI (blue) for nuclei visualization and with anti-albumin antibody (red). GFP$^+$ cells (green) on liver parenchyma did not express albumin and did not assume hepatocyte-like polygonal morphology. The section was counterstained with DAPI for nuclei visualization (blue). (B) Quantification of GFP$^+$ cells in livers of BMC-treated mice at different time-points after APAP injection. Data represent the means $\pm$ SEM of 3–5 mice/group/time-point. (C) The presence of GFP$^+$ cells (green) in the spleen section of a BMC-transplanted mouse. The section was counterstained with DAPI for nuclei visualization (blue). Bar = 50 μm. (D) GFP gene expression in bone marrow, spleen and liver of mice 6 h after APAP injection, showing increased recruitment of transplanted BMC to the bone marrow, followed by spleen and liver. Data represent mean $\pm$ SEM of seven mice/group. Scale bars represent 50 μm. $^*P < 0.05$; $^{**}P < 0.001$; $^{***}P < 0.0001$.

most of the cells migrated to the bone marrow and the spleen, and very few cells were retained in the liver 6 h after APAP injection (Figure 4D).

To evaluate the number of inflammatory cells, liver sections were submitted to immunofluorescence analysis using an antibody against the pan-leukocyte marker CD45. Mice injected with APAP had CD45$^+$ cell infiltrates of mild intensity after 6 h (Figure 5A), which increased after 14 h (Figure 5B). The percentage of CD45$^+$ cells did not differ significantly between BMC-treated and saline-injected groups (Figure 5C).

BMC transplantation protects the BBB integrity

We next evaluated leakage in the BBB by EB injection 18 h after APAP injection. The number of EB-stained neurons was significantly attenuated in brains of mice from the BMC-treated group in comparison with saline-injected mice (Figure 6A–C). However,

we did not observe migration of GFP$^+$ cells to the brains of BMC-transplanted mice by fluorescence microscopy.

Because hyperammonemia is implicated in the pathogenesis of brain edema in acute liver damage (7), we determined the serum ammonia levels after APAP injection in cell- and saline-treated mice. Ammonia levels were similar in both groups (BMC, 680 ± 30.4 μg/dL; saline, 730 ± 57.7 μg/dL; $P = 0.4859$). These data indicated that the reduction in the brain vessel permeability associated with BMC transplantation was probably because of an ammonia-independent mechanism.

Another factor that may contribute to disruption of the BBB is the increased activity of metalloproteinases (MMP (14–16). We evaluated the activity of MMP-9 in the sera of mice submitted to APAP-induced injury. No significant differences in the activity of MMP-9 were found when BMC-treated and saline-injected mice were compared (Figure 6D). We
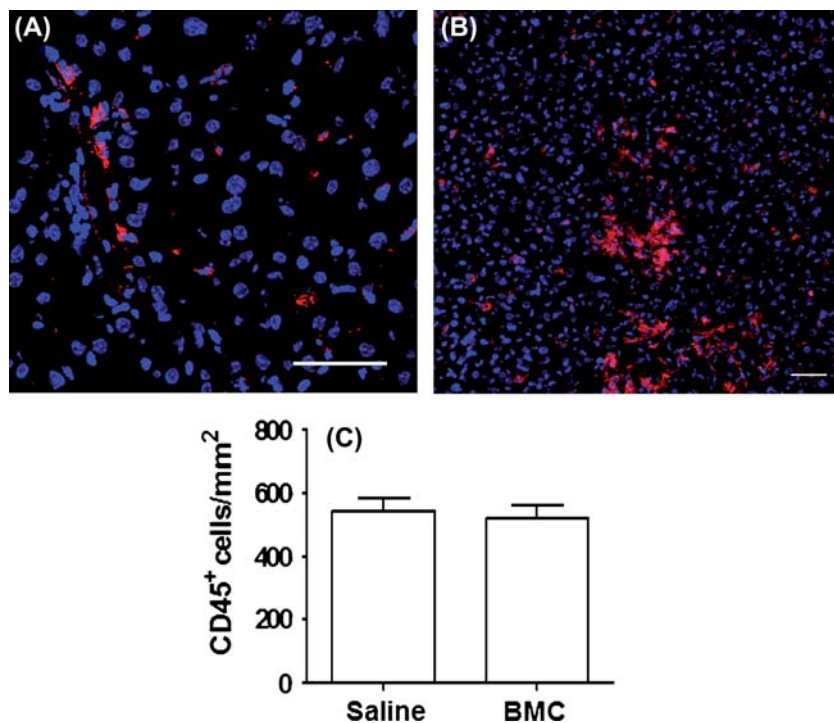
Figure 5. BMC transplantation does not affect the number of inflammatory cells in the liver. (A) Immunofluorescence showing mild infiltration of CD45$^+$ cells (red) into the injured liver 6 h after APAP injection. (B) Infiltration of CD45$^+$ cells into the liver increases 14 h after APAP injection. (C) Quantification of CD45$^+$ cells in the liver, showing similar numbers of infiltrating cells in both BMC- and saline-treated groups. Scale bars represent 50 μm. The data represent means $\pm$ SEM of seven mice/group.

then hypothesized that BMC could act by modulating the expression of adrenomedullin and endothelin-1, two peptides known for their role in the regulation of BBB permeability (17). Although the gene expression of adrenomedullin and endothelin-1 was found to be elevated in the brains of mice 14 h after APAP injection, no statistically significant difference was found between BMC- and saline-treated mice (Figure 6E, F).

Modulation of APAP-induced cytokine production after BMC transplantation

Because increased production of TNF-α is strongly associated with hepatic encephalopathy in acute liver failure (8), we measured the concentrations of TNF-α in the liver and serum of mice submitted to APAP-induced injury, as well as in normal controls. Saline-injected mice had increased TNF-α concentrations in the liver (Figure 7A) and serum (Figure 7C) when compared with normal controls. When BMC-treated mice were evaluated 14 h after APAP injection, we observed a significant reduction of TNF-α in the serum, but not in the liver, compared with saline-injected mice (Figure 7A, C).

To investigate the mechanisms by which BMC modulate TNF-α production, we measured the concentrations of the anti-inflammatory cytokine IL-10. IL-10 concentrations in the livers of BMC-transplanted and saline-injected mice were not significantly different (Figure 7B). However, when the expression of IL-10 mRNA was evaluated, a marked increase was observed in the spleen and bone marrow of BMC-transplanted mice 6 h after APAP injection (Figure 8A–D). Fourteen hours after APAP injection, gene expression of TNF-α was suppressed in the spleen, while IL-10 was up-regulated (Figure 8E, F).

Discussion

We have demonstrated a protective effect of BMC transplantation in mice with ALF induced by APAP. This was evidenced by a reduction in mortality, modulation of the production of inflammatory mediators and decreased damage to the BBB. This was only achieved when the cells were transplanted early (up to 6 h after APAP challenge), indicating that early events modulated by the cell therapy may be determinants of disease outcome.

The protective effect of BMC transplantation observed in our study did not correlate with an improvement in liver necrosis or function (ALT, AST and ammonia). However, in a rat model of ALF, improvement of liver function and decreased area of necrosis were observed after transplantation of BMC (18). This difference may be because of a slower evolution of the disease in the rat model
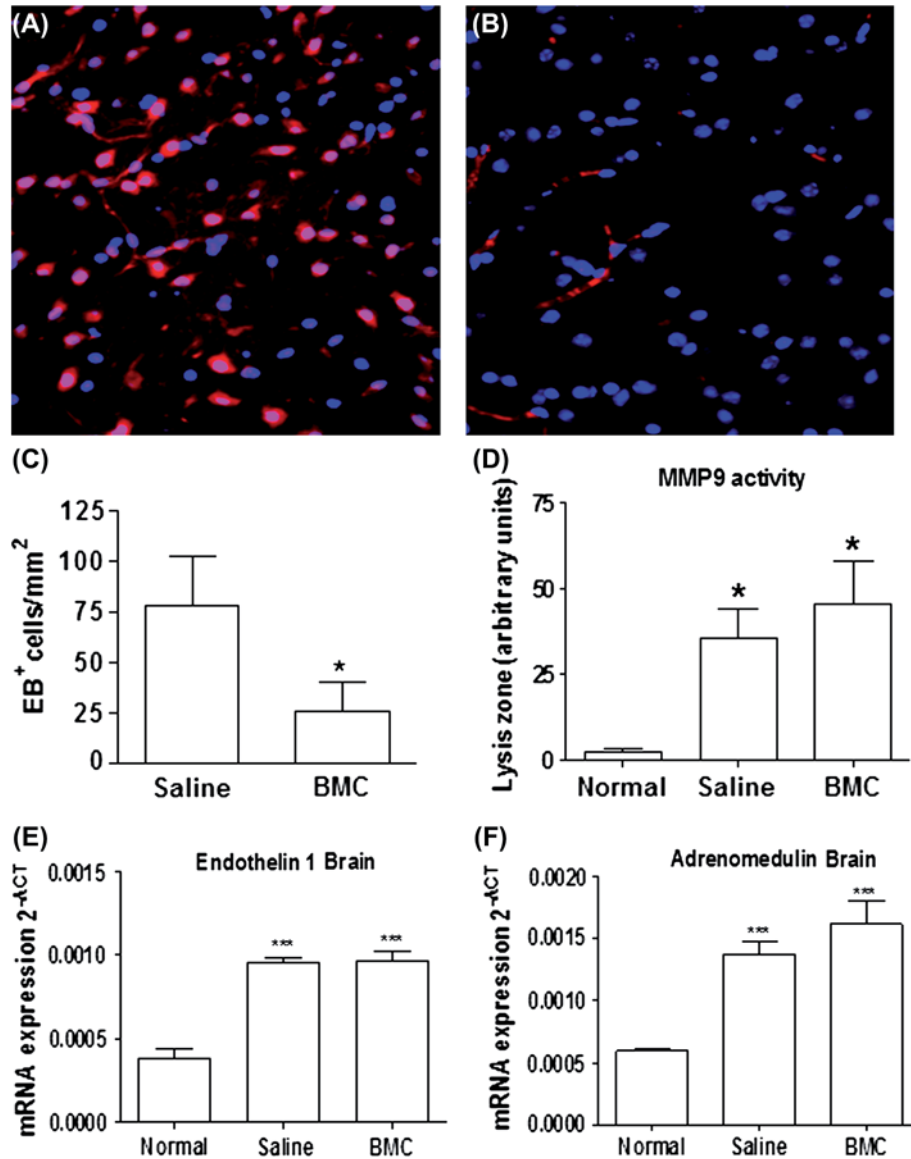
Figure 6. Evaluation of brain edema 18 h after APAP injection. Mice were injected with EB and killed 30 min later. Brains were processed as described in the Methods. (A, B) Fluorescence microscopy of brain sections obtained from saline- and BMC-treated mice, respectively. BMC induced low impregnation of cells with EB (red). Nuclei were stained with DAPI (blue). (C) EB staining cells were quantified in brain sections, and were reduced in BMC-treated mice. Data represent the means $\pm$ SEM of 3–5 mice/group. $^*P < 0.05$. (D) Zymogram for detection of serum MMP-9 activity 14 h after APAP injection, showing similar lysis area between BMC- and saline-treated groups. Data represent one of two experiments, presented as the means $\pm$ SEM of 12–14 mice/group. (E, F) qPCR analysis of gene expression of endothelin-1 (E) and adrenomedullin (F) in the brains of mice 14 h after APAP injection. Data represent the means $\pm$ SEM of 5–7 mice/group. $^{***}P < 0.0001$.

compared with the mouse model used in our study; most of the mice had died 24 h after APAP injection, whereas in the rat model mortality started after the first 24 h. Thus it is possible that, in our study, the fast evolution of the disease renders it difficult for the transplanted cells to promote any improvement of liver regeneration.

A few transplanted cells migrated to the liver, and no contribution of GFP$^+$ cells to hepatocyte formation was observed during all the time-points analyzed. Thus it is likely that the transplanted

BMC act via a paracrine effect, causing the modulation of cytokine production in this model. In fact, a decrease in serum TNF-α concentrations and an increase in IL-10 mRNA expression in the bone marrow and spleen were observed after BMC transplantation in our model of ALF. The modulation of cytokine production and inflammatory response by BMC transplantation has been observed in other disease models, such as chronic chagasic cardiomyopathy (19), epilepsy (20) and chronic liver diseases (21).
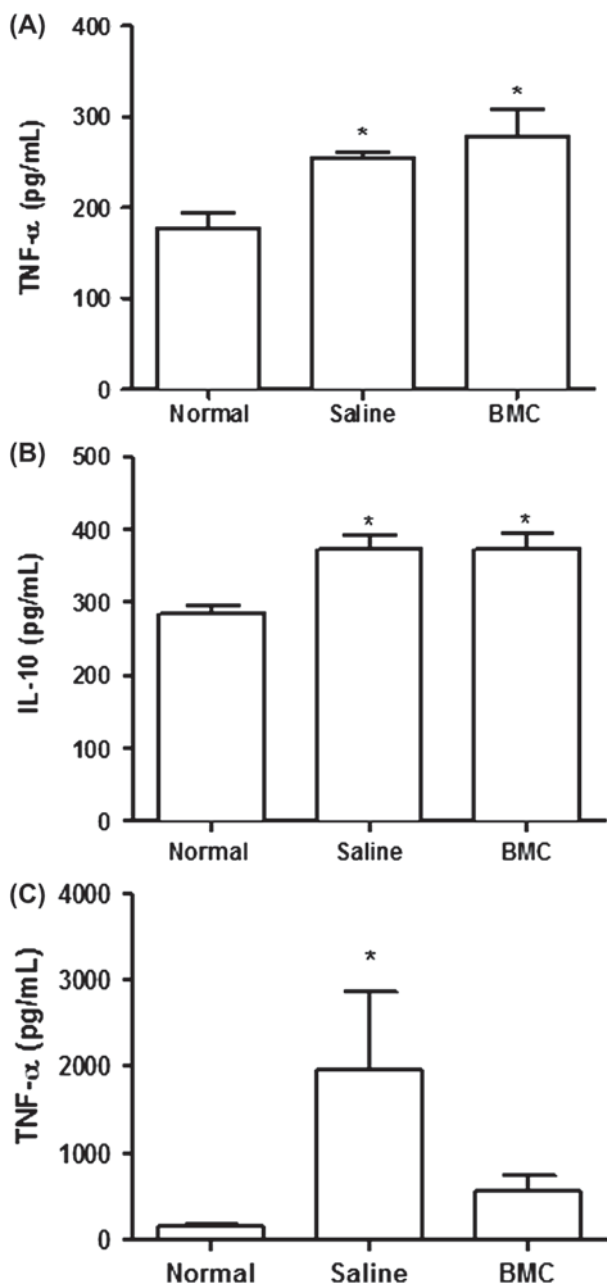
Figure 7. Assessment of cytokines in the liver and serum 14 h after APAP injection. Concentrations of TNF-α (A, C) and IL-10 (B) were determined in liver extracts (A, B) and serum (C) in saline- and BMC-treated mice 14 h after APAP injection. Data represent the means ± SEM of 5–7 mice/group. ***$P < 0.0001$.

The increase in TNF-α during the course of ALF seems to be a crucial event determining the disease outcome (22,23). TNF-α is a pleiotropic cytokine the effects of which may contribute in different ways to disease progression, including apoptosis induction, endothelial cell and platelet activation, increased vascular permeability and induction of soluble mediators (24). TNF-α elevation in ALF is indicated as one of the main causes of hepatic encephalopathy, and the severity of encephalopathy correlates with TNF-α serum concentration in patients with ALF (25). Elevated serum levels of TNF-α has been shown previously to correlate with increased permeability of the BBB in mice with APAP-induced ALF (26). Furthermore, Bemeur *et al.* (27), using an experimental model of ALF induced by azoxymethane in mice, have shown successfully that TNFR1 knockout mice are protected against the onset of coma and brain edema. Thus it is possible that the modulation of TNF-α production by transplanted BMC causes a decreased leakage in the BBB, consequently decreasing the development of hepatic encephalopathy and death rate of mice after APAP challenge.

TNF-α production was modulated in the serum but not in the liver of mice submitted to BMC transplantation after APAP challenge. This suggested a systemic immunomodulatory effect of the transplanted cells, and in fact an increase in IL-10 mRNA expression was observed both in the spleen as well as the bone marrow of BMC-treated mice 3 h after cell transplantation. The spleen and bone marrow are sites in which transplanted cells are preferentially retained (28), and this was confirmed in our study by qRT-PCR analysis. The production of IL-10, a potent anti-inflammatory cytokine with well-known suppressive activities over TNF-α production, has been described previously to occur in BMC cultures *in vitro* and *in vivo* in a model of myocardial infarct (29). Thus it is possible that both cell populations, transplanted cells as well as resident cells in the spleen and bone marrow, contribute to the increase in IL-10 mRNA expression.

In summary, we observed that peripheral transplantation of BMC reduced mortality in an APAP-induced model of acute liver failure potentialized by ethanol without improving liver damage. Transplanted cells did not differentiate into hepatocytes and did not up-regulate the liver function, as showed by serum ammonia dosage. Nonetheless, mice that received BMC transplantation showed less BBB injury. Studies are needed to evaluate the therapeutically active subpopulations in the BMC fraction and to describe the protective mechanisms involved.
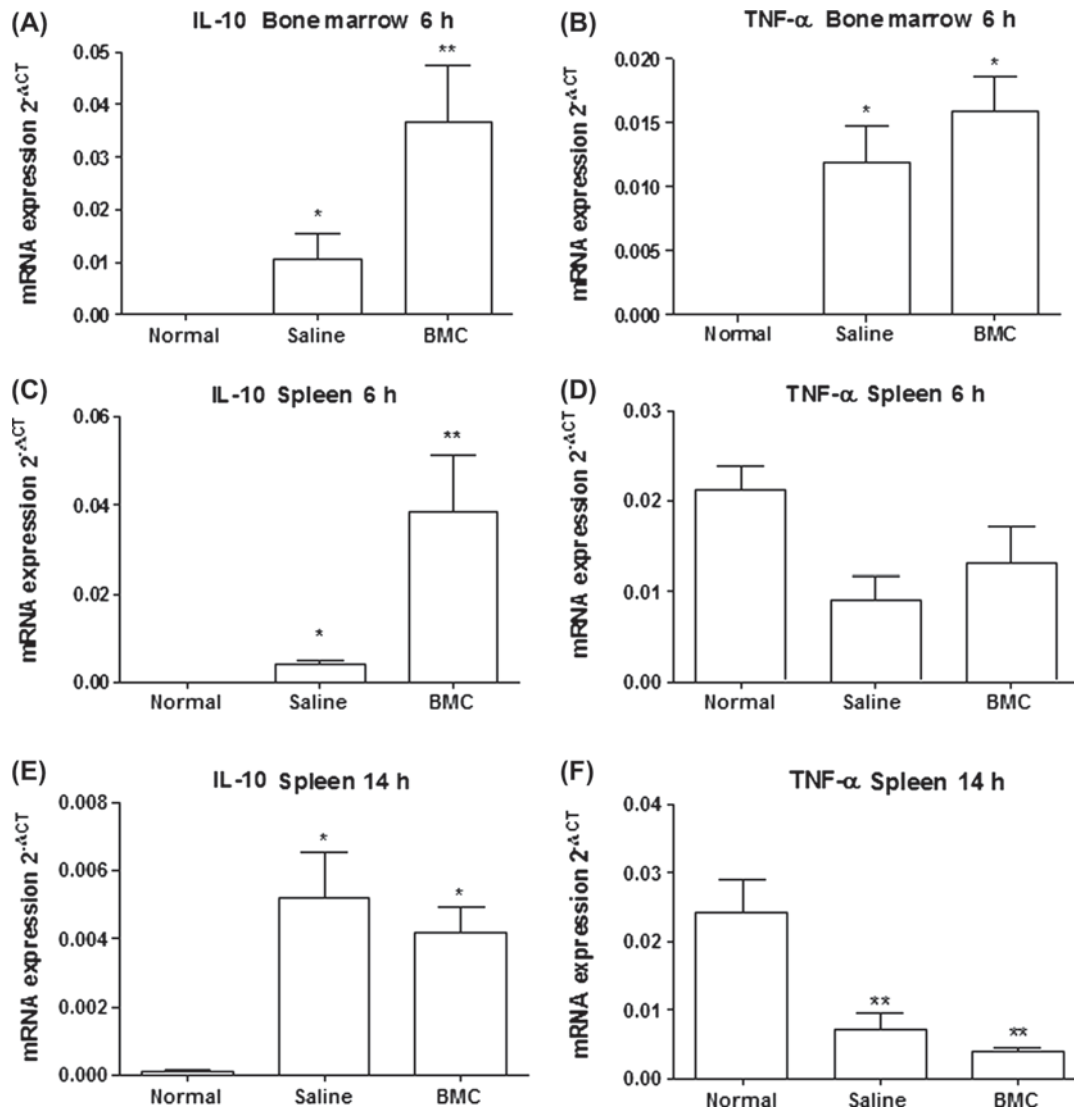
Acknowledgments

Figure 8. Measurement of cytokine gene expression in the bone marrow and spleen. (A, B) Analysis of IL-10 (A) and TNF-α (B) mRNA expression in the bone marrow 6 h after APAP injection. (C–F) Analysis of IL-10 (C, E) and TNF-α (D, F) mRNA expression in the spleen 6 (C, D) and 14 (D, F) h after APAP injection. Data represent the means ± SEM of 6–7 mice/group. $*P < 0.05$; $**P < 0.001$.

BA, for transaminase evaluation; and the Laboratory of Clinical Analysis of the Hospital São Rafael, Salvador, BA, for assessment of serum ammonia.

Conflict of interest statement: The authors claim they have no conflict of interest in this study.

References

1. Larson AM, Polson J, Fontana RJ, Davern TJ, Lalani E, Hynan LS, et al. Acetaminophen-induced acute liver failure: results of a United States multicenter, prospective study. Hepatology. 2005;42:1364–72.

2. Slattery JT, Nelson SD, Thummel KE. The complex interaction between ethanol and acetaminophen. Clin Pharmacol Ther. 1996;60:241–6.

3. Whitcomb DC, Block GD. Association of acetaminophen hepatotoxicity with fasting and ethanol use. J AM MED ASSOC. 1994;272:1845–50.

4. Potter WZ, Davis DC, Mitchell JR, Jollow DJ, Gillette JR, Brodie BB. Acetaminophen-induced hepatic necrosis. III. Cytochrome P-450-mediated covalent binding in vitro. J Pharmacol Exp Ther. 1973;187:203–10.

5. Masubuchi Y, Suda C, Horie T. Involvement of mitochondrial permeability transition in acetaminophen-induced liver injury in mice. J Hepatol. 2005;42:110–16.

6. Kosenko E, Kaminsky Y, Lopata O, Muravyov N, Kaminsky A, Hermenegildo C, et al. Nitroarginine, an inhibitor of nitric oxide synthase, prevents changes in superoxide radical and antioxidant enzymes induced by ammonia intoxication. Metab Brain Dis. 1998;13:29–41.

7. Chung C, Gottstein J, Blei AT. Indomethacin prevents the development of experimental ammonia-induced brain edema in rats after portacaval anastomosis. Hepatology. 2001;34:249–54.

8. Odeh M. Pathogenesis of hepatic encephalopathy: the tumour necrosis factor-alpha theory. Eur J Clin Invest. 2007;37:291–304.

9. Bernal W, Wendon J. Liver transplantation in adults with acute liver failure. J Hepatol. 2004;40:192–7.

10. Jalan R. Acute liver failure: current management and future prospects. J Hepatol. 2005;42(Suppl):S115–23.

11. Simpson K, Hogaboam CM, Kunkel SL, Harrison DJ, Bone-Larson C, Lukacs NW. Stem cell factor attenuates liver damage in a murine model of acetaminophen-induced hepatic injury. Lab Invest. 2003;83:199–206.

12. van Poll D, Parekkadan B, Cho CH, Berthiaume F, Nahmias Y, Tilles AW, et al. Mesenchymal stem cell-derived molecules directly modulate hepatocellular death and regeneration in vitro and in vivo. Hepatology. 2008;47:1634–43.

13. Abraham CS, Deli MA, Joo F, Megyeri P, Torpier G. Intracarotid tumor necrosis factor-alpha administration increases the blood–brain barrier permeability in cerebral cortex of the newborn pig: quantitative aspects of double-labelling studies and confocal laser scanning analysis. Neurosci Lett. 1996; 208:85–8.

14. Van Lint P, Wielockx B, Puimège L, Noël A, López-Otin C, Libert C. Resistance of collagenase-2 (matrix metalloproteinase-8)-deficient mice to TNF-induced lethal hepatitis. J Immunol. 2005;175:7642–9.

15. Wielockx B, Lannoy K, Shapiro SD, Itoh T, Itohara S, Vandekerckhove J, Libert C. Inhibition of matrix metalloproteinases blocks lethal hepatitis and apoptosis induced by tumor necrosis factor and allows safe antitumor therapy. Nat Med. 2001;7:1202–8.

16. Nguyen JH, Yamamoto S, Steers J, Sevlever D, Lin W, Shimojima N, et al. Matrix metalloproteinase-9 contributes to brain extravasation and edema in fulminant hepatic failure mice. J Hepatol. 2006;44:1105–14.

17. Kis B, Chen L, Ueta Y, Busija DW. Autocrine peptide mediators of cerebral endothelial cells and their role in the regulation of blood–brain barrier. Peptides. 2006;27: 211–22.

18. Belardinelli MC, Pereira F, Baldo G, Vicente Tavares AM, Kieling CO, da Silveira TR, et al. Adult derived mononuclear bone marrow cells improve survival in a model of acetaminopheninduced acute liver failure in rats. Toxicology. 2008;247:1–5.

19. Soares MB, Lima RS, Souza BS, Vasconcelos JF, Rocha LL, Dos Santos RR, et al. Reversion of gene expression alterations in hearts of mice with chronic chagasic cardiomyopathy after transplantation of bone marrow cells. Cell Cycle. 2011;10: 1448–55.

20. Costa-Ferro ZS, Souza BS, Leal MM, Kaneto CM, Azevedo CM, da Silva IC, et al. Transplantation of bone marrow mononuclear cells decreases seizure incidence, mitigates neuronal loss and modulates pro-inflammatory cytokine production in epileptic rats. Neurobiol Dis. 2012;46:302–13.

21. de Oliveira SA, de Freitas Souza BS, Barreto EP, Kaneto CM, Neto HA, Azevedo CM, et al. Reduction of galectin-3 expression and liver fibrosis after cell therapy in a mouse model of cirrhosis. Cytotherapy. 2012;14:339–49.

22. Streetz K, Leifeld L, Grundmann D, Ramakers J, Eckert K, Spengler U, et al. Tumor necrosis factor alpha in the pathogenesis of human and murine fulminant hepatic failure. Gastroenterology. 2000;119:446–60.

23. Nagaki M, Iwai H, Naiki T, Ohnishi H, Muto Y, Moriwaki H. High levels of serum interleukin-10 and tumor necrosis factor-alpha are associated with fatality in fulminant hepatitis. J Infect Dis. 2000;182:1103–8.

24. Idriss HT, Naismith JH. TNF alpha and the TNF receptor superfamily: structure-function relationship(s). Microsc Res Tech. 2000;50:184–95.

25. Odeh M. Pathogenesis of hepatic encephalopathy: the tumour necrosis factor-alpha theory. Eur J Clin Invest. 2007;37: 291–304.

26. Wang W, Lv S, Zhou Y, Fu J, Li C, Liu P. Tumor necrosis factor-α affects blood–brain barrier permeability in acetaminophen-induced acute liver failure. Eur J Gastroenterol Hepatol. 2011;23:552–8.

27. Bemeur C, Qu H, Desjardins P, Butterworth RF. IL-1 or TNF receptor gene deletion delays onset of encephalopathy and attenuates brain edema in experimental acute liver failure. Neurochem Int. 2010;56:213–15.

28. Aizawa S, Tavassoli T. Molecular basis of the recognition of intravenously transplanted hemopoietic cells by bone marrow. Proc Natl Acad Sci USA 1988;85:3180–3183.

29. Burchfield JS, Iwasaki M, Koyanagi M, Urbich C, Rosenthal N, Zeiher AM, Dimmeler S. Interleukin-10 from transplanted bone marrow mononuclear cells contributes to cardiac protection after myocardial infarction. Circ Res. 2008; 103:203–11.

5 DISCUSSÃO

O presente estudo avaliou os efeitos do transplante de células mononucleares da medula óssea no modelo experimental de insuficiência hepática aguda induzida por APAP e potencializada por etanol. O pré-tratamento com etanol é comprovadamente capaz de aumentar o tamanho do retículo endoplasmático liso nos hepatócitos e elevar a expressão das enzimas hepáticas microssomais, como a CYP2E1, sendo esta isoforma particularmente importante para o metabolismo oxidativo do APAP (RUBIN *et al.*, 1968). Consequentemente, o pré-tratamento com etanol aumenta a toxicidade hepática induzida por APAP, levando a uma redução significativa da DL50 (PRESCOTT *et al.*, 2000). Em um estudo prévio, na ausência de pré-tratamento com etanol, foi determinada como DL_{50} em camundongos a dose de 1000 mg/kg (KOFMAN *et al.*, 2005). No entanto, no presente estudo, o pré-tratamento com etanol permitiu que a dose de APAP a 300 mg/kg de APAP levasse à mortalidade de 70% a 80% dos animais, de modo homogêneo e reproduzível nos experimentos realizados. Esta taxa de mortalidade é compatível com a mortalidade associada à IHA em pacientes não submetidos ao transplante hepático (RIORDAN *et al.*, 2008). Assim como o observado em pacientes com IHA, a mortalidade dos animais nos modelos experimentais de IHA tem sido associada a causas extra-hepáticas, que incluem insuficiência renal aguda, disfunção múltipla de órgãos e edema cerebral (RAHMAN *et al.*, 2000; NEWSOME *et al.*, 2000).

Observou-se, ainda, que a mortalidade dos animais, de modo reproduzível, começa a ser observada em torno de 12 horas após a injeção de APAP e ocorria principalmente dentro das primeiras 24 horas. Este dado trouxe a perspectiva de avaliação dos efeitos da terapia celular dentro de uma janela temporal definida. Foi observado que o impacto da terapia sobre a mortalidade estava associado à precocidade com que a terapia era estabelecida. Na realidade, neste trabalho identificou-se uma janela terapêutica de seis horas, após a injeção de APAP, para que fosse observado algum efeito da administração de CMMO sobre a mortalidade dos animais. Quando o tratamento foi realizado dentro das primeiras três horas, observou-se uma redução significativa da mortalidade: após cinco dias de acompanhamento, a taxa de sobrevivência foi de 60% no grupo tratado com células da medula óssea, enquanto que uma sobrevivência de apenas 20% foi observada no grupo controle injetado com salina.

O momento em que o tratamento é administrado na IHA parece ser crítico para determinar o seu sucesso não apenas em nosso estudo de terapia celular. Já foi previamente observado que outras intervenções terapêuticas na IHA tendem a ser mais eficazes quanto mais cedo são iniciadas. Isto é observado, por exemplo, com a N-acetilcisteína, cujos efeitos

benéficos também são reduzidos em estágios avançados de IHA (KEAYS *et al.*, 1991; LEE *et al.*, 2009). Em outros modelos experimentais, como é o caso do acidente vascular encefálico, também foi identificada uma janela terapêutica para que o tratamento com células mononucleares da medula óssea fosse eficaz (DE VASCONCELOS DOS SANTOS *et al.*, 2010).

A escolha da via endovenosa para o transplante de células mononucleares da medula óssea foi baseada em estudos prévios, na qual foi possível detectar a migração das células transplantadas para o fígado em modelos experimentais de cirrose hepática e infecção crônica por *Schistosoma mansoni* (OLIVEIRA *et al.*, 2008; OLIVEIRA *et al.*, 2011). Além disso, a via endovenosa é segura para o transplante de células mononucleares da medula óssea, diferentemente do que é observado para as células-tronco mesenquimais, que costumam levar ao quadro de embolia pulmonar devido ao seu tamanho aumentado em relação aos capilares pulmonares (FURLANI *et al.*, 2009). É bem conhecida a capacidade das células da medula óssea, mesmo quando injetadas sistemicamente, de migrar para sítios de lesão seguindo gradientes quimiotáticos, principalmente com papel do eixo SDF-1/CXCR4, mas também de outras moléculas quimiotáticas, dentre elas a MMP9, que se encontram aumentadas em modelos experimentais de IHA (CUI *et al.*, 2007; NGUYEN *et al.*, 2006, LEI *et al.*, 2010).

Apesar da presença das células transplantadas no fígado durante todo o período avaliado, não encontramos nenhuma evidência da ocorrência de transdiferenciação ou fusão celular. Este resultado demonstrou que a regeneração hepática observada após cinco dias da injeção de APAP foi baseada nas células do receptor, não tendo sido observada a presença de hepatócitos expressando GFP nos animais transplantados com CMMO. Outros estudos conseguiram demonstrar um grande repovoamento hepático após o transplante de células da medula óssea. Isto foi particularmente evidenciado em camundongos deficientes para a enzima fumarilacetoacetato hidrolase (Fah$^{-/-}$), um modelo experimental de tirosinemia do tipo I, quando há grande vantagem seletiva à proliferação dos hepatócitos derivados do doador selvagem sobre os hepatócitos do receptor mutante (JANG *et al.*, 2004; VASSILOPOULOS *et al.*, 2003). Entretanto, em outros modelos experimentais de lesão hepática aguda e crônica, a freqüência relatada de hepatócitos derivados da medula óssea tem sido em geral baixa (OLIVEIRA *et al.*, 2008; OLIVEIRA *et al.*, 2011; THORGEIRSSON *et al.*, 2006; DAHLKE *et al.*, 2003).

No presente estudo, o efeito da terapia celular sobre a mortalidade não foi associado à regeneração hepática aumentada, ou mesmo a um efeito hepatoprotetor. Não foram observadas reduções nos níveis séricos de transaminases ou amônia, bem como não houve

diferença entre a área de necrose presente nos animais do grupo tratado com células mononucleares da medula óssea e controles injetados com salina. Este resultado está em desacordo com o observado em um estudo prévio realizado em modelo experimental de IHA induzida por APAP em ratos, no qual foram relatados efeitos benéficos do transplante celular sobre a lesão hepática e os níveis séricos de transaminases (BELARDINELLI *et al.*, 2008). Tendo em vista que o transplante foi realizado neste estudo de Belardinelli e colaboradores somente após 24 horas da injeção de APAP, quando no nosso modelo, já ocorreu grande parte da mortalidade, é possível que diferenças relacionadas ao modelo experimental, como dose ou grau de susceptibilidade à lesão hepática dos animais, cause uma lesão hepática mais branda e de progressão mais lenta, permitindo a observação de um efeito benéfico das células sobre a lesão hepática. Além disso, esses autores realizaram a infusão de células mononucleares da medula óssea diretamente na veia porta, o que teoricamente poderia levar a uma maior distribuição de células no fígado, justificando o potencial efeito hepatoprotetor descrito. Entretanto, não é possível confirmar esta hipótese, uma vez que faltam dados neste estudo quanto à migração das células infundidas para o fígado.

Em um estudo recente, foi avaliada a necessidade de migração celular preferencialmente para o fígado para que seja observado efeito hepatoprotetor das células de medula óssea. Foi realizado o transplante de células mononucleares da medula óssea, por via endovenosa sistêmica, em modelo experimental de lesão hepática aguda induzida por tetracloreto de carbono e acetaminofluoreno em camundongos. Observou-se que, quando o transplante foi associado à injeção intraperitoneal de SDF-1, ocorria uma migração mais intensa das células transplantadas para o fígado, levando a um menor dano hepático e à regeneração acelerada neste grupo experimental (JIN *et al.*, 2009). O mesmo grupo demonstrou, posteriormente, que o efeito terapêutico das células mononucleares da medula óssea sobre a lesão e a regeneração hepática é aumentado quando as células são induzidas a superexpressar o HGF (JIN *et al.*, 2011).

É importante salientar que as células mononucleares da medula óssea compõem um grupo heterogêneo de células, não sendo tão simples determinar que populações são de interesse terapêutico na IHA. É possível ainda que diferentes populações celulares possam desempenhar papéis importantes. O transplante, por via endovenosa sistêmica, de células-tronco mesenquimais da medula óssea em modelo experimental de lesão hepática aguda induzida por tetracloreto de carbono em ratos promoveu reduções nos níveis séricos de transaminases e no dano hepático (JIN *et al.*, 2012). Por se tratar de um tipo celular diferente, também é possível que este efeito hepatoprotetor esteja associado às células-tronco

mesenquimais, que perfazem não mais do que 0,01% do total de células mononucleares da medula óssea (PITTENGER *et al.*, 1999). No entanto, os resultados benéficos observados após o tratamento com GCSF de animais com IHA induzida por D-galactosamina apontam para um importante papel terapêutico de outras populações celulares, como células CD34$^+$, que são mobilizadas para a periferia após o tratamento com este fator de crescimento, e foram capazes de estimular a regeneração hepática neste modelo (ZHANG *et al.*, 2011). De um modo geral, é possível afirmar que a ausência de efeito hepatoprotetor observada no presente estudo não está de acordo com estudos prévios da literatura utilizando diferentes estratégias em terapia celular (SOUZA *et al.*, 2009).

Tendo em vista o efeito observado sobre a sobrevivência dos animais, foi necessário o desenvolvimento e teste de novas hipóteses para explicar os mecanismos de ação das células mononucleares da medula óssea neste modelo experimental. Buscou-se investigar um potencial efeito da terapia celular sobre a resposta inflamatória local e sistêmica, baseando-se em observações de estudos prévios desenvolvidos pelo nosso grupo, envolvendo a terapia com células mononucleares da medula óssea em outros modelos experimentais. Um estudo, utilizando modelo experimental de cirrose hepática em camundongos, demonstrou que a redução da fibrose hepática observada após o transplante de células mononucleares da medula óssea estava associada à redução de células inflamatórias no fígado, bem como a uma redução do número de macrófagos ativados positivos para galectina-3, uma molécula associada à inflamação e fibrose (OLIVEIRA *et al.*, 2011, ANEXO I). Além disso, o transplante de células mononucleares da medula óssea modula a miocardite, levando à redução de fibrose no coração em modelo experimental miocardiopatia chagásica crônica (SOARES *et al.*, 2011, ANEXO II). Neste modelo observou-se, através da análise de microarranjo de DNA, que após a terapia celular ocorre uma mudança global da expressão gênica no coração. De um total de 1702 genes com expressão alterada pela doença, a maioria relacionada à inflamação, resposta imune e apoptose, 96% retornou aos níveis observados em animais normais, correlacionando-se com a redução de fibrose, miocardite e níveis de citocinas pró-inflamatórias observada neste modelo. Além disso, em um modelo experimental de epilepsia induzida por lítio e pilocarpina, o transplante de células mononucleares da medula óssea, realizado na fase crônica e mesmo em estágio avançado da doença, foi associado a diversos efeitos benéficos, como reduções na freqüência de crises convulsivas espontâneas e recorrentes, morte neuronal no hipocampo e gliose. Estes efeitos estavam associados à redução da expressão de citocinas pró-inflamatórias e ao aumento de citocinas anti-inflamatórias no cérebro e na periferia (COSTA-FERRO *et al.*, 2011, ANEXO III). Estas evidências provenientes de diferentes

modelos dão suporte à hipótese de que efeitos imunomodulatórios e anti-inflamatórios são responsáveis pelos efeitos benéficos observados em diferentes modelos experimentais.

O papel benéfico da modulação da inflamação hepática sobre a evolução da IHA foi demonstrado em estudo realizado por Parekkadan e colaboradores, no qual foi observado que a infusão, por via endovenosa, de moléculas derivadas de culturas de células-tronco mesenquimais da medula óssea em ratos com IHA induzida por d-galactosamina foi associada a um menor dano hepático e acelerada regeneração do fígado (PAREKKADAN *et al.*, 2007). Este resultado foi atribuído a um menor influxo de leucócitos para o fígado, uma vez que grande parte das moléculas infundidas nos animais tinha ação quimiotática, alterando agudamente o gradiente quimiotático em favor da permanência dos leucócitos no compartimento intravascular. No entanto, os autores não observaram benefício quanto à modulação de inflamação hepática quando as células-tronco mesenquimais foram transplantadas, sendo a eficácia da terapia supostamente restrita exclusivamente à infusão de moléculas derivadas de células-tronco. No presente estudo, a avaliação da resposta inflamatória local no fígado foi baseada na quantificação de leucócitos infiltrantes e na determinação dos níveis hepáticos das citocinas TNF-α e IL-10. Todas as análises foram feitas em animais submetidos à eutanásia 14 horas após a injeção de APAP, momento no qual supostamente os efeitos da terapia deveriam ser detectáveis, uma vez que se trata do início do intervalo de tempo no qual ocorre significativa mortalidade. Não foi possível detectar diferenças na atividade inflamatória no fígado entre os grupos experimentais, sugerindo que a modulação da resposta inflamatória local não era um mecanismo importante neste modelo. É possível se fazer uma analogia ao resultado observado por Parekkadan e colaboradores quanto ao transplante de células-tronco mesenquimais, mesmo considerando que foi utilizado outro tipo de células. No entanto, trata-se de um dado contrastante quanto comparado às observações realizadas após o transplante de células mononucleares da medula óssea em outros modelos, provavelmente por se tratar de um modelo de lesão aguda, em oposição aos estudos previamente realizados em modelos experimentais de doenças crônicas, no qual os efeitos da terapia foram avaliados algumas semanas depois de sua realização.

A investigação da resposta inflamatória sistêmica revelou a presença de modulação dos níveis séricos de TNF-α 14 horas após a injeção de APAP. O TNF-α é uma citocina pró-inflamatória que desempenha um importante papel na síndrome da resposta inflamatória sistêmica e na disfunção múltipla de órgãos, independentemente da etiologia (STRIETER *et al.*, 1993). Esta citocina está associada a uma grande parte dos efeitos sistêmicos observados na IHA, como o edema cerebral e a síndrome da resposta inflamatória sistêmica. Observou-se

previamente que, em pacientes com IHA, os níveis séricos de TNF-α são significativamente maiores em pacientes que vão a óbito quando comparados àqueles que sobrevivem (NAGAKI *et al.*, 2000; STREETZ *et al.*, 2000). É bem estabelecido o envolvimento do TNF-α no aumento da permeabilidade da barreira hemato-encefálica em diversas doenças neurológicas, incluindo acidente vascular encefálico, trauma, malária cerebral e esclerose múltipla (MAYHAN *et al.*, 2002; SHARIEF *et al.*, 1992). Já foi demonstrado que os níveis séricos de TNF-α se correlacionam diretamente com o aumento da permeabilidade vascular cerebral ao corante azul de Evans em modelo experimental de IHA induzida por APAP em camundongos, estando associados ao componente vasogênico do edema cerebral na IHA (WANG *et al.*, 2011). Também foi demonstrado, em estudos *in vitro*, que o TNF-α ativa a via do NFκB em células endoteliais cerebrais, levando a uma redução da expressão gênica da claudina-5, um importante componente das junções de oclusão no endotélio vascular cerebral (ASLAM *et al.*, 2012). Elevados níveis séricos de mediadores inflamatórios, dentre eles o TNF-α, também podem atuar indiretamente através da estimulação à secreção aumentada de peptídeos que aumentam a permeabilidade da barreira hemato-encefálica, como é o caso da substância P (KIS *et al.*, 2006).

Tendo em vista que a modulação do TNF-α não ocorreu no fígado, foi realizada a quantificação de citocinas em outros órgãos onde pode estar ocorrendo a atividade imunomodulatória das células mononucleares da medula óssea. Verificou-se que, após 14 horas da injeção de APAP, a expressão gênica no baço demonstrava aumento de IL-10 e redução de TNF-α em ambos os grupos, em relação ao normal. Este resultado pode indicar que, apesar da manutenção de níveis sistêmicos elevados da citocina TNF-α, a expressão gênica já estava direcionada a um controle anti-inflamatório, conhecido como fase de resolução. A primeira linha de defesa contra o dano é rápida e composta da ativação de células da resposta imune inata. Observa-se, em modelo experimental de sepse, um pico de expressão gênica do mRNA de TNF-*a* entre duas e quatro horas após o desafio com LPS, enquanto que o nível da citocina apresenta um pico horas depois (DEFORGE *et al.*, 1991). Foi previamente descrito que a expressão aumentada de genes pró-inflamatórios como TNF−α, IL-6 e IL-1β, em células de Kupffer, os macrófagos residentes do fígado, pode ser detectada uma hora pós a injeção de APAP em camundongos (MARTIN-MURPHY *et al.*, 2010). Após o início da resposta inflamatória, de um modo geral, o sistema tenta retornar à homeostase pela indução de expressão gênica reguladores negativos, como as citocinas anti-inflamatórias (ALAM *et al.*, 2011). Como a ativação de células do sistema imune fora do

fígado supostamente ocorre em períodos curtos após a injeção de APAP, é provável que a expressão gênica observada no baço 14 horas após a injeção de APAP reflete a fase de resolução da atividade inflamatória, apesar de ainda ser possível detectar elevados níveis de TNF-*a* no grupo controle injetado com salina, sugerindo que a modulação da resposta inflamatória observada no grupo tratado com células mononucleares da medula óssea poderia ter ocorrido em um ponto mais precoce.

A avaliação dos níveis de expressão gênica da IL-10 em ponto mais precoce, seis horas após a injeção de APAP ou três horas após a terapia celular, revelou o aumento da expressão gênica desta citocina no baço e na medula óssea dos animais tratados com células mononucleares da medula óssea quando comparados aos animais controles injetados com salina. A IL-10 é uma das citocinas com maior ação anti-inflamatória, sendo capaz de inibir a síntese de citocinas pró-inflamatórias, tais como IFN-γ, IL-2, TNF-α e GM-CSF (OUYANG *et al.*, 2011). A IL-10, além de reduzir a expressão gênica do TNF-α, é também capaz de realizar a inibição pós-transcricional da expressão de TNF-α (RAJASINGH *et al.*, 2006; KONTOYIANNIS *et al.*, 2001). As principais fontes de secreção de IL-10 são os monócitos, linfócitos Th2, mastócitos, células T regulatórias ($CD4^+CD25^+FoxP3^+$) e células-tronco mesenquimais (FUJIO *et al.*, 2010; SABAT *et al.*, 2010). Já foi previamente descrito que as células-tronco mesenquimais são capazes de antagonizar os efeitos do TNF-α através da expressão, em condições inflamatórias, de citocinas anti-inflamatórias, tais como a IL-10, promovendo o aumento da sobrevivência em modelo experimental de sepse (MEI *et al.*, 2010).

Os efeitos exercidos pela IL-10 podem representar o mecanismo que leva à modulação do TNF-α observada no presente estudo, mas outros mecanismos não podem ser excluídos. Existem outros mecanismos relacionados que podem contribuir para a redução na expressão de TNF-α após a terapia celular, como a secreção de outras moléculas com atividade imunomodulatória, como a prostaglandina E_2 (GHANNAM *et al.*, 2010) e IL-6 (SCHINDLER *et al.*, 1990). Um estudo prévio demonstrou ainda que células-tronco mesenquimais secretam a forma solúvel do receptor I do TNF (sTNFRI), levando à neutralização da citocina *in vivo,* com subseqüente atenuação da resposta inflamatória sistêmica no modelo experimental de choque séptico (YAGI *et al.*, 2010).

Dentre as possíveis conseqüências da redução dos níveis séricos de TNF-α, foi observada uma redução da permeabilidade da barreira hemato-encefálica 18 horas após a injeção de APAP no grupo tratado com células mononucleares da medula óssea. Um estudo

recente demonstrou que o transplante de células-tronco mesenquimais por via endovenosa é capaz de modular a permeabilidade da barreira hemato-encefálica, reduzindo o edema cerebral e aumentando a sobrevivência em um modelo experimental de trauma crânio-encefálico (WALKER *et al.*, 2010). De modo similar ao que foi observado no presente estudo, Walker e colaboradores demonstraram que interações celulares ocorrem entre as células-tronco mesenquimais e as células do baço, promovendo o aumento de células T CD4^{+} com perfil regulatório e secreção aumentada de IL-10 e IL-4 capazes de induzir proteção à distância contra o dano à integridade da barreira hemato-encefálica.

Além da interação com outras células, como as do baço e da própria medula óssea, é possível que as células transplantadas, sobretudo em condições de stress causadas pela lesão hepática, liberem fatores que promovem a modulação da produção de TNF-α. Isso foi visto em modelo de infarto agudo do miocárdio, no qual foi realizado o transplante xenogênico de células da medula óssea humanas (BURCHFIELD *et al.*, 2008). Por ser um transplante xenogênico, esse modelo permite que as células transplantadas produzem grande quantidade de IL-10 *in vitro* e quando injetadas no miocárdio.

Outros mecanismos supostamente envolvidos na quebra da barreira hemato-encefálica na IHA, como um desbalanço entre a expressão de TIMP-1 e MMP9, levando a uma maior atividade da MMP9 com subseqüente degradação das proteínas das junções de oclusão, como claudina-5 e ocludina, foram relatados em estudos prévios (NGUYEN *et al.*, 2006; YAMAMOTO *et al.*, 2006). No presente estudo foi verificada a presença de atividade aumentada da MMP9 no soro dos animais injetados com APAP quando comparados aos animais do grupo normal, porém não se observou diferença entre o grupo tratado com células mononucleares da medula óssea e o grupo injetado com salina. Este resultado indica que, apesar de um aumento na atividade sistêmica da MMP9 poder estar envolvido na patogênese do edema cerebral na IHA, este parâmetro não foi alterado pela terapia celular, não sendo este um mecanismo de ação relevante exercido pelas células da medula óssea neste modelo experimental.\

Observamos também que os níveis de expressão gênica de adrenomedulina e endotelina-1, dois peptídeos com papel conhecido sobre a regulação da permeabilidade da barreira hemato-encefálica, estão elevados em ambos os grupos experimentais, quando comparados aos animais normais. Condições extremas, como hipóxia podem levar ao aumento da expressão de adrenomedulina (KIS *et al.*, 2006). A indução do aumento da expressão de adrenomedulina foi previamente apontada como um importante mecanismo de ação envolvido na terapia celular com células-tronco mesenquimais em modelo experimental

de insuficiência cardíaca e com células mononucleares da medula óssea em pacientes com isquemia de membros (LI *et al.*, 2009; TACHI *et al.*, 2008). No presente estudo, no entanto, a terapia celular não foi capaz de alterar a expressão dos genes codificadores destas moléculas.

Um resumo dos principais resultados observados em nosso estudo, que podem explicar os efeitos do transplante de células mononucleares da medula óssea no modelo de IHA, está representado na figura 5. Por fim, outros estudos devem ser realizados para que haja uma melhor compreensão dos mecanismos de atuação das células de medula óssea nesse modelo. Muito embora a janela terapêutica do tratamento investigado seja pequena, o entendimento dos mecanismos de patogênese da IHA e dos efeitos protetores do tratamento com células mononucleares da medula óssea poderão servir de base para o desenho de novas estratégias de intervenção em momentos mais avançados da doença.
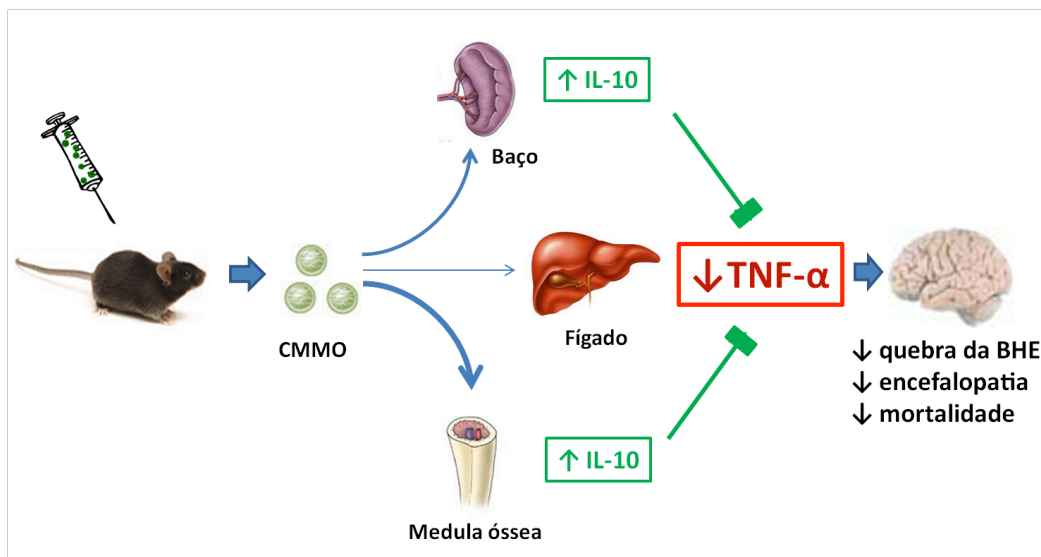

Figura 6. Efeitos observados da terapia com células mononucleares da medula óssea em camundongos com IHA induzida por APAP.

6 CONCLUSÕES / SUMÁRIO DE RESULTADOS

O presente estudo demonstra que:

- A administração de células mononucleares da medula óssea em camundongos com IHA induzida por APAP causa uma redução na taxa de mortalidade;

- A proteção induzida pelas células mononucleares da medula óssea não está correlacionada à proteção contra o dano hepático causado pelo APAP;

- A administração de células mononucleares da medula óssea modula a produção de citocinas, diminuindo a concentração sérica da citocina pró-inflamatória TNF-α e aumentando a expressão do mRNA da citocina anti-inflamatória IL-10 no baço e na medula óssea;

- Camundongos tratados com células mononucleares da medula óssea apresentaram menor permeabilidade da BHE do que os controles injetados com salina, indicando uma proteção induzida pelas células mononucleares da medula óssea na quebra da barreira hemato-encefálica.

7 REFERÊNCIAS

ALAM, M. M.; O'NEILL, L. A. MicroRNAs and the resolution phase of inflammation in macrophages. **Eur. J. Immunol.,** v. 41, n. 9, p. 2482-5, Sep 2011.

ALBRECHT, J.; NORENBERG, M. D. Glutamine: a Trojan horse in ammonia neurotoxicity. **Hepatology,** v. 44, n. 4, p. 788-94, Oct 2006.

ASLAM, M. et al. TNF-alpha induced NFκB signaling and p65 (RelA) overexpression repress Cldn5 promoter in mouse brain endothelial cells. **Cytokine,** v. 57, n. 2, p. 269-75, Feb 2012.

BACCARANI, U. et al. Human hepatocyte transplantation for acute liver failure: state of the art and analysis of cell sources. **Transplant. Proc.,** v. 37, n. 6, p. 2702-4, 2005 Jul-Aug 2005.

BAINE, A. M. et al. Fulminant liver failure models with subsequent encephalopathy in the mouse. **Hepatobiliary Pancreat. Dis. Int.,** v. 10, n. 6, p. 611-9, Dec 2011.

BAUMGARTNER, D. et al. Effects of intrasplenic injection of hepatocytes, hepatocyte fragments and hepatocyte culture supernatants on D-galactosamine-induced liver failure in rats. **Eur. Surg. Res.,** v. 15, n. 3, p. 129-35, 1983.

BELARDINELLI, M. C. et al. Adult derived mononuclear bone marrow cells improve survival in a model of acetaminophen-induced acute liver failure in rats. **Toxicology,** v. 247, n. 1, p. 1-5, May 2008.

BERNAL, W. et al. Acute liver failure. **Lancet,** v. 376, n. 9736, p. 190-201, Jul 2010.

BJERRING, P. N. et al. The brain in acute liver failure. A tortuous path from hyperammonemia to cerebral edema. **Metab. Brain. Dis.,** v. 24, n. 1, p. 5-14, Mar 2009.

BONKOVSKY, H. L. et al. Acute hepatic and renal toxicity from low doses of acetaminophen in the absence of alcohol abuse or malnutrition: evidence for increased susceptibility to drug toxicity due to cardiopulmonary and renal insufficiency. **Hepatology,** v. 19, n. 5, p. 1141-8, May 1994.

BOURDI, M. et al. Protection against acetaminophen-induced liver injury and lethality by interleukin 10: role of inducible nitric oxide synthase. **Hepatology,** v. 35, n. 2, p. 289-98, Feb 2002.

BRADBURY, M. W. The blood-brain barrier. **Exp. Physiol.,** v. 78, n. 4, p. 453-72, Jul 1993.

BURCHFIELD, J. S. et al. Interleukin-10 from transplanted bone marrow mononuclear cells contributes to cardiac protection after myocardial infarction. **Circ. Res.,** v. 103, n. 2, p. 203-11, Jul 2008.

CARPENTIER, B.; GAUTIER, A.; LEGALLAIS, C. Artificial and bioartificial liver devices: present and future. **Gut,** v. 58, n. 12, p. 1690-702, Dec 2009.

CHEN, F. et al. Disruptions of occludin and claudin-5 in brain endothelial cells in vitro and in brains of mice with acute liver failure. **Hepatology,** v. 50, n. 6, p. 1914-23, Dec 2009.

CHIANG, C. H. et al. Investigation of hepatoprotective activity of induced pluripotent stem cells in the mouse model of liver injury. **J. Biomed. Biotechnol.,** v. 2011, p. 219060, 2011.

COSTA-FERRO, Z. S. et al. Transplantation of bone marrow mononuclear cells decreases seizure incidence, mitigates neuronal loss and modulates pro-inflammatory cytokine production in epileptic rats. **Neurobiol. Dis.,** Dec 2011a.

CUI, X. et al. Nitric oxide donor upregulation of stromal cell-derived factor-1/chemokine (CXC motif) receptor 4 enhances bone marrow stromal cell migration into ischemic brain after stroke. **Stem Cells,** v. 25, n. 11, p. 2777-85, Nov 2007.

DAHLKE, M. H. et al. Liver regeneration in a retrorsine/CCl4-induced acute liver failure model: do bone marrow-derived cells contribute? **J. Hepatol.,** v. 39, n. 3, p. 365-73, Sep 2003.

DAN, Y. Y.; YEOH, G. C. Liver stem cells: a scientific and clinical perspective. **J. Gastroenterol. Hepatol.,** v. 23, n. 5, p. 687-98, May 2008.

DE VASCONCELOS DOS SANTOS, A. et al. Therapeutic window for treatment of cortical ischemia with bone marrow-derived cells in rats. **Brain Res.,** v. 1306, p. 149-58, Jan 2010.

DEFORGE, L. E.; REMICK, D. G. Kinetics of TNF, IL-6, and IL-8 gene expression in LPS-stimulated human whole blood. **Biochem. Biophys. Res. Commun.,** v. 174, n. 1, p. 18-24, Jan 1991.

DUFFY, T. J.; VERGEER, P. P. Amanita poisoning: treatment and role of liver transplantation. **Am. J. Med.,** v. 87, n. 2, p. 244, Aug 1989.

FUJIO, K.; OKAMURA, T.; YAMAMOTO, K. The Family of IL-10-secreting CD4+ T cells. **Adv. Immunol.,** v. 105, p. 99-130, 2010.

FURLANI, D. et al. Is the intravascular administration of mesenchymal stem cells safe? Mesenchymal stem cells and intravital microscopy. **Microvasc. Res.,** v. 77, n. 3, p. 370-6, May 2009.

GAILLARD, P. J.; DE BOER, A. G. A novel opportunity for targeted drug delivery to the brain. **J. Control. Release,** v. 116, n. 2, p. e60-2, Nov 2006.

GHANNAM, S. et al. Immunosuppression by mesenchymal stem cells: mechanisms and clinical applications. **Stem Cell Res. Ther.,** v. 1, n. 1, p. 2, 2010.

GILL, R. Q.; STERLING, R. K. Acute liver failure. **J. Clin. Gastroenterol.,** v. 33, n. 3, p. 191-8, Sep 2001.

GORINI, P.; FOGLI, L.; MORSIANI, E. [Acute and fulminant liver failure: experimental models]. **Ann. Ital. Chir.,** v. 71, n. 3, p. 293-300, 2000 May-Jun 2000.

HABIBULLAH, C. M. et al. Human fetal hepatocyte transplantation in patients with fulminant hepatic failure. **Transplantation,** v. 58, n. 8, p. 951-2, Oct 1994.

HINSON, J. A.; ROBERTS, D. W.; JAMES, L. P. Mechanisms of acetaminophen-induced liver necrosis. **Handb. Exp. Pharmacol.**, n. 196, p. 369-405, 2010.

HOOFNAGLE, J. H. et al. Fulminant hepatic failure: summary of a workshop. **Hepatology,** v. 21, n. 1, p. 240-52, Jan 1995.

IDRISS, H. T.; NAISMITH, J. H. TNF alpha and the TNF receptor superfamily: structure-function relationship(s). **Microsc. Res. Tech.,** v. 50, n. 3, p. 184-95, Aug 2000.

ISHIDA, Y. et al. A pivotal involvement of IFN-gamma in the pathogenesis of acetaminophen-induced acute liver injury. **FASEB J.,** v. 16, n. 10, p. 1227-36, Aug 2002.

JAESCHKE, H. et al. Complement activates Kupffer cells and neutrophils during reperfusion after hepatic ischemia. **Am. J. Physiol.,** v. 264, n. 4 Pt 1, p. G801-9, Apr 1993.

JAESCHKE, H. et al. Acetaminophen hepatotoxicity and repair: the role of sterile inflammation and innate immunity. **Liver Int.,** v. 32, n. 1, p. 8-20, Jan 2012.

JANG, Y. Y. et al. Hematopoietic stem cells convert into liver cells within days without fusion. **Nat. Cell Biol.,** v. 6, n. 6, p. 532-9, Jun 2004.

JIN, S. Z. et al. Ex vivo-expanded bone marrow stem cells home to the liver and ameliorate functional recovery in a mouse model of acute hepatic injury. **Hepatobiliary Pancreat. Dis. Int.,** v. 11, n. 1, p. 66-73, Feb 2012a.

JIN, S. Z. et al. Stromal cell derived factor-1 enhances bone marrow mononuclear cell migration in mice with acute liver failure. **World J. Gastroenterol.,** v. 15, n. 21, p. 2657-64, Jun 2009.

JIN, S. Z. et al. Hepatocyte growth factor promotes liver regeneration induced by transfusion of bone marrow mononuclear cells in a murine acute liver failure model. **J. Hepatobiliary Pancreat. Sci.,** v. 18, n. 3, p. 397-405, May 2011a.

JOLLOW, D. J. et al. Acetaminophen-induced hepatic necrosis. VI. Metabolic disposition of toxic and nontoxic doses of acetaminophen. **Pharmacology,** v. 12, n. 4-5, p. 251-71, 1974.

KEAYS, R. et al. Intravenous acetylcysteine in paracetamol induced fulminant hepatic failure: a prospective controlled trial. **BMJ,** v. 303, n. 6809, p. 1026-9, Oct 1991.

KIS, B. et al. Autocrine peptide mediators of cerebral endothelial cells and their role in the regulation of blood-brain barrier. **Peptides,** v. 27, n. 1, p. 211-22, Jan 2006.

KOFMAN, A. V. et al. Dose- and time-dependent oval cell reaction in acetaminophen-induced murine liver injury. **Hepatology,** v. 41, n. 6, p. 1252-61, Jun 2005.

KONTOYIANNIS, D. et al. Interleukin-10 targets p38 MAPK to modulate ARE-dependent TNF mRNA translation and limit intestinal pathology. **EMBO J.,** v. 20, n. 14, p. 3760-70, Jul 2001.

KUAI, X. L. et al. Treatment of surgically induced acute liver failure by transplantation of HNF4-overexpressing embryonic stem cells. **Chin. J. Dig. Dis.,** v. 7, n. 2, p. 109-16, 2006.

LAGASSE, E. et al. Purified hematopoietic stem cells can differentiate into hepatocytes in vivo. **Nat. Med.,** v. 6, n. 11, p. 1229-34, Nov 2000.

LEE, W. M. et al. Intravenous N-acetylcysteine improves transplant-free survival in early stage non-acetaminophen acute liver failure. **Gastroenterology,** v. 137, n. 3, p. 856-64, 864.e1, Sep 2009.

LEE, W. M. et al. Acute liver failure: Summary of a workshop. **Hepatology,** v. 47, n. 4, p. 1401-15, Apr 2008.

LEE, W. M.; STRAVITZ, R. T.; LARSON, A. Introduction to the revised AASLD position paper on acute liver failure 2011. **Hepatology**, Dec 2011.

LEI, Y. et al. G-CSF enhanced SDF-1 gradient between bone marrow and liver associated with mobilization of peripheral blood CD34+ cells in rats with acute liver failure. **Dig. Dis. Sci.,** v. 55, n. 2, p. 285-91, Feb 2010.

LEROU, P. H. et al. Derivation and maintenance of human embryonic stem cells from poor-quality in vitro fertilization embryos. **Nat. Protoc.,** v. 3, n. 5, p. 923-33, 2008.

LI, L. et al. Paracrine action mediate the antifibrotic effect of transplanted mesenchymal stem cells in a rat model of global heart failure. **Mol. Biol. Rep.,** v. 36, n. 4, p. 725-31, Apr 2009.

LIDOFSKY, S. D. Liver transplantation for fulminant hepatic failure. **Gastroenterol. Clin. North Am.,** v. 22, n. 2, p. 257-69, Jun 1993.

LORENZ, E.; CONGDON, C.; UPHOFF, D. Modification of acute irradiation injury in mice and guinea-pigs by bone marrow injections. **Radiology,** v. 58, n. 6, p. 863-77, Jun 1952.

LOTZE, M. T.; TRACEY, K. J. High-mobility group box 1 protein (HMGB1): nuclear weapon in the immune arsenal. **Nat. Rev. Immunol.,** v. 5, n. 4, p. 331-42, Apr 2005.

MAKOWKA, L. et al. Cellular transplantation in the treatment of experimental hepatic failure. **Science,** v. 210, n. 4472, p. 901-3, Nov 1980.

MARTIN-MURPHY, B. V.; HOLT, M. P.; JU, C. The role of damage associated molecular pattern molecules in acetaminophen-induced liver injury in mice. **Toxicol. Lett.,** v. 192, n. 3, p. 387-94, Feb 2010a.

MASUBUCHI, Y.; SUDA, C.; HORIE, T. Involvement of mitochondrial permeability transition in acetaminophen-induced liver injury in mice. **J. Hepatol.,** v. 42, n. 1, p. 110-6, Jan 2005.

MAYHAN, W. G. Cellular mechanisms by which tumor necrosis factor-alpha produces disruption of the blood-brain barrier. **Brain Res.,** v. 927, n. 2, p. 144-52, Feb 2002.

MCCLAIN, C. J. et al. Potentiation of acetaminophen hepatotoxicity by alcohol. **JAMA,** v. 244, n. 3, p. 251-3, Jul 1980.

MEERMAN, L. et al. Acute liver failure: spontaneous recovery or transplantation? **Scand. J. Gastroenterol. Suppl.,** v. 223, p. 55-9, 1997.

MEI, S. H. et al. Mesenchymal stem cells reduce inflammation while enhancing bacterial clearance and improving survival in sepsis. **Am. J. Respir. Crit. Care Med.,** v. 182, n. 8, p. 1047-57, Oct 2010.

NAGAKI, M. et al. High levels of serum interleukin-10 and tumor necrosis factor-alpha are associated with fatality in fulminant hepatitis. **J. Infect. Dis.,** v. 182, n. 4, p. 1103-8, Oct 2000.

NEUBERGER, J. M. Halothane and hepatitis. Incidence, predisposing factors and exposure guidelines. **Drug Saf.,** v. 5, n. 1, p. 28-38, 1990 Jan-Feb 1990.

NEWSOME, P. N. et al. Animal models of fulminant hepatic failure: a critical evaluation. **Liver Transpl.,** v. 6, n. 1, p. 21-31, Jan 2000.

NGUYEN, J. H. et al. Matrix metalloproteinase-9 contributes to brain extravasation and edema in fulminant hepatic failure mice. **J. Hepatol.,** v. 44, n. 6, p. 1105-14, Jun 2006a.

NORENBERG, M. D.; JAYAKUMAR, A. R.; RAMA RAO, K. V. Oxidative stress in the pathogenesis of hepatic encephalopathy. **Metab. Brain Dis.,** v. 19, n. 3-4, p. 313-29, Dec 2004.

ODEH, M. Pathogenesis of hepatic encephalopathy: the tumour necrosis factor-alpha theory. **Eur. J. Clin. Invest.,** v. 37, n. 4, p. 291-304, Apr 2007.

OKAYA, T.; LENTSCH, A. B. Cytokine cascades and the hepatic inflammatory response to ischemia and reperfusion. **J. Invest. Surg.,** v. 16, n. 3, p. 141-7, 2003 May-Jun 2003.

OLIVEIRA, S. A. et al. Reduction of galectin-3 expression and liver fibrosis after cell therapy in a mouse model of cirrhosis. **Cytotherapy**, Dec 2011a.

OLIVEIRA, S. A. et al. Therapy with bone marrow cells reduces liver alterations in mice chronically infected by Schistosoma mansoni. **World J. Gastroenterol.,** v. 14, n. 38, p. 5842-50, Oct 2008.

OSTAPOWICZ, G. et al. Results of a prospective study of acute liver failure at 17 tertiary care centers in the United States. **Ann. Intern. Med.,** v. 137, n. 12, p. 947-54, Dec 2002.

OUYANG, W. et al. Regulation and functions of the IL-10 family of cytokines in inflammation and disease. **Annu. Rev. Immunol.,** v. 29, p. 71-109, Apr 2011.

PAREKKADAN, B. et al. Mesenchymal stem cell-derived molecules reverse fulminant hepatic failure. **PLoS One,** v. 2, n. 9, p. e941, 2007.

PITTENGER, M. F. et al. Multilineage potential of adult human mesenchymal stem cells. **Science,** v. 284, n. 5411, p. 143-7, Apr 1999.

PRESCOTT, L. F. Paracetamol, alcohol and the liver. **Br. J. Clin. Pharmacol.,** v. 49, n. 4, p. 291-301, Apr 2000.

RAHMAN, T. M.; HODGSON, H. J. Animal models of acute hepatic failure. **Int. J. Exp. Pathol.,** v. 81, n. 2, p. 145-57, Apr 2000.

RAJASINGH, J. et al. IL-10-induced TNF-alpha mRNA destabilization is mediated via IL-10 suppression of p38 MAP kinase activation and inhibition of HuR expression. **FASEB J.,** v. 20, n. 12, p. 2112-4, Oct 2006.

RATAJCZAK, M. Z. et al. Pivotal role of paracrine effects in stem cell therapies in regenerative medicine - can we translate stem cell-secreted paracrine factors and microvesicles into better therapeutic strategies? **Leukemia**, Dec 2011.

RIORDAN, S. M.; WILLIAMS, R. Perspectives on liver failure: past and future. **Semin. Liver Dis.,** v. 28, n. 2, p. 137-41, May 2008.

ROGER, V. et al. Internal bioartificial liver with xenogeneic hepatocytes prevents death from acute liver failure: an experimental study. **Ann. Surg.,** v. 228, n. 1, p. 1-7, Jul 1998.

ROLANDO, N. et al. The systemic inflammatory response syndrome in acute liver failure. **Hepatology,** v. 32, n. 4 Pt 1, p. 734-9, Oct 2000.

RUBIN, E.; HUTTERER, F.; LIEBER, C. S. Ethanol increases hepatic smooth endoplasmic reticulum and drug-metabolizing enzymes. **Science,** v. 159, n. 3822, p. 1469-70, Mar 1968a.

SABAT, R. et al. Biology of interleukin-10. **Cytokine Growth Factor Rev.,** v. 21, n. 5, p. 331-44, Oct 2010.

SCAFFIDI, P.; MISTELI, T.; BIANCHI, M. E. Release of chromatin protein HMGB1 by necrotic cells triggers inflammation. **Nature,** v. 418, n. 6894, p. 191-5, Jul 2002.

SCHINDLER, R. et al. Correlations and interactions in the production of interleukin-6 (IL-6), IL-1, and tumor necrosis factor (TNF) in human blood mononuclear cells: IL-6 suppresses IL-1 and TNF. **Blood,** v. 75, n. 1, p. 40-7, Jan 1990.

SCHIODT, F. V. et al. Etiology and outcome for 295 patients with acute liver failure in the United States. **Liver Transpl. Surg.,** v. 5, n. 1, p. 29-34, Jan 1999.

SHARIEF, M. K.; THOMPSON, E. J. In vivo relationship of tumor necrosis factor-alpha to blood-brain barrier damage in patients with active multiple sclerosis. **J. Neuroimmunol.,** v. 38, n. 1-2, p. 27-33, May 1992.

SHIMOJIMA, N. et al. Altered expression of zonula occludens-2 precedes increased blood-brain barrier permeability in a murine model of fulminant hepatic failure. **J. Invest. Surg.,** v. 21, n. 3, p. 101-8, 2008 May-Jun 2008.

SOUZA, B. S. et al. Current status of stem cell therapy for liver diseases. **Cell Transplant.,** v. 18, n. 12, p. 1261-79, 2009.

STREETZ, K. et al. Tumor necrosis factor alpha in the pathogenesis of human and murine fulminant hepatic failure. **Gastroenterology,** v. 119, n. 2, p. 446-60, Aug 2000.

STRIETER, R. M.; KUNKEL, S. L.; BONE, R. C. Role of tumor necrosis factor-alpha in disease states and inflammation. **Crit. Care Med.,** v. 21, n. 10 Suppl, p. S447-63, Oct 1993.

STROM, S. C. et al. Hepatocyte transplantation as a bridge to orthotopic liver transplantation in terminal liver failure. **Transplantation,** v. 63, n. 4, p. 559-69, Feb 1997.

TACHI, Y. et al. Changes in angiogenesis-related factors in serum following autologous bone marrow cell implantation for severe limb ischemia. **Expert. Opin. Biol. Ther.,** v. 8, n. 6, p. 705-12, Jun 2008.

THEISE, N. D. et al. Liver from bone marrow in humans. **Hepatology,** v. 32, n. 1, p. 11-6, Jul 2000.

THORGEIRSSON, S. S.; GRISHAM, J. W. Hematopoietic cells as hepatocyte stem cells: a critical review of the evidence. **Hepatology,** v. 43, n. 1, p. 2-8, Jan 2006.

TILG, H. et al. Serum levels of cytokines in chronic liver diseases. **Gastroenterology,** v. 103, n. 1, p. 264-74, Jul 1992.

TREDGER, J. M. et al. Effects of ethanol ingestion on the hepatotoxicity and metabolism of paracetamol in mice. **Toxicology,** v. 36, n. 4, p. 341-52, Sep 1985.

VAN LINT, P. et al. Resistance of collagenase-2 (matrix metalloproteinase-8)-deficient mice to TNF-induced lethal hepatitis. **J. Immunol.,** v. 175, n. 11, p. 7642-9, Dec 2005.

VAN POLL, D. et al. Mesenchymal stem cell-derived molecules directly modulate hepatocellular death and regeneration in vitro and in vivo. **Hepatology,** v. 47, n. 5, p. 1634-43, May 2008.

VASSILOPOULOS, G.; WANG, P. R.; RUSSELL, D. W. Transplanted bone marrow regenerates liver by cell fusion. **Nature,** v. 422, n. 6934, p. 901-4, Apr 2003.

WALKER, P. A. et al. Intravenous multipotent adult progenitor cell therapy for traumatic brain injury: preserving the blood brain barrier via an interaction with splenocytes. **Exp. Neurol.,** v. 225, n. 2, p. 341-52, Oct 2010.

WANG, W. et al. Tumor necrosis factor-α affects blood-brain barrier permeability in acetaminophen-induced acute liver failure. **Eur. J. Gastroenterol. Hepatol.,** v. 23, n. 7, p. 552-8, Jul 2011.

WANG, X. et al. Cell fusion is the principal source of bone-marrow-derived hepatocytes. **Nature,** v. 422, n. 6934, p. 897-901, Apr 2003.

WARE, A. J.; D'AGOSTINO, A. N.; COMBES, B. Cerebral edema: a major complication of massive hepatic necrosis. **Gastroenterology,** v. 61, n. 6, p. 877-84, Dec 1971.

WATANABE, K. et al. Adrenomedullin reduces ischemic brain injury after transient middle cerebral artery occlusion in rats. **Acta Neurochir. (Wien),** v. 143, n. 11, p. 1157-61, Nov 2001.

WHITCOMB, D. C.; BLOCK, G. D. Association of acetaminophen hepatotoxicity with fasting and ethanol use. **JAMA,** v. 272, n. 23, p. 1845-50, Dec 1994.

WRIGHT, T. L. et al. Hepatitis B virus and apparent fulminant non-A, non-B hepatitis. **Lancet,** v. 339, n. 8799, p. 952-5, Apr 1992.

YAGI, H. et al. Reactive bone marrow stromal cells attenuate systemic inflammation via sTNFR1. **Mol. Ther.,** v. 18, n. 10, p. 1857-64, Oct 2010.

YAMAMOTO, S.; NGUYEN, J. H. TIMP-1/MMP-9 imbalance in brain edema in rats with fulminant hepatic failure. **J. Surg. Res.,** v. 134, n. 2, p. 307-14, Aug 2006.

YTREBØ, L. M. et al. N-acetylcysteine increases cerebral perfusion pressure in pigs with fulminant hepatic failure. **Crit Care Med.,** v. 29, n. 10, p. 1989-95, Oct 2001.

YU, Y. et al. Cell therapies for liver diseases. **Liver Transpl.,** v. 18, n. 1, p. 9-21, Jan 2012a.

ZAGO, M. A. Terapia com células-tronco. Fundamentos, oportunidades e obstáculos. Revista da Sociedade Brasileira de Hipertensão, v.8, n.4, p.145-150, 2005.

ZHANG, B. et al. Effects of bone marrow and hepatocyte transplantation on liver injury. **J. Surg. Res.,** v. 157, n. 1, p. 71-80, Nov 2009.

ZHANG, L. et al. Granulocyte colony-stimulating factor treatment ameliorates liver injury and improves survival in rats with D-galactosamine-induced acute liver failure. **Toxicol. Lett.,** v. 204, n. 1, p. 92-9, Jul 2011.

ZHAO, E. et al. Bone marrow and the control of immunity. **Cell. Mol. Immunol.,** v. 9, n. 1, p. 11-9, Jan 2012.

ZIMMERMAN, H. J.; MADDREY, W. C. Acetaminophen (paracetamol) hepatotoxicity with regular intake of alcohol: analysis of instances of therapeutic misadventure. **Hepatology,** v. 22, n. 3, p. 767-73, Sep 1995.

8 ANEXOS

8.1 ANEXO I

OLIVEIRA, S. A. et al. Reduction of galectin-3 expression and liver fibrosis after cell therapy in a mouse model of cirrhosis. Cytotherapy, v. 14, n. 3, Mar, p. 339-349, 2012.

Reduction of galectin-3 expression and liver fibrosis after cell therapy in a mouse model of cirrhosis

SHEILLA ANDRADE DE OLIVEIRA[1,2]*, BRUNO SOLANO DE FREITAS SOUZA[2,3]*,
ELTON PEREIRA SÁ BARRETO[2], CARLA MARTINS KANETO[3],
HÉLIO ALMEIDA NETO[2,3], CARINE MACHADO AZEVEDO[2,3],
ELISALVA TEIXEIRA GUIMARÃES[2], LUIZ ANTONIO RODRIGUES DE FREITAS[3,4],
RICARDO RIBEIRO-DOS-SANTOS[2,3] & MILENA BOTELHO PEREIRA SOARES[2,3]

[1]*Centro de Pesquisas Aggeu Magalhães, Fundação Oswaldo Cruz, Recife, Pernambuco, Brazil,* [2]*Centro de Pesquisas Gonçalo Moniz, Fundação Oswaldo Cruz, Salvador, Bahia, Brazil,* [3]*Hospital São Rafael, Salvador, Bahia, Brazil, and* [4]*Universidade Federal da Bahia, Salvador, Bahia, Brazil*

Abstract

Background aims. Cirrhosis, end-stage liver disease, is caused by different mechanisms of injury, associated with persistent inflammation. Galectin-3 is an important regulator of fibrosis that links chronic inflammation to fibrogenesis. We investigated the role of bone marrow cell (BMC) transplantation in chronic inflammation and hepatic fibrosis. *Methods.* Liver cirrhosis was induced by administration of carbon tetrachloride and ethanol to wild-type C57BL/6 or bone marrow chimeric mice. Bone marrow chimeras were generated by lethal irradiation and transplantation with BMC obtained from green fluorescent protein (GFP$^+$)donors. Wild-type cirrhotic mice were transplanted with BMC without irradiation. Livers from chimeras and cirrhotic transplanted mice were obtained for evaluation of inflammation, fibrosis and regulatory factors [galectin-3, matrix metallopeptidase (MMP)-9, tissue inhibitor of metalloproteinase (TIMP)-1 and transforming growth factor (TGF)-β]. *Results.* The development of cirrhosis was associated with increased expression of galectin-3 by F4/80$^+$ cells and intense migration of BMC to the liver. Furthermore, when transplanted after the establishment of cirrhosis, BMC also migrated to the liver and localized within the fibrous septa. Two months after BMC therapy, cirrhotic mice had a significant reduction in liver fibrosis and expression of type I collagen. We did not find any difference in levels of TGF-β, TIMP-1 and MMP-9 between saline and BMC groups. However, the numbers of inflammatory cells, phagocytes and galectin-3$^+$ cells were markedly lower in the livers of cirrhotic mice treated with BMC. *Conclusions.* Our results demonstrate an important role for BMC in the regulation of liver fibrosis and that transplantation of BMC can accelerate fibrosis regression through modulatory mechanisms.

Key Words: *carbon tetrachloride, galectin-3, hepatic cirrhosis, mice, stem cells*

Introduction

Cirrhosis is the end stage of many chronic liver diseases and represents a therapeutic challenge world-wide (1–3). The development of cirrhosis is initiated after repeated insults that cause chronic liver tissue damage, consequently inducing fibrosis and nodular regeneration of liver cells. This process is frequently associated with an inflammatory response and the activation of hepatic stellate cells, known as the most important source of extracellular matrix (ECM) production, along with different subtypes of myofibroblasts, such as fibrogenic cells from the epithelial-to-mesenchymal transition, periportal fibrocytes, and bone marrow-derived fibrocytes that synthesize ECM proteins (4,5). Persistent noxious stimuli lead to chronic activation of macrophages and synthesis of molecules that promote fibrogenesis, such as galectin-3, a lectin that regulates a wide variety of biologic phenomena, establishing a link between chronic inflammation and fibrogenesis (6).

It has been shown that galectin-3 activates and stimulates the proliferation of myofibroblasts as well as increases their synthesis of collagen (7). Furthermore, galectin-3 expression has been associated with the development of fibrosis in a variety of organs, such as the kidney, liver, gut and heart (8,9). As a result of the persistent stimulus to fibrogenesis, with increased galectin-3 expression, profound alterations in the liver architecture occur, modifying the relationship between stromal components, vessels and hepatocytes, ultimately characterizing liver cirrhosis (10).

Liver transplantation is the only effective treatment available for patients with cirrhosis presenting chronic hepatic failure (2,11), and it remains a high-risk procedure limited by the availability of donated organs. In this context, the development of new therapeutic strategies for liver failure is necessary. Stem cell therapy has emerged as a potential tool in the treatment of liver disease (12). In recent years, many experimental studies have been carried out to evaluate the therapeutic efficacy of stem cells in models of acute hepatic injuries (13–24). Although the results have been promising, further studies on models of chronic liver disease are necessary. There is also a need to understand the mechanisms by which stem cell therapy can be beneficial in treating liver disease (25).

Cell therapy can act through a variety of mechanisms, either directly or indirectly by secretion of molecules that can counteract fibrogenesis, such as soluble mediators and metalloproteinases (21,26). The present study evaluated the effects of bone marrow cells (BMC) transplanted in mice with cirrhosis induced by long-term administration of carbon tetrachloride and ethanol (CCl_4 + EtOH). Our results demonstrate the therapeutic potential of BMC in a well-established cirrhosis model and reinforce the idea that galectin-3 may be a potential intervention target in the treatment of liver fibrosis.

Methods

Ethics statement

Prior to undertaking the studies described here, approval for all the experiments using mice was obtained from the Gonçalo Moniz Research Center (CPqGM), Fundação Oswaldo Cruz (FIOCRUZ; Salvador, Bahia, Brazil) Ethics Committee and certified as 001/2007, protocol number 24.

Animals

Three-week-old male C57BL/6 wild-type and female enhanced green fluorescent protein (eGFP)-transgenic mice were used as recipients and donors of BMC, respectively. All the animals, weighing between 20 and 23 g, were raised and maintained at the Gonçalo Moniz Research Center/FIOCRUZ, in rooms with a controlled temperature ($22 \pm 2°C$) and humidity ($55 \pm 10\%$) environment under continuous air renovation conditions. Animals were housed in a 12-h light/12-h dark cycle (6.00–18.00) with rodent diet and water *ad libitum*.

Generation of bone marrow chimeras

C57BL/6 female mice were irradiated with 6 Gy for depletion of BMC (Figure 1A) in a [137]Cesium source irradiator (CisBio International, Gif Sur Yvette France). BMC were obtained from the femurs and tibiae of male eGFP transgenic mice and used to reconstitute irradiated mice. The mononuclear cells were purified by centrifugation in Ficoll gradient at 1000 *g* for 15 min (Histopaque 1119 and 1077; 1:1; Sigma, St Louis, MO, USA). After two washings in Dulbecco's modified Eagle medium (DMEM) medium (Sigma), the cells were filtered and resuspended in saline. Each irradiated mouse received an injection of 10^7 cells. Two weeks later, representative animals were killed and BMC were harvested to confirm repopulation by donor cells using flow cytometry analysis.

Induction of hepatic injury and cirrhosis

Experimental cirrhosis was induced in wild-type and chimeric mice by administration of 0.2 mL 20% CCl_4 dissolved in a mineral oil solution (Merck, Darmstadt, Germany) and diluted in olive oil through gavage twice a week, combined with 5% (v/v) ethanol (EtOH) in the drinking water (Figure 1B). Control mice were maintained in the same housing conditions as the experimental groups. Groups of animals were killed for evaluation after periods of 24 days, 2–3 months and 5–6 months.

Morphologic and morphometric hepatic analyzes

Mice under anesthesia were perfused through the heart with 50 mL phosphate-buffered saline (PBS) followed by 200 mL paraformaldehyde at 4°C. Liver slices were fixed in 10% formalin and embedded in paraffin. Five micrometer-thick sections were stained with either hematoxylin-eosin (H&E) for histologic analysis and to quantify inflammation, or picrosirius red to quantify fibrosis. Analyzes were performed on whole liver sections after slide scanning using the Aperio ScanScope system (Aperio Technologies, Vista, CA, USA). The images were analyzed used the Image Pro program (version 7.0; Media Cybernetics, San Diego, CA, USA). A mean area of 54 636 978 μm^2/mouse was analyzed.

Cirrhosis was defined by the presence of hepatic cell nodules delimited by fibrosis occupying most of the liver parenchyma. The morphologic parameters analyzed were presence of steatosis, ballooning cells, apoptosis, necrosis, Mallory–Denk bodies, ductular proliferation and inflammation (portal and acinar). These parameters were classified according to intensity in five grades, ranging from 0 to 4.

Transplantation of BMC to wild-type C57BL/6 mice

Six months after treatment with CCl_4 + EtOH, the administration of these drugs was suspended and the
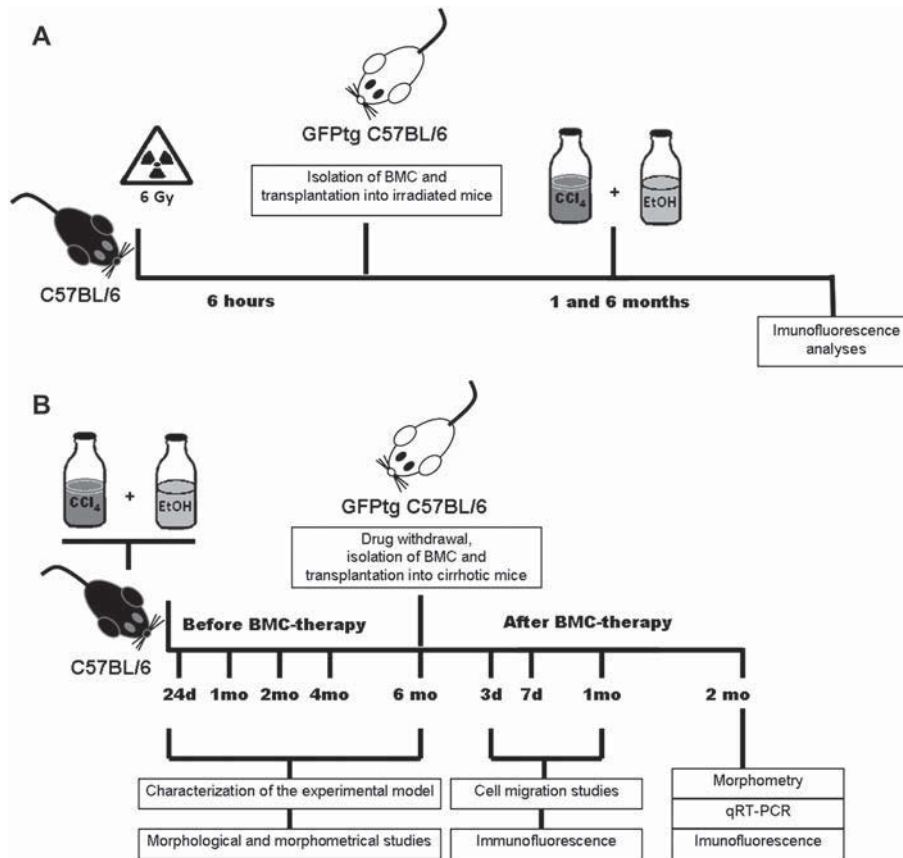
Figure 1. A schematic illustration of the experimental design. Generation of bone marrow chimeras and hepatic injury (A). C57BL/6 female mice were irradiated (6 Gy) and transplanted with BMC obtained from GFP$^+$ donors (10^7 cells/mouse). Chimeric mice were submitted to a cirrhosis-induction protocol with administration of CCl_4 + EtOH, and were killed 1 month ($n=5$) or 6 months ($n=5$) later. Control chimeric mice remained without injury at the same time-points ($n=10$). Induction of experimental liver cirrhosis and therapy with BMC (B). Groups of mice were treated with CCl_4 + EtOH. Normal controls were maintained in the same housing conditions. Mice were killed for morphologic evaluations and characterization of the experimental model ($n=4$/time-point) after different periods of CCl_4 + EtOH administration (24 days and 2, 3, 5 and 6 months). Cirrhotic mice (treated for 6 months with CCl_4 + EtOH) were transplanted with BMC or injected with saline and killed 2 months later for morphometric, immunofluorescence and qRT-PCR studies ($n=5$–8 mice/group).

wild-type C57BL/6 mice were submitted to BMC transplantation (Figure 1B). BMC were obtained from femurs and tibiae of C57BL/6 eGFP transgenic mice. BMC were purified by centrifugation in a Ficoll gradient (Histopaque 1119 and 1077, 1:1; Sigma-Aldrich, St Louis, MO, USA) at 1000 g for 15 min. BMC were suspended in saline and injected into the cirrhotic wild-type C57BL/6 mice. The isolated BMC were analyzed using flow cytometry with the following conjugated antibodies from Becton Dickinson (San Diego, CA, USA): stem cell antigen-1(Sca-1)–phycoerythrin (PE)/Cyanine (Cy)5, CD45–Allophycocyanin(APC), CD44–PE, CD34–PE, CD11b–PE and CD117–PE. Acquisition and analysis were performed in a FACScalibur flow cytometer (Becton Dickinson). The following percentages were obtained: 96.51 ± 1.32 for GFP$^+$ cells, 0.11 ± 0.032 for Sca-1$^+$ cells, 96.35 ± 3.12 for CD45$^+$ cells, 92.72 ± 3.23 for CD44$^+$ cells, 0.02 ± 0.05 for CD34$^+$ cells,; 60.22 ± 5.71 for CD11b$^+$ cells and 0.17 ± 0.04 for CD117$^+$ cells.

One or three doses of 3×10^7 cells/mouse were administered intravenously, via the retro-orbital plexus, with 7 days between injections. Control cirrhotic mice received saline injections at similar intervals. Mice were killed at various time-points after cell treatment.

Immunofluorescence analysis

The 5-μm frozen sections obtained from the livers of mice were fixed in 4% cold paraformaldehyde in a 0.1 M phosphate buffer. The presence of transplanted GFP$^+$ BMC in the liver tissue was analyzed using direct fluorescence microscopy. The following antibodies were used: anti-cytokeratin-18, diluted 1:100 (Santa Cruz Biotechnology, Santa Cruz, California, USA); anti-CD45, diluted 1:100 (Caltag, Buckingham, UK); anti-albumin, diluted 1:400 (DAKO, Glostrup, Denmark); and anti-galectin-3, diluted 1:50 (Santa Cruz Biotechnology). Nuclei were counterstained with 4,6-dismidino-2-phenylindole (VectaShield hard set mounting

medium with DAPI H-1500; Vector Laboratories, Burlingame, CA, USA). The presence of fluorescent cells was observed using an AX70 microscope with an epifluorescence system plus grid to enhance the fluorescence resolution (Optigrid, structured light imaging system; Thales Optem Inc., Olympus, Center Valley, PA, USA), using appropriate filters (Olympus) in a FluoView1000 confocal microscope (Olympus, Optigrid, Fairport, NY, USA). Quantification of galectin-3$^+$ cells, autofluorescent cells and type I collagen were performed in 10 random fields per section. Cell images were captured using $400 \times$ magnification and analyzed using Image Pro Plus software.

Real-time–polymerase chain reaction

Total RNA was isolated from the livers using TRIzol reagent (Invitrogen, Carlsbad, CA, USA), and the concentration was determined by photometric measurement. A high-capacity cDNA reverse transcription kit (Applied Biosystems, Foster City, CA, USA) was used to synthesize cDNA from 1 μg RNA, in accordance with manufacturer's recommendations. Real-time–polymerase chain reaction (qRT-PCR) assays were performed to detect the expression levels of transforming growth factor (TGF)-β1, tissue inhibitor of metalloproteinase (TIMP)-1 and matrix metallopeptidase (MMP)-9 genes. qRT-PCR amplification mixtures contained 20 ηg template cDNA, and Taqman master mix (10 μL) (Applied Biosystems) probes for TGF-β (Mm00441724_m1), TIMP-1 (Mm00441818_m1) and MMP-9 (Mm00442991_m1) in a final volume of 20 μL. All reactions were run in duplicate on an ABI7500 sequence detection system (Applied Biosystems) under standard thermal cycling conditions. The mean cycle threshold (Ct) values from duplicate measurements were used to calculate expression of the target gene, with normalization to an internal control glyceraldehyde-3-phosphate dehydrogenase (GAPDH) using the $2 - DCt$ formula. Experiments with coefficients of variation greater than 5% were excluded. A no-template control (NTC) and no-reverse transcription controls (No-RT) were also included.

Statistical analysis

Data were analyzed using a Student's t-test or ANOVA, followed by Newman–Keuls (TGF-β and morphometry) or Tukey (qRT-PCR) tests, using Prism Software (version 5.0; GraphPad Software, San Diego, CA, USA). Differences were considered significant if P was equal to or less than 0.05.

Results

Cirrhosis induction in mice chronically treated with $CCl_4 + EtOH$

Chronic administration of $CCl_4 + EtOH$ caused progressive morphologic alterations in the liver. After 6 months of repeated administration of $CCl_4 + EtOH$, the livers exhibited morphologic alterations, such as a nodular surface and brownish coloring (Figure 2A, B). The normal parenchyma was replaced by regenerative nodules (Figure 2C, D) measuring 453 ± 199 μm in diameter (ranging from 196 to 770 μm) delimited by fibrous septa. Vascular alterations, including portal vein dilation, were observed (Figure 2A). The survival
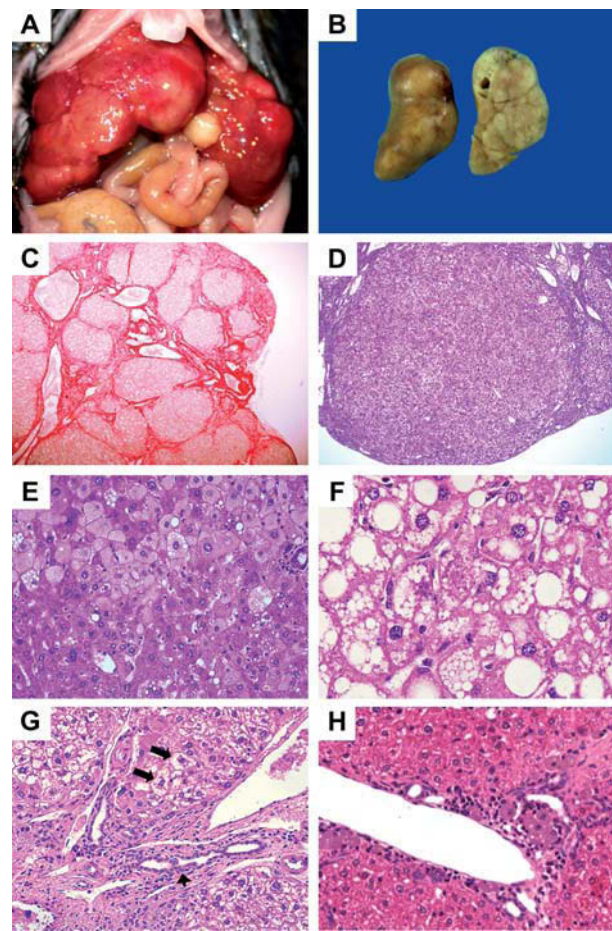

Figure 2. Macroscopic and morphologic aspects of cirrhosis in mice submitted to $CCl_4 + EtOH$ administration for 6 months. Prominent areas of nodules on the liver surface of cirrhotic mice (A,B). Hepatic nodules of variable size subdivided into irregular fibrous septa could be seen in the picrosirius red-stained section by optical microscopy (c) ($40 \times$). Regenerative macronodule (D) (H&E, $100 \times$). Ballooning cells (E) (H&E, $200 \times$) and the presence of micro- and macrovacuolar steatosis (F) (H&E, $400 \times$). Proliferation of ductular cells (G) and the presence of Mallory bodies (G, arrows) (H&E, $200 \times$). After 6 months of $CCl_4 + EtOH$ treatment, the foci of periportal chronic inflammation associated with large phagocytic cells (D, arrows) were seen with H&E staining (H) ($200 \times$).

during 6 months of $CCl_4 + EtOH$ administration was about 70% (37/53).

Short-term administration (24 days) of $CCl_4 + EtOH$ induced hepatic cell necrosis and a mixed inflammatory infiltrate with a predominance of mononuclear cells, especially in centrilobular areas (data not shown). At this time-point, mild hepatocellular ballooning without steatosis was observed. Some incomplete fibrous septa linking vascular structures were also observed. After a longer period of $CCl_4 + EtOH$ administration (2–5 months), the normal liver architecture was partially replaced by nodules of regenerating liver cells surrounded by fibrous septa. At this time-point, a mild ductular proliferation was present within portal tracts, as well as in fibrous septa (data not shown).

Cirrhosis was established after 6 months of continuous $CCl_4 + EtOH$ administration, and characterized by a diffuse liver alteration with fibrous tissue completely surrounding nodules of regenerative hepatocytes, resulting in profound alteration of the liver architecture (Figure 2C, D). Some cirrhotic nodules showed microvacuolar hepatocellular steatosis and foci ballooning cells (Figure 2E, F), and hyaline Mallory–Denk bodies were frequently observed

(Figure 2G). Ductular cell proliferation was observed in connective tissue (Figure 2G).

Foci of inflammatory cells were seen within the fibrous septa (Figure 2H) Immunostaining for $F4/80^+$, a macrophage cell marker, demonstrated that many of the inflammatory cells were macrophages (Figure 3A). Among these cells, some showed an abundant clear brown cytoplasm. These cells had autofluorescent granules, were positive for the $F4/80^+$ marker and also for galectin-3 (Figure 3B, C). These cells were observed in greater quantities at later time-points (Figure 3D–F), although some $F4/80^+$ cells remained negative for galectin-3 (Figure 3C, detail).

Migration of BMC to injured liver

In order to evaluate the recruitment of BMC during the development of cirrhosis, bone marrow chimeras were generated and submitted to treatment with $CCl_4 + EtOH$ or remained as uninjured controls. Acute and chronic hepatic injury induced by $CCl_4 + EtOH$ resulted in an increase in the recruitment of BMC to the liver, compared with control animals. GFP^+ cell numbers were found to be 2-fold increased in acutely
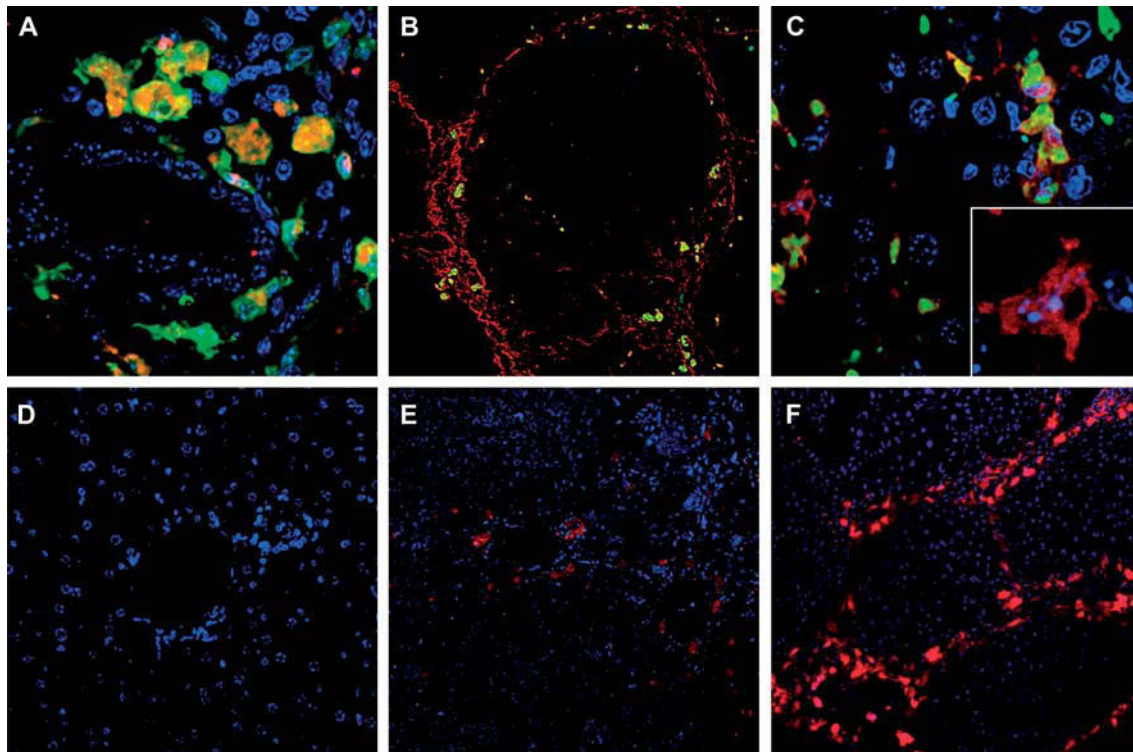

Figure 3. Presence of galectin-3$^+$ cells during the establishment of experimental cirrhosis. Phagocytic cells found in inflammatory infiltrates had deposits of autofluorescent material (red) and were also positive for F4/80 (green) (A) (1200×). Picrosirius staining visualized by fluorescence microscopy showed the presence of autofluorescent cells (yellow) associated with fibrous septa (red) (B) (100×). Most galectin-3$^+$ (red) cells co-stained with F4/80 (green; C) (1200×) and a few galectin-3$^+$ cells were F4–80$^-$ (C, detail). Immunofluorescence staining with anti-galectin-3 (red) and DAPI (blue) in liver sections of non-injured mice (D) (400×) and $CCl_4 + EtOH$-treated mice for 2 months (E) (200×) and 6 months (F) (200×), which showed increased numbers of galectin-3$^+$ cells with time and their typical localization in areas of fibrous septa (F) (200×).
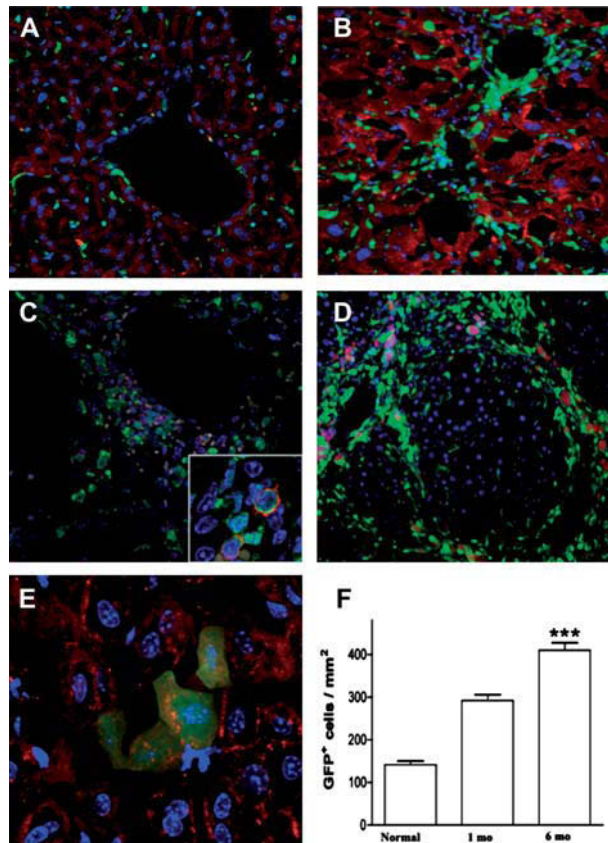
Figure 4. BMC migrate to the injured liver in chimeric mice. Immunofluorescence for detection of GFP (green), albumin (red) and nuclear counterstaining with DAPI (blue). Bone marrow GFP^{+} positive cells were found in small numbers in sinusoids of non-injured chimeras (A) (400×) and at greater numbers in perivascular regions of acutely injured chimeras after 30 days of CCl_4 + EtOH treatment (B) (400×). Most infiltrating GFP^{+} cells (green) were found in periportal inflammatory infiltrates at 30 days of CCl_4 + EtOH treatment and co-stained with CD45 (red) (C, detail) (200×). At 6 months of CCl_4 + EtOH treatment, GFP^{+} cells (green) were mostly found in fibrous septa and some presented autofluorescent cytoplasmic deposits (red) (D) (200×). Rarely, hepatocytes co-stained with albumin (red) and GFP (green) were visualized after 6 months of CCl_4 + EtOH treatment (E) (800×). The GFP^{+} cells were quantified in non-injured, 30-day injured and 6-months injured chimeras (F). Data are represented as the means ± SEM of five animals per group. *$P < 0.05$ (F).

injured livers compared with uninjured controls (Figure 4B, F), and the number was three times greater in chronically injured mice (Figure 4C–F). In the non-injured control group, GFP^{+} cells were found predominantly in sinusoids (Figure 4A).

However, in acutely injured livers GFP^{+} cells were seen around the central vein in the hepatic lobules (Figure 4C), whereas in chronically injured livers they were found mainly within the fibrous septa (Figure 4D). Few cells co-expressing GFP and albumin could be found in the hepatic parenchyma in chronically injured mice (Figure 4E), with none found in uninjured controls. The number of GFP^{+} cells in the parenchyma of chimeric

mice significantly increased at later time-points (Figure 4F).

In order to investigate whether BMC migrate to the livers of non-irradiated mice with established cirrhosis, the animals were transplanted intravenously with 3×10^7 bone marrow mononuclear cells obtained from GFP transgenic mice. GFP[+] BMC were found in the liver sections of cirrhotic mice 3 days after transplantation (Figure 5A). At this time-point, GFP^{+} cells were mostly small and round in shape and were found in portal area tracts. One week after transplantation, GFP^{+} cells, mostly with an elongated shape, were found within the fibrous septa (Figure 5B). GFP^{+} cells were not seen in the liver sections of mice analyzed 1 and 2 months after transplantation (data not shown).

Effects of BMC transplantation in livers of cirrhotic mice

To evaluate the effects of the transplanted cells into non-irradiated cirrhotic mice, liver sections were analyzed 2 months after the therapy with BMC. Mice were submitted to a 3-week protocol, with 1-weekly intravenous injections of 3×10^7 cells. A reduction in fibrosis was observed in the BMC-treated mice, compared with controls (Figure 5C, D), which was confirmed by morphometric evaluation (Figure 6A). A marked reduction in collagen I was observed in the fibrous septa of livers from BMC-treated mice, compared with controls (Figure 6B). In addition, the number of inflammatory and large autofluorescent cells significantly decreased after BMC therapy (Figure 6C, D). In contrast with these results, transplantation of BMC to mice that were still receiving CCl_4 + EtOH between 4 and 6 months of the protocol did not lead to lower levels of fibrosis, compared with mice injected with saline (data not shown).

To investigate the mechanisms by which BMC therapy resulted in a reduction of fibrosis, we tested whether BMC transplantation modulated the production of the fibrogenic cytokine TGF-β. Liver TGF-β mRNA levels in cirrhotic mice were increased compared with normal controls. However, no differences were observed in the group treated with BMC compared with saline-treated cirrhotic mice, as investigated by qRT-PCR analysis (Figure 6E). Two additional factors associated with fibrosis, TIMP-1 and MMP-9, were also evaluated at the gene expression level. The same pattern of expression as found at the TGF-β mRNA level was also observed with TIMP-1, a pro-fibrogenic factor. The expression of MMP-9, an anti-fibrogenic factor, was
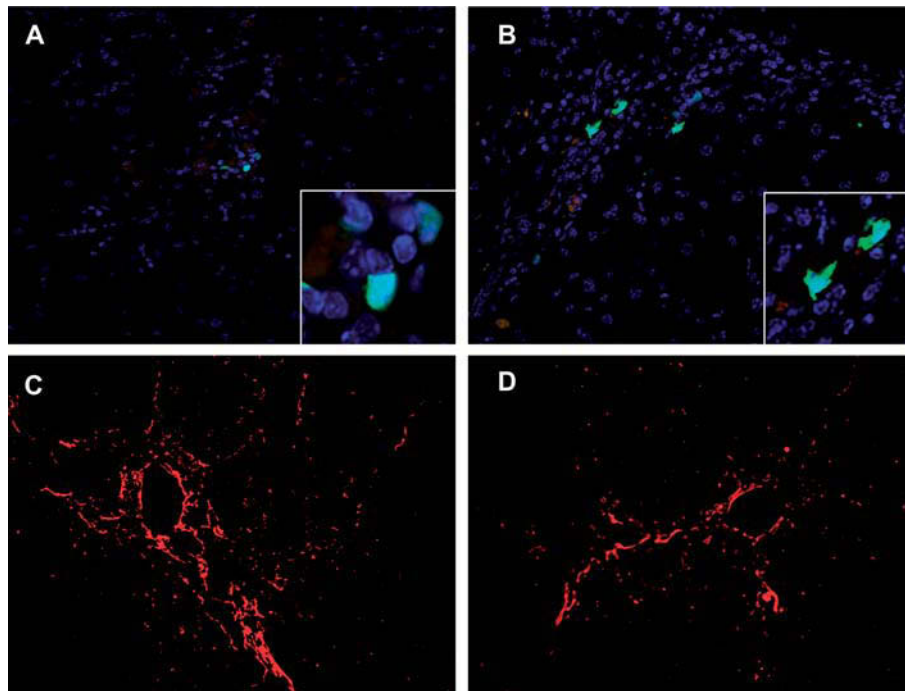
Figure 5. BMC migrate to cirrhotic liver and promote fibrosis reduction. Mice were transplanted intravenously with BMC after the establishment of cirrhosis and were killed 1 or 7 days later for fluorescence microscopy analysis. For visualization of GFP$^+$ cells (green), sections were mounted with nuclear counterstaining with DAPI (blue). Small, round-shaped GFP$^+$ cells were seen 1 day after the transplantation (A and detail), while GFP$^+$ with elongated shapes were seen in fibrous septa after 7 days (B and detail). Picrosirius red staining for detection of collagen in liver sections of saline-treated © and BMC-treated (D) mice.

found to be similar among all groups analyzed (data not shown).

Reduction of galectin-3 expression after BMC treatment in livers of cirrhotic mice

The expression of galectin-3 in the livers of cirrhotic mice was evaluated. Galectin-3+ cells were observed mainly in portal tracts and in fibrous septa in cirrhotic mice treated with saline (Figure 7A), whereas in the livers of BMC-treated cirrhotic mice galectin-3$^+$ cells were observed only in portal tracts (Figure 7B). Morphometric analysis revealed a marked decrease in the number of galectin-3$^+$ cells in the livers of mice 2 months after BMC transplantation, compared with saline-treated cirrhotic controls ($P < 0.0001$; Figure 7C).

Discussion

A growing number of reports have shown that BMC transplantation mitigates liver damage in acute experimental models (13–16,18–20,22). In the present study we report the beneficial effects of BMC transplantation in an experimental model of cirrhosis, induced by chronic administration of $CCl_4 + EtOH$. C57BL/6 mice chronically receiving $CCl_4 + EtOH$ developed morphologic alterations that characterize liver cirrhosis, providing a useful tool for studying mechanisms of fibrogenesis and fibrosis regression, as well as for the development of novel potential therapies.

The bone marrow mononuclear cell fraction tested in our study comprises a number of cell types and therefore additional studies are needed to identify which cell populations are responsible for the beneficial effects observed. However, despite being a heterogeneous population, transplantation of BMC is already a well-established procedure in medical practice, which helps translation of the results to clinical studies. In this regard, initial clinical studies using autologous BMC transplantation in patients with chronic liver disease have been conducted by our group and others (25,27).

Different populations of bone marrow-derived cells have been implicated in both the development as well as the regression of cirrhosis (21,28). The establishment of chronic liver injury and its progression to cirrhosis involves the activation of hepatic stellate cells, which are converted into fibroblasts and myofibroblasts and become the main source of ECM in liver fibrosis. Furthermore, the potential role of other fibroblast subpopulations has been described, such as fibrogenic cells from the epithelial-to-mesenchymal transition, periportal fibrocytes and bone marrow-derived cells (5). The role of BMC as another source
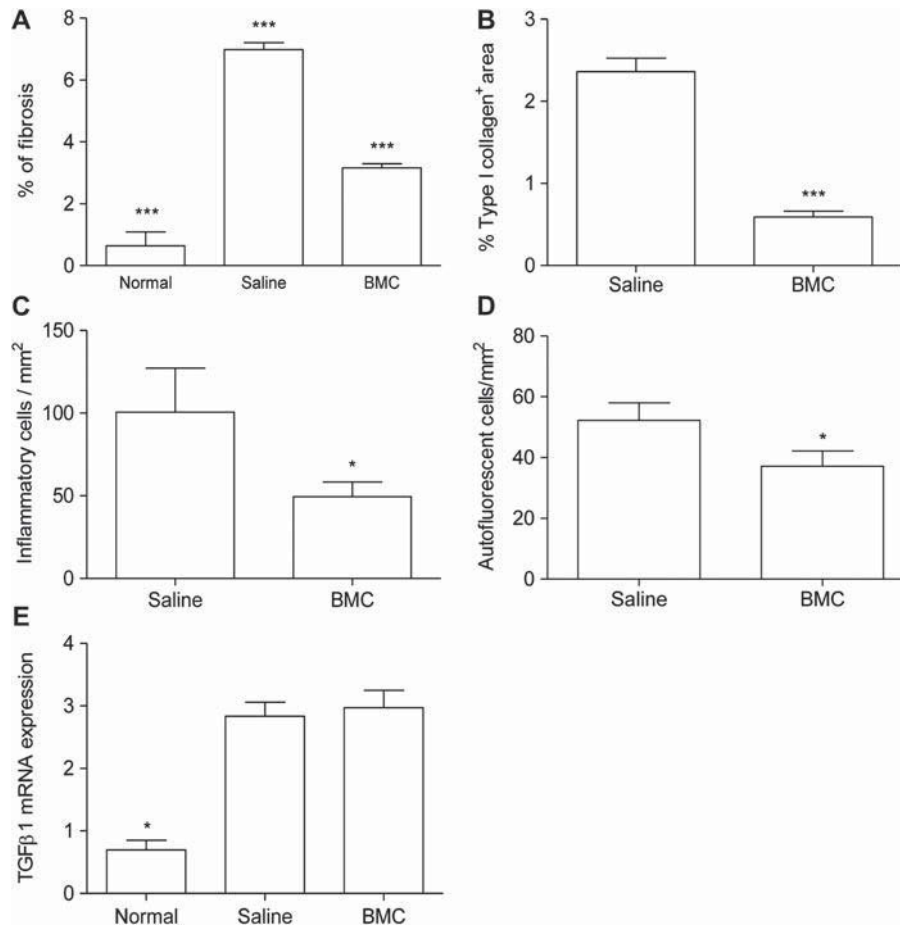
Figure 6. Effects observed after 2 months of BMC therapy on liver cirrhosis. Morphometric quantification of the percentage area of liver fibrosis assessed by picrosirius red staining (A) and immunostaining with anti-type I collagen (B), demonstrating fibrosis reduction in the BMC-treated group compared with the saline-treated group. Quantification of inflammatory cells (C) and autofluorescent cells (D) in liver sections showing reduced numbers in the BMC-treated group compared with the saline-treated group. TGF-β levels assessed in liver homogenates by qRT-PCR (E). Data are represented graphically as the mean $\pm$ SEM of five to eight mice/group. $*P < 0.05$, $***P < 0.0001$.

of liver fibrocytes during fibrogenesis has been studied before by Higashiyama *et al.* (9), who reported that these cells were not important for the development of liver fibrosis. Kupffer cells and infiltrating bone marrow-derived macrophages are a crucial link between chronic inflammation and liver fibrosis (29). However, diverse populations of macrophages are involved in promoting anti-inflammatory effects, as well fibrolysis (29). Macrophage depletion has been shown to compromise fibrolysis during the regression of liver fibrosis (30).

Using bone marrow chimeric mice, the present study has demonstrated the migration of bone marrow-derived cells to the liver, particularly to the fibrous septa, during the development of cirrhosis. A small number of BMC participated in the generation of hepatocytes in chimeric mice submitted to a cirrhosis-inducing protocol. A few GFP$^+$ hepatocytes were also found in chimeric mice and in BMC-transplanted mice chronically infected with

Schistosoma mansoni (31). Previous reports have indicated that the finding of bone marrow-derived hepatocytes may be the result of fusion of BMC with hepatocytes (32). As we did not observe the presence of bone marrow-derived hepatocytes 2 months after cell transplantation, the contribution of these cells to hepatocyte renewal was not found to be relevant to the repair process.

BMC were found mainly in the fibrous septa of BMC-transplanted cirrhotic mice, and promoted regression of fibrosis, suggesting the potential anti-fibrogenic role of BMC by accelerating the process of fibrosis regression that was observed naturally 2 months after the withdrawal of $CCl_4 + EtOH$. This result was only achieved in the groups of mice treated with repeated injections of BMC over a 3-week period, and after the withdrawal of $CCl_4 + EtOH$. We were unable to detect any improvement in liver fibrosis when mice were treated with BMC during the cirrhosis induction protocol. In another study,
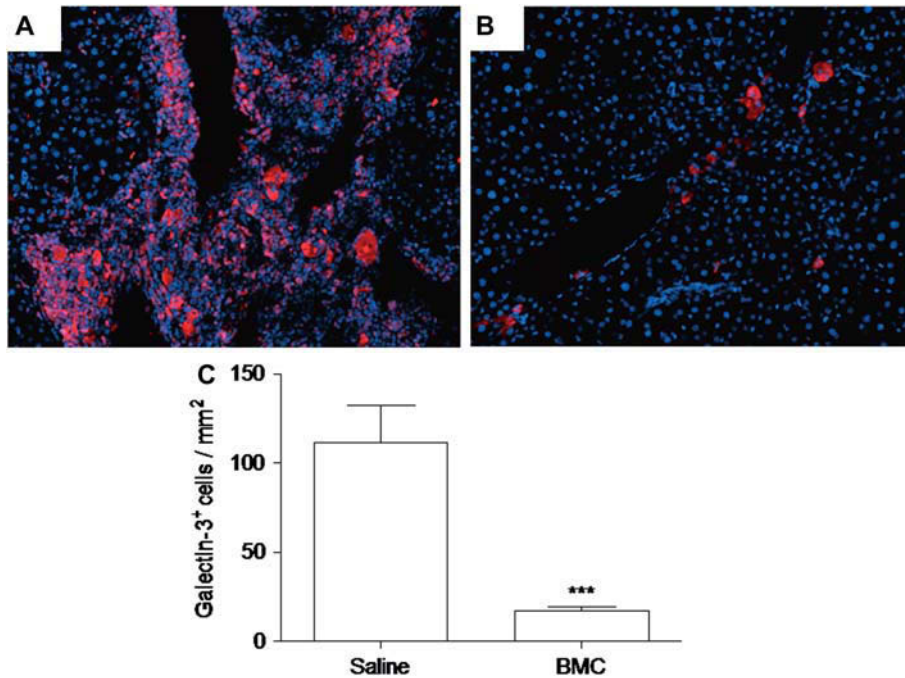
Figure 7. Reduced numbers of galectin-3$^+$ cells in livers of BMC-treated mice 2 months after therapy. Immunofluorescence for galectin-3 detection (red) in 5-mm frozen liver slices of saline-treated (A) (400×) and BMC-treated (B) (400×) mice, counterstained with DAPI (blue) for nuclei visualization. Quantification of galectin-3$^+$ cells in saline-treated and BMC-treated groups (C). Data represent the means ± SEM of five to eight animals/group. ***$P < 0.0001$.

increased fibrosis was found when unfractionated BMC were transplanted into mice that were still being injured by CCl_4 (33).

The reduction of fibrosis after BMC transplantation may be because of the modulatory effects exerted by the transplanted cells on non-parenchymatous liver cells. We observed a reduction in the total number of inflammatory cells, including phagocytes. Moreover, in our chronic experimental model, there was a strong relationship between the amount of fibrous tissue and the numbers of galectin-3$^+$ cells, which were mostly F4/80$^+$ macrophages. Macrophages have been shown to be key modulator cells in fibrogenesis, because they produce a number of mediators, including galectin-3 (29). There is evidence that galectin-3 induces a variety of intracellular signaling pathways that lead to the proliferation of hepatic stellate cells (8). This factor is an important activator of fibroblasts (6–8) and plays a pro-fibrotic role by regulating myofibroblast activation during fibrogenesis (7).

TGF-β1, a cytokine that promotes fibrosis in many organs, is mainly produced by hepatic stellate cells and stimulates the production of ECM components (34). The present study did not find any significant differences in TGF-β1 mRNA levels between saline- and BMC-treated groups. Similar results were obtained with protein assessment by enzyme-linked immunosorbent assays (ELISA) in liver fragments (data not shown). This could be

explained by the fact that TGF-β1, as well as being a known pro-fibrogenic cytokine because of its effect on myofibroblast proliferation and collagen production, it is also a very important anti-inflammatory cytokine (35). In fact, this duality may explain the failure of TGF-β1-signaling inhibitors in the treatment of other fibrotic diseases (35). It is possible that a modulation of pro-fibrotic macrophage subsets, rather than a direct modulation of the production of TGF-β1, could explain our results. Studies using galectin-3-null mice treated with CCl_4 showed that galectin-3 may be required for TGF-β-mediated myofibroblast activation and ECM production (7). Thus the marked reduction in galectin-3 expression after BMC transplantation suggests that the TGF-β-mediated pathway and, consequently, ECM deposition might be affected by transplanted BMC.

Previous reports have shown the expression of MMP, which are associated with a reduction of liver fibrosis after cell transplantation, by bone marrow-derived cells (19,36). It has also been reported previously that liver macrophages can recruit neutrophils during the recovery phase. These cells also express MMP, which promote fibrolysis (37). Although the present study did not find alterations in MMP-9 and TIMP-1 gene expression levels among saline- and BMC-treated cirrhotic mice, it is possible that other MMP, such as MMP-13, may be involved in the

process of fibrosis regression after cell transplantation (36,38).

In conclusion, the present study has established a mouse model of cirrhosis with morphologic characteristics similar to those found in human cirrhosis, and shown that transplanted BMC migrate to the liver, where they modulate inflammation and fibrosis. The findings of a reduction in fibrous tissue and low galectin-3 expression in animals submitted to cell transplantation reiterate the role this molecule plays in the development of fibrosis, and calls attention to its importance as a target for anti-fibrotic therapies. Additional studies attempting to understand BMC cell populations better and the mechanisms by which BMC transplantation ameliorates hepatic diseases should be conducted to develop successful clinical therapies for liver fibrosis.

Conflict of interest statement: The authors claim they have no conflict of interest in this study.

References

1. Corrao G, Arico S. Independent and combined action of hepatitis C virus infection and alcohol consumption on the risk of symptomatic liver cirrhosis. Hepatology. 1998;27:914–19.
2. Keeffe EB. Liver transplantation: current status and novel approaches to liver replacement. Gastroenterology. 2001;120: 749–62.
3. Tsui JI, Pletcher MJ, Vittinghoff E, Seal K, Gonzales R. Hepatitis C and hospital outcomes in patients admitted with alcohol-related problems. J Hepatol. 2006;44:262–6.
4. Dranoff JA, Wells RG. Portal fibroblasts: underappreciated mediators of biliary fibrosis. Hepatology. 2010;51:1438–44.
5. Forbes SJ, Parola M. Liver fibrogenic cells. Best Pract Res Clin Gastroenterol. 2011;25:207–17.
6. Sasaki S, Bao Q, Hughes RC. Galectin-3 modulates rat mesangial cell proliferation and matrix synthesis during experimental glomerulonephritis induced by anti-Thy1. 1 antibodies. J Pathol. 1999;187:481–9.
7. Henderson NC, Mackinnon AC, Farnworth SL, Poirier F, Russo FP, Iredale JP, et al. Galectin-3 regulates myofibroblast activation and hepatic fibrosis. Proc Natl Acad Sci USA. 2006;103:5060–5.
8. Maeda N, Kawada N, Seki S, Arakawa T, Ikeda K, et al. Stimulation of proliferation of rat hepatic stellate cells by galectin-1 and galectin-3 through different intracellular signaling pathways. J Biol Chem. 2003;278:18938–44.
9. Higashiyama R, Moro T, Nakao S, Mikami K, et al. Negligible contribution of bone marrow-derived cells to collagen production during hepatic fibrogenesis in mice. Gastroenterology. 2009:137:1459–66.
10. Bataller R, Brenner DA. Liver fibrosis. J Clin Invest. 2005;115: 209–18.
11. Neuberger J. Liver transplantation. J Hepatol. 2000;32:198–207.
12. Mimeault M, Hauke R, Batra SK. Stem cells: a revolution in therapeutics – recent advances in stem cell biology and their therapeutic applications in regenerative medicine and cancer therapies. Clin Pharmacol Ther. 2007;82:252–64.
13. Lagasse E, Connors H, Al-Dhalimy M, Reitsma M, Dohse M, et al. Purified hematopoietic stem cells can differentiate into hepatocytes in vivo. Nat Med. 2000;6:1229–34.
14. Oyagi S, Hirose M, Kojima M, Okuyama M, Kawase M, et al. Therapeutic effect of transplanting HGF-treated bone marrow mesenchymal cells into CCl$_4$-injured rats. J Hepatol. 2006;44:742–8.
15. Vassilopoulos G, Wang PR, Russell DW. Transplanted bone marrow regenerates liver by cell fusion. Nature. 2003;422:901–4.
16. Jang YY, Collector MI, Baylin SB, Diehl AM, Sharkis SJ. Hematopoietic stem cells convert into liver cells within days without fusion. Nat Cell Biol. 2004;6:532–9.
17. Caplan AI, Dennis JE. Mesenchymal stem cells as trophic mediators. J Cell Biochem. 2006;98:1076–84.
18. Fang B, Shi M, Liao L, Yang S, Liu Y, et al. Systemic infusion of FLK1(+) mesenchymal stem cells ameliorate carbon tetrachloride-induced liver fibrosis in mice. Transplantation. 2004;78:83–8.
19. Sakaida I, Terai S, Yamamoto N, Aoyama K, Ishikawa T, et al. Transplantation of bone marrow cells reduces CCl$_4$-induced liver fibrosis in mice. Hepatology. 2004;40:1304–11.
20. Zhao DC, Lei JX, Chen R, Yu WH, Zhang XM, et al. Bone marrow-derived mesenchymal stem cells protect against experimental liver fibrosis in rats. World J Gastroenterol. 2005;11:3431–40.
21. Higashiyama R, Inagaki Y, Hong YY, Kushida M, Nakao S, et al. Bone marrow-derived cells express matrix metalloproteinases and contribute to regression of liver fibrosis in mice. Hepatology. 2007;45:213–22.
22. Yannaki E, Athanasiou E, Xagorari A, Constantinou V, Batsis I, et al. G-CSF-primed hematopoietic stem cells or G-CSF per se accelerate recovery and improve survival after liver injury, predominantly by promoting endogenous repair programs. Exp Hematol. 2005;33:108–19.
23. Di Campli C, Piscaglia AC, Pierelli L, Rutella S, Bonanno G, et al. A human umbilical cord stem cell rescue therapy in a murine model of toxic liver injury. Dig Liver Dis. 2004;36:603–13.
24. Tang XP, Yang X, Tan H, Ding YL, Zhang M, et al. Clinical and experimental study on the therapeutic effect of umbilical cord blood transplantation on severe viral hepatitis. World J Gastroenterol. 2003;9:1999–2003.
25. Souza BS, Nogueira RC, De Oliveira SA, De Freitas LA, Lyra LG, et al. Current status of stem cell therapy for liver diseases. Cell Transplant. 2009;18:1261–79.
26. Danguy A, Camby I, Kiss R. Galectins and cancer. Biochim Biophys Acta. 2002;1572:285–93.
27. Lyra AC, Soares MB, da Silva LF, Braga EL, et al. Infusion of autologous bone marrow mononuclear cells through hepatic artery results in a short-term improvement of liver function in patients with chronic liver disease: a pilot randomized controlled study. Eur J Gastroenterol Hepatol. 2010;22:33–42.
28. Kisseleva T, Uchinami H, Feirt N, Quintana-Bustamante O, et al. Bone marrow-derived fibrocytes participate in pathogenesis of liver fibrosis. J Hepatol. 2006;45:429–38.
29. Wynn TA, Barron L. Macrophages: master regulators of inflammation and fibrosis. Semin Liver Dis. 2010;30:245–57.
30. Duffield JS, Forbes SJ, Constandinou CM, Clay S, Partolina M, et al. Selective depletion of macrophages reveals distinct, opposing roles during liver injury and repair. J Clin Invest. 2005;115:56–65.
31. Oliveira SA, Souza BS, Guimaraes-Ferreira CA, Barreto ES, Souza SC, et al. Therapy with bone marrow cells reduces liver alterations in mice chronically infected by Schistosoma mansoni. World J Gastroenterol. 2008;14:5842–50.
32. Wang X, Willenbring H, Akkari Y, Torimaru Y, Foster M, et al. Cell fusion is the principal source of bone-marrow-derived hepatocytes. Nature. 2003;422:897–901.
33. Thomas JA, Pope C, Wojtacha D, Robson AJ, Gordon-Walker TT, et al. Macrophage therapy for murine liver fibrosis recruits

host effector cells improving fibrosis, regeneration and function. Hepatology. 2011;53:2003–15.

34. Gressner AM, Weiskirchen R, Breitkopf K, Dooley S. Roles of TGF-beta in hepatic fibrosis. Front Biosci. 2002;7:793–807.

35. Fattouh R, Jordana M. TGF-beta, eosinophils and IL-13 in allergic airway remodeling: a critical appraisal with therapeutic considerations. Inflamm Allergy Drug Targets. 2008; 7:224–36.

36. Rabani V, Shahsavani M, Gharavi M, Piryaei A, Azhdari Z, et al. Mesenchymal stem cell infusion therapy in a carbon tetrachloride-induced liver fibrosis model affects matrix metalloproteinase expression. Cell Biol Int. 2010;34: 601–5.

37. Harty MW, Papa EF, Huddleston HM, Young E, Nazareth S, et al. Hepatic macrophages promote the neutrophil-dependent resolution of fibrosis in repairing cholestatic rat livers. Surgery. 2008;143:667–78.

38. Fallowfield JA, Mizuno M, Kendall TJ, Constandinou CM, Benyon RC, et al. Scar- associated macrophages are a major source of hepatic matrix metalloproteinase-13 and facilitate the resolution of murine hepatic fibrosis. J Immunol. 2007; 178:5288–95.

8.2 ANEXO II

SOARES, M. B. et al. Reversion of gene expression alterations in hearts of mice with chronic chagasic cardiomyopathy after transplantation of bone marrow cells. Cell Cycle, v. 10, n. 9, May, p. 1448-1455, 2011.

Reversion of gene expression alterations in hearts of mice with chronic chagasic cardiomyopathy after transplantation of bone marrow cells

Milena B.P. Soares,[1,2,]* Ricardo S. Lima,[3] Bruno S.F. Souza,[1,2] Juliana F. Vasconcelos,[1,2] Leonardo L. Rocha,[1]
Ricardo Ribeiro dos Santos,[1,2] Sanda Iacobas,[4] Regina C. Goldenberg,[5] Michael P. Lisanti,[9] Dumitru A. Iacobas,[4]
Herbert B. Tanowitz,[6,7,]* David C. Spray[4,6] and Antonio C. Campos de Carvalho[4,5,8]

[1]Centro de Pesquisas Gonçalo Moniz; Fundação Oswaldo Cruz; [2]Hospital São Rafael; Salvador, Brazil; [3]Departamento de Medicina; Universidade Federal do Vale do São Francisco; Petrolina, Pe Brazil; [4]Dominick P. Purpura Department of Neuroscience; Albert Einstein College of Medicine; Bronx, NY USA; [5]Instituto de Biofísica Carlos Chagas Filho; Universidade Federal do Rio de Janeiro; [8]Instituto Nacional de Cardiologia; Rio de Janeiro, Brazil; [6]Department of Medicine; [7]Department of Pathology; Albert Einstein College of Medicine; Bronx, NY USA; [9]Department of Stem Cell Biology and Regenerative Medicine; Kimmel Cancer Center; Thomas Jefferson University; Philadelphia, PA USA

Chronic chagasic cardiomyopathy is a leading cause of heart failure in Latin American countries, being associated with intense inflammatory response and fibrosis. We have previously shown that bone marrow mononuclear cell (BMC) transplantation improves inflammation, fibrosis and ventricular diameter in hearts of mice with chronic Chagas disease. Here we investigated the transcriptomic recovery induced by BMC therapy by comparing the heart transcriptomes of chagasic mice treated with BMC or saline with control animals. Out of the 9,390 unique genes quantified in all samples, 1,702 had their expression altered in chronic chagasic hearts compared to those of normal mice. Major categories of significantly upregulated genes were related to inflammation, fibrosis and immune responses, while genes involved in mitochondrion function were downregulated. When BMC-treated chagasic hearts were compared to infected mice, 96% of the alterations detected in infected hearts were restored to normal levels, although an additional 109 genes were altered by treatment. Transcriptomic recovery, a new measure that considers both restorative and side effects of treatment, was remarkably high (84%). Immunofluorescence and morphometric analyses confirmed the effects of BMC therapy in the pattern of inflammatory-immune response and expression of adhesion molecules. In conclusion, by using large-scale gene profiling for unbiased assessment of therapeutic efficacy we demonstrate immunomodulatory effects of BMC therapy in chronic chagasic cardiomyopathy and identify potentially relevant factors involved in the pathogenesis of the disease that may provide new therapeutic targets.

Introduction

The discovery of stem cells with potential therapeutic properties to promote tissue regeneration recovery has opened new avenues for the treatment of degenerative and traumatic disorders, including heart failure. Patients with Chagas disease, one of the main causes of heart failure in Latin American countries, could possibly benefit from a stem cell-based therapy aiming to ameliorate the heart function deteriorated by the chronic infection with *Trypanosoma cruzi*. Currently, heart transplantation is the only efficient therapy for chagasic patients with heart failure, a procedure limited by the scarcity of donated organs and complications when performed in *T. cruzi*-infected patients due to the risk of a resurgence of parasitemia and tissue parasitism upon administration of immunosuppressive drugs. Therefore, instead of replacing the hearts of chagasic heart

failure individuals, the perspective of decreasing the damage of the heart and restoring pre-infection status with cell-based therapies presents an attractive option that should be investigated.[1]

Chronic chagasic cardiomyopathy is a progressive disease characterized by focal or disseminated inflammation causing myocytolysis, necrosis and progressive deposition of collagen.[2] Transplantation of bone marrow cells (BMC) was reported to reduce inflammation and fibrosis in the heart. The decrease in inflammatory cells correlated with an increase in apoptotic cells in the inflammatory infiltrate.[3] A regression of right ventricular dilation, typically observed in a specific chagasic mouse model, was observed in mice treated with BMC, as detected by magnetic resonance image analysis.[4] In addition, administration of granulocyte-colony stimulating factor (G-CSF), a cytokine capable of mobilizing BMCs to the peripheral blood, to chagasic mice caused a decrease in inflammation
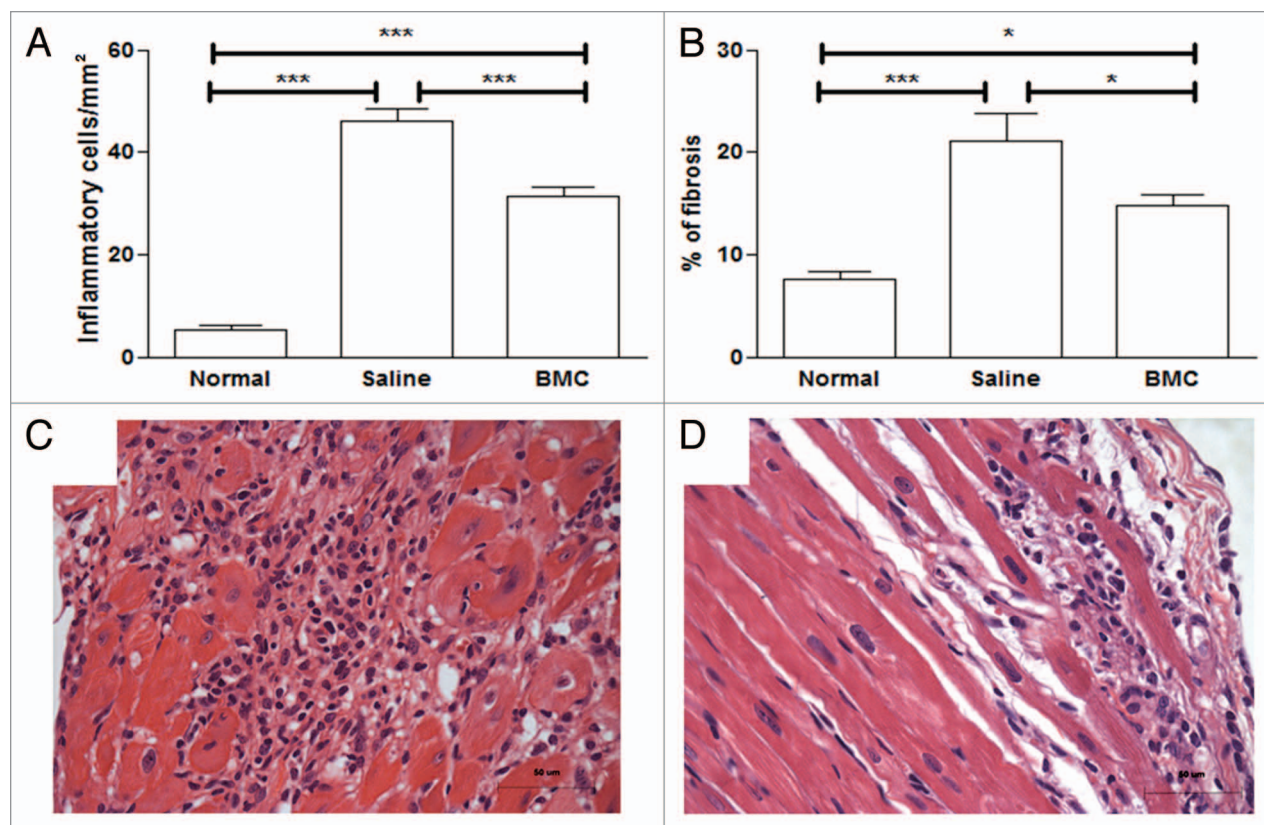
Figure 1. Transplantation of BMC decreases inflammation and fibrosis in hearts of C57Bl/6 mice chronically infected with Colombian strain *T. cruzi*. Mice were infected with 1,000 trypomastigote forms of Colombian strain *T. cruzi*. Inflammation (A) and fibrosis (B) were quantified in heart sections of normal mice, mice 8 months after infection injected with saline (Saline) or with bone marrow cells (BMC), stained with H&E and Sirius red. Bars represent the means ± SEM of 5–8 animals/group at six months after infection. *$p < 0.05$; ***$p < 0.001$. Heart sections of chagasic mice injected with saline (C) or with BMC (D), stained with H&E (original magnification x40).

and fibrosis and improvement of cardiopulmonary function.[5] Altogether, these results suggest a paracrine effect of BMC therapy, modulating the immune response that causes tissue aggression and fibrosis deposition in the heart.[1]

The identification of the mechanisms by which BMCs modulate the immune-inflammatory response and promote improvement of cardiac damage in infected mice may contribute to the development of more efficient therapies for chagasic patients. We have previously shown that a number of genes related to inflammation and fibrosis are altered in the hearts of chagasic mice compared to normal controls.[6] In this study we have used cDNA microarray analysis as an unbiased, high throughput approach to evaluate the efficacy of transplantation of BMC to restore the normal transcriptome in the myocardium of mice chronically infected with *T. cruzi*. Our results show a marked transcriptomic recovery caused by the BMC therapy in the hearts of mice with chronic chagasic cardiomyopathy and suggest that such an analytical approach may be useful to evaluate efficacy of other treatments for various pathological conditions.

Results

Injection of BMCs in mice with chronic chagasic cardiomyopathy reduces inflammation and fibrosis. Mice infected with

the Colombian strain of *T. cruzi* develop a progressive myocarditis accompanied by fibrosis during the chronic phase of infection. Treatment with BMCs caused a decrease in the number of inflammatory cells (**Fig. 1A**) and a reduction in fibrosis (**Fig. 1B**) compared to saline-treated controls. An intense multifocal inflammatory response composed mainly by mononuclear cells, associated with myocytolysis, was observed in sections of saline-treated chagasic mice (**Fig. 1C**). Smaller and less frequent foci of inflammatory cells were found in heart sections of chagasic mice treated with BMCs (**Fig. 1D**).

Gene regulation by BMC transplantation. We compared transcriptomic changes in the BMC-treated and untreated infected mouse hearts with respect to the uninfected hearts, defining as significantly regulated those genes whose mean expression level changed by more than 1.5-fold and that were different at the 0.05 level of significance when the variation among the four biological replicas was considered. Microarray results have been deposited in www.ncbi.nlm.nih.gov/gds as GSE24088. Two months after transplantation of BMC (at eight months after infection), 9,390 genes were quantifiable on all twelve arrays (from uninfected controls, infected and saline-treated and BMC treated infected hearts); of these, 480 (5.12%) were downregulated and 1,222 (13.01%) were upregulated in the infected saline-treated hearts. GenMapp analysis was used to determine whether regulated

genes encoding proteins performing specific functions were differentially affected. Of the upregulated genes, most prominent Gene Ontology (GO) terms that corresponded to these pathways were immune system process/immune response, chemokine receptor binding and chemokine activity, including inflammatory response and chemotaxis genes *Ccl12, Ccl6, Ccl7, Ccl8* (50-fold upregulated), *Ccl9* (40-fold upregulated) and *Cxcl1*. Downregulated genes in the infected hearts were most prominently associated with mitochondria (cofactor binding, TCA cycle, glycoloysis, oxidative phsophorylation, coenzyme biosynthesis, oxydoreductase activity, electron transport, NADH, RNA biosynthesis), although other affected pathways included axon guidance receptor (*Ephb3, Q8c419),* negative regulation of BMP signaling *(Htra1, Twsg1, Flt1)*, transmembrane receptor tyrosine kinase activity (*Erbb3, Ephb3, Q8c419*), cell cycle arrest (*Ak1, Cdkn1b, Cdkn1c, Sesn1*) and multidrug transport (*Slc47a1*).

In the infected hearts of mice treated with BMC, we found that expression of 103 genes (1.21% of the quantified genes) were upregulated compared to controls and 77 (0.91%) were downregulated. Most prominent categories of upregulated genes were those associated with angiogenesis and blood vessel development (*Casp8, Col18a1, Dicer1, Myh9, Pdgfa, Tnfrsf12a, Cxcl12, Fgf8, Serpinf1, Stab1, Btg1, Notch1*) and endothelial cell development (*Vezf1*), thiamin transport and folate carrier activity (*Slc19a2*) and vitamin biosynthesis (*Itgb1bp3*), cyclin binding (*Cdkn1a*) and purine catabolism (*Ampd2*). Downregulated gene categories included nuclear transport (*Rangrf, Akt1*), cofactor metabolic process (*Akt1, Ndufs1, Ldhd, Acss1, Idh3a, Sdha, Sucla2, Suclg2, Coq5, Coq6, Coq9*) and isomerase activity (*flbp10, hsd367, Fkpb10, Hsd3b7, Tpi1*), calcium ion binding (*Eef2k, Fkbp10, Frem2*) and cell cycle arrest (*Ak1, Cdkn1b)*. The remarkable restoration of the control gene expression pattern by BMC therapy of infected mice is summarized in **Figure 2** and is quantified by the TRE score, calculated as follows:

$$
TRE = \frac{\overbrace{454}^{DX} + \overbrace{1166}^{UX} - \overbrace{62}^{XD} - \overbrace{46}^{XU}}{\underbrace{454}_{DX} + \underbrace{1166}_{UX} + \underbrace{62}_{XD} + \underbrace{46}_{XU} + \underbrace{39}_{DD} + \underbrace{0}_{DU} + \underbrace{1}_{UD} + \underbrace{31}_{UU}} \times 100\% = 84\%
$$

where initials above the numbers indicate whether the genes were down (D), up (U) or not (X) regulated in the infected and saline-treated hearts (first letter) or BMC-treated hearts (second letter) with respect to control hearts. Note that only 70 genes (of 1,702) retained their up (31) or down (39) regulation in the chagasic heart following BMC therapy and only a single gene was switched between up and downregulated (UD).

Alterations in the expression pattern of galectin-3 and syndecan-4 in hearts of mice with chronic chagasic cardiomyopathy after BMC transplantation. The expression of two proteins encoded by genes upregulated by *T. cruzi* infection and modulated by BMC therapy was investigated by confocal analysis. Galectin-3 was found highly expressed in macrophages of the inflammatory infiltrate in chagasic hearts, when compared to non-infected controls (**Figs. 3A, 4A and C**). Upon BMC treatment, the number of galectin-3 positive cells was significantly

reduced in heart sections of chagasic mice (**Figs. 3A and 4E**). Syndecan-4, a heparan-sulfate proteoglycan that regulates cell-matrix interactions and is present in focal adhesions, was found highly expressed in endothelial cells in chagasic hearts compared to normal mice (**Fig. 4B and D**). Heart sections of BMC-treated mice showed a significant reduction in the intensity of syndecan-4 staining and in the number of syndecan-4+ blood vessels (**Figs. 3B, C and 4F**). In contrast, the total number of blood vessels was similar in the three groups, as indicated by staining with antibodies against von Willebrand Factor (**Fig. 3D**).

Discussion

Stem cell transplantation has become an attractive therapeutic possibility for patients with cardiac diseases, including chronic chagasic cardiomyopathy. The demonstration that BMC transplantation has beneficial effects in hearts of mice with chronic chagasic cardiomyopathy has raised several questions and the determination of the molecular and cellular mechanisms by which these cells exert their action may contribute to the development of new therapeutic strategies for chronic chagasic cardiomyopathy based on cell transplantation and/or cell factors. Here we performed a microarray analysis in an attempt to understand some of the mechanisms involved in the activity of BMC in the mouse model of chronic chagasic cardiomyopathy. Gene expression analysis was carried out comparing hearts of mice with chronic chagasic cardiomyopathy treated or not with BMC and non-infected controls. We have found that most of the genes altered by infection are modulated by BMC therapy, indicating a dramatic effect of these cells in the mechanisms of pathogenesis of the disease. The use of large-scale gene profiling for unbiased assessment of therapeutic efficacy is thus a major contribution of the present work to cell based therapies.

Previously we have shown that a significant number of genes with expression altered in the heart by infection with the Colombian *T. cruzi* strain are related to inflammation and fibrosis.[6] As expected, since BMC therapy causes a significant decrease in inflammation and fibrosis, we found that most of these upregulated genes in chronic chagasic cardiomyopathy have their expression in the heart decreased after cell therapy.

The decrease in inflammation observed two months after BMC therapy (at a total of eight months post-infection) was previously associated with an increased number of apoptotic cells compared to untreated chagasic controls.[3] In contrast to the high number of inflammatory cells undergoing apoptosis during the indeterminate stage,[7] a reduced number (about 0.5%) of cells in the inflammatory infiltrate were found undergoing apoptosis in hearts of individuals with chronic chagasic cardiomyopathy.[8] We found several genes related to apoptosis altered by *T. cruzi* infection and modulated by BMC therapy. Analysis such as the one used in this study will detect global alterations in gene expression, representing all cell types present in the heart, including cardiomyocytes and inflammatory cells. Thus, additional studies are needed to clarify which mechanisms are involved in the prevention of apoptosis of inflammatory cells in chronic chagasic cardiomyopathy, as well as those promoting apoptosis after BMC therapy.
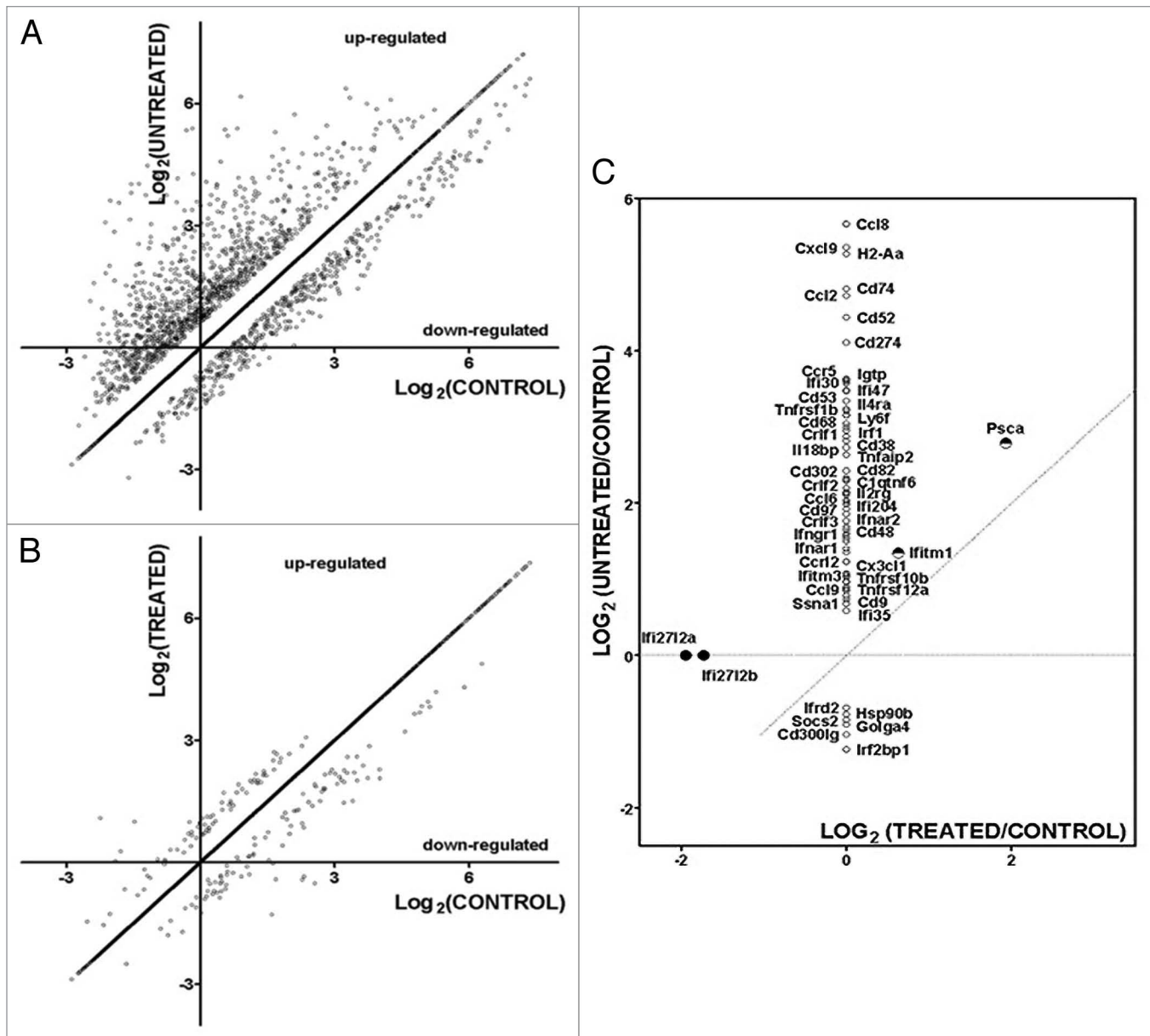
Figure 2. Significantly regulated genes in BMC-untreated (injected with saline) (A) and BMC-treated (B) infected hearts with respect to controls. A substantial reduction in the number of regulated genes was observed in treated hearts. Significantly regulated immune response genes in untreated (vertical axis) and treated (horizontal axis) (C). Symbols of certain regulated genes were written close to their representative points. Note that, while the upregulation of *ifitm1* and psca was reduced by treatment, the regulation of all other immune response gene was fully recovered. However, *Ifi27l2a* and *Ifi27l2b*, whose expression was not significantly altered by the infection, were found as downregulated in treated hearts.

The inflammatory infiltrate present in hearts of mice with chronic chagasic cardiomyopathy is mainly composed by mononuclear cells found adhered to myofibers, many of them in process of myocytolysis.[2] Macrophages are one of the main populations found in the inflammatory site, and are highly activated by IFNγ and TNFα, two cytokines produced in the hearts of chagasic mice.[6] Here we found that the expression of galectin-3 (also known as Mac-2), a member of a large family of lectins that are highly conserved throughout animal evolution, upregulated in chagasic mice, is modulated by BMC therapy. By immunofluorescence analysis, we showed that this molecule is expressed mainly in macrophages within the inflammatory infiltrate in the hearts of chagasic mice. A previous study has demonstrated, in a model of hypertrophied heart in rats, that galectin-3 was the most overexpressed gene in failing versus functionally compensated hearts.[9] Galectin-3 colocalized with activated myocardial macrophages and treatment of rats with recombinant galectin-3 induced cardiac fibroblast proliferation, collagen production, cyclin D1 expression and left ventricular dysfunction.[9] In addition, galectin-3 is known to play important roles in inflammatory responses, including suppression of T-cell apoptosis and its expression is induced by IFNγ in macrophages found in
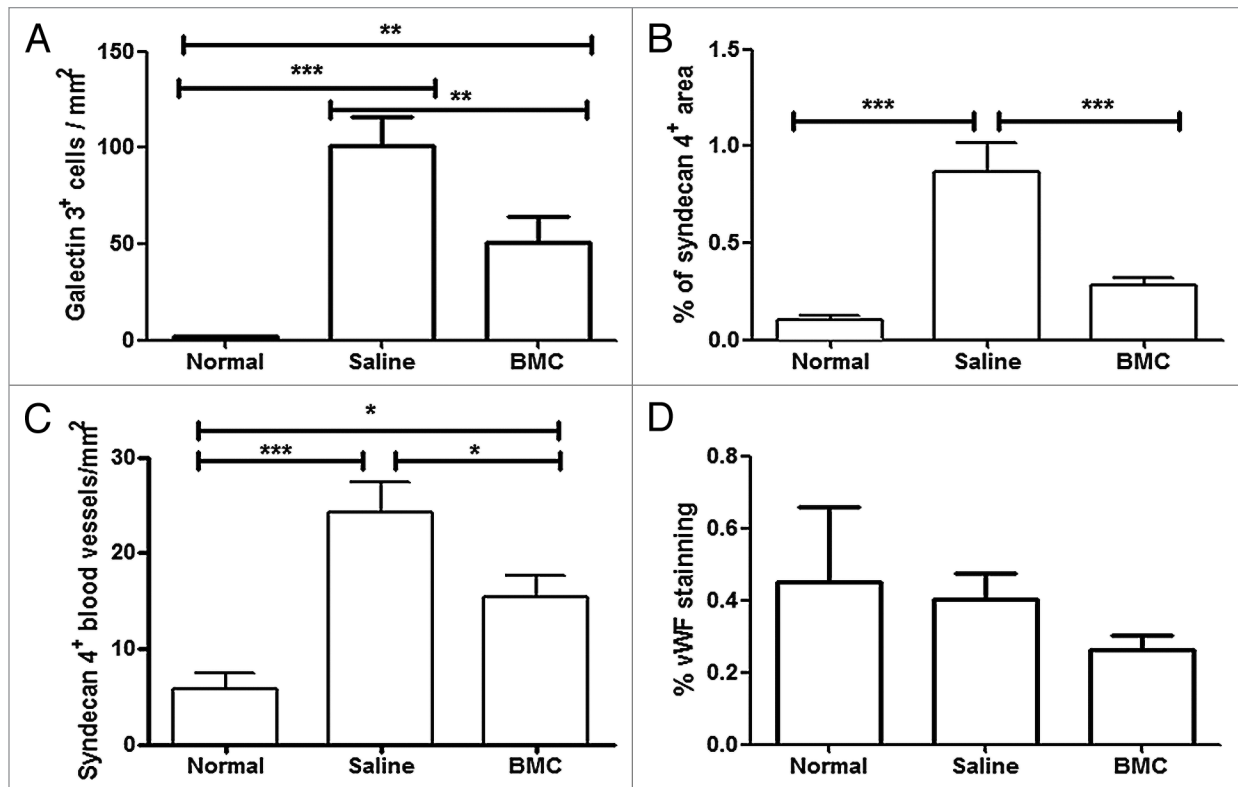
Figure 3. Quantification of galectin-3, syndecan-4 and vWF. Expression of galectin-3 (A), syndecan-4 (B and C) and vWF (D) were quantified by immunohistochemistry and morphometric analysis in heart sections of normal or eight month chagasic mice that had been injected at six months after infection with saline (Saline) or with bone marrow cells (BMC). Bars represent the means ± SEM of 3 animals/group. *p < 0.05; **p < 0.01; ***p < 0.001.

inflammatory infiltrates in the heart.[10,11] Altogether, these data suggest an important role of galectin-3 in the pathogenesis of chronic chagasic cardiomyopathy, and indicate this molecule as a target for development of new treatments for chronic chagasic cardiomyopathy. In fact, galectin-3 production has recently been pointed out as a novel marker of heart failure in patients.[12]

Another molecule with its gene expression modulated by BMC therapy was syndecan-4, a heparin sulfate-carrying cell surface protein expressed by a number of different cell types, including endothelial cells, smooth muscle cells and cardiac myocytes that participates in processes of cell signaling, adhesion and migration.[13,14] Little is known about the regulation of syndecan-4, but it has been reported to increase after various forms of tissue injury including vascular wall injury,[13] or myocardial infarction.[14] Syndecan-4 expression has been shown to be increased with migration of blood-derived macrophages after myocardial infarction.[14] Zhang et al. (1999) have shown that TNFα is the principal factor produced by the ischemic myocytes responsible for induction of endothelial cell syndecan-4 expression.[15] To our knowledge, this is the first study investigating the expression of syndecan-4 in Chagas disease. The fact that TNFα levels are increased in chronic chagasic hearts may explain the finding of enhanced expression of syndecan-4 observed herein.[6] Furthermore, the modulation of the chronic inflammatory response in chagasic hearts induced by BMC therapy may explain the reduction of syndecan-4 expression found in BMC-treated animals.

A correlation between intensity of expression of syndecan-4 in endothelial cells was found in close association with inflammatory infiltrates, but this was not due to an increase in the number of vWF+ blood vessels. The microarray analysis suggested an increase in angiogenesis in hearts of chronic chagasic mice after BMC therapy, but this was not confirmed by the immunohistochemistry analysis. This apparent disparity may be explained by the fact that the genes upregulated after BMC therapy, participate in a number of other biological processes in addition to those related to blood vessel formation, such as apoptosis.[16-18]

We previously commented on the prominent upregulation of immune response genes in the chagasic heart and validated substantial numbers of these gene products using ELISA, real-time PCR and confocal microscopy.[6] The identification of mitochondria-associated genes as one of the pathways that are most downregulated in the infected heart is entirely consistent with reports by Garg and others indicating that mitochondrial function is a prominent target of infection in acute and chronic states.[19-21]

Gene expression profiling with microarrays has been widely used to characterize tissue and cell responses to various stimuli, to identify disease biomarkers and to reveal components and interplay within and between gene regulatory networks. The application of this unbiased high throughput method to compare a pathological situation with changes occurring after a therapeutic regimen here revealed a striking degree of recovery of control gene expression status in infected mice treated with BMC. As
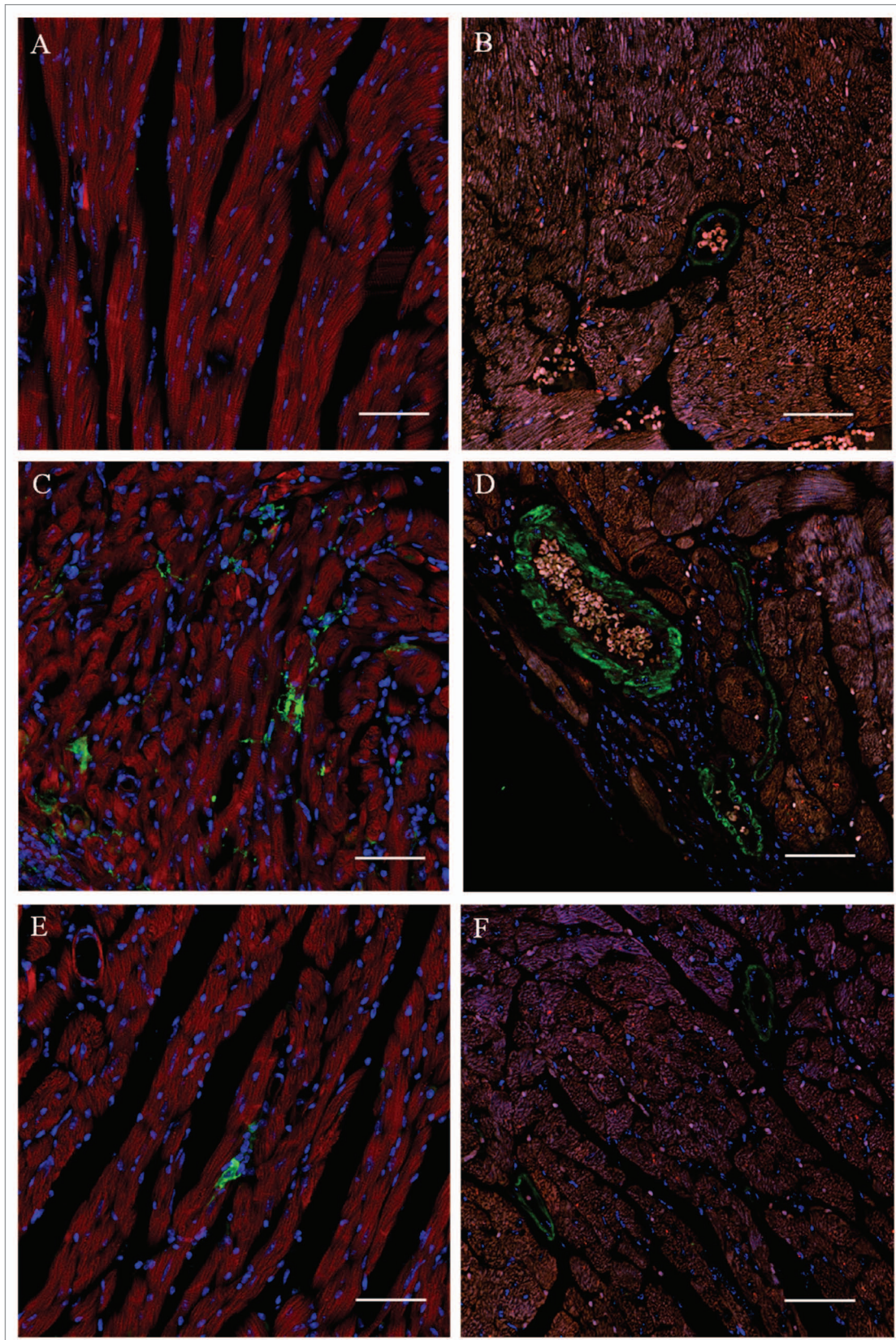
Figure 4. Expression of galectin-3 and syndecan-4 in hearts of chronic chagasic mice treated with bone marrow cells. Heart sections of normal mice (A and B), of mice injected with saline (C and D) or with BMC (E and F). Sections were stained (red) with anti-galectin-3 (A, C and E) or anti-syndecan-4 (B, D and F). Nuclei (blue) were stained with DAPI. Scale bars: 50 μm (original magnification x40).

we previously showed in a study examining structural and physiological parameters of hearts of chagasic mice, the BMC therapy not only prevents further damage over time but also reverses the damage that was present before the stem cells were injected.[4]

In conclusion, this unbiased global gene expression analysis indicated a potent restorative effect of BMC in the hearts of mice with chronic chagasic cardiomyopathy, with over 90% recovery of normal expression level of genes altered by *T. cruzi* infection. This impressive effect is most probably mediated by a paracrine effect through the secretion of soluble mediators. From this global expression profile identification of such factors is possible and may lead to the association or the replacement of cell therapy by these cellular hormones in order to achieve the desired repair to the damaged chagasic heart.

Materials and Methods

Animals. Four week-old female and male C57Bl/6 mice were used for *T. cruzi* infection. All animals, weighing 20–23 g, were raised and maintained at the Gonçalo Moniz Research Center/FIOCRUZ in rooms with controlled temperature (22 ± 2°C) and humidity (55 ± 10%) and continuous air flow. Animals were housed in a 12 h light/12 h dark cycle (6 am–6 pm) and provided with rodent diet and water ad libitum. Animals were handled according to the NIH guidelines for animal experimentation. All procedures described had prior approval from the local IACUC (Albert Einstein College of Medicine and Fiocruz, Bahia).

Infection with *Trypanosoma cruzi*. Trypomastigotes of the myotropic Colombian *T. cruzi* strain were obtained from culture supernatants of infected LCC-MK2 cells. Infection of C57Bl/6 mice was performed by intraperitoneal injection of 1,000 *T. cruzi* trypomastigotes in saline. Parasitemia of infected mice was evaluated at various times after infection by counting the number of trypomastigotes in peripheral blood aliquots.

Bone marrow cell (BMC) transplantation. BMCs obtained from femurs and tibiae of C57Bl/6 mice were used in transplantation experiments.[3,4] Briefly, BMCs were purified by centrifugation in Ficoll gradient at 1,000 g for 15 minutes (Histopaque 1119 and 1077, 1:1; Sigma, St. Louis, MO). After two washings in RPMI medium (Sigma), the cells were resuspended in saline, filtered over nylon wool and injected intravenously in chagasic mice (3 x 10^6 cells/mouse) six months after infection. Non-transplanted control mice received intravenous injections of the same volume (200 µl) of saline.

Morphometric analysis. Groups of mice were sacrificed at two months after BMC or saline injection (at eight months after infection) and hearts removed and fixed in 10% buffered formalin. Heart sections were analyzed by light microscopy after paraffin embedding, followed by standard hematoxylin/eosin staining. Inflammatory cells infiltrating heart tissue were counted using a digital morphometric evaluation system. Images were digitized using a color digital video camera adapted to a microscope. The images were analyzed using the Image Pro Program (Media Cybernetics, San Diego, CA), such that the inflammatory cells were counted and integrated with respect to area. Ten fields per section were counted in 5–10 sections per heart. The percentage

of fibrosis was determined using Sirius red-stained heart sections and the Image Pro Plus v.7.0 Software to integrate the areas.

Immunofluorescence. Frozen or formalin-fixed paraffin embedded hearts were sectioned and 4 µm-thick sections were used for detection of galectin-3 and syndecan-4 expression by immunofluorescence. First, paraffin embedded sections were deparaffinized and a heat-induced antigen retrieval step in citrate buffer (pH = 6.0) was performed. Then, sections were incubated overnight with the following primary antibodies: anti-galectin-3, 1:50 (Santa Cruz Biotechnology), anti-syndecan-4, 1:50 (Santa Cruz Biotechnology) or anti-vWF, 1:100 (Dako). On the following day, sections were incubated with Alexa fluor 633 conjugated Phalloidin, 1:50, mixed with one of the secondary antibodies Alexa fluor 488-conjugated anti-goat IgG, 1:200 or Alexa fluor 488-conjugated anti-rabbit IgG, 1:200 (Molecular Probes) for 1 hour. Nuclei were stained with 4,6-diamidino-2-phenylindole (VectaShield Hard Set mounting medium with DAPI H-1500; Vector Laboratories). The presence of fluorescent cells was determined by observation on a FluoView 1000 confocal microscope (Olympus). Approximately 10 random fields per animal were captured using a 40x objective. Morphometric analyses were performed using Image Pro Plus v.7.0 software.

DNA microarray and data analysis. We compared RNA samples extracted from whole hearts of 4 control, 4 chagasic and 4 BMC-treated chagasic mice by analyzing hybridization to MO30k microarrays printed by Duke University (www.ncbi.nlm.nih.gov/geo/query/acc.cgi?acc=GPL8938) spotted with 70-mer oligonucleotides (mouse Operon version 3.0). The hybridization protocol has already been described in reference 6, the slide type and the scanner settings were uniform throughout the entire experiment to minimize the technical noise. Briefly, 20 µg total RNA extracted in Trizol from each of the twelve samples (individual hearts) was reverse transcribed in the presence of fluorescent Alexa Fluor® 555- and Alexa Fluor®647-aha-dUTPs (Invitrogen, Carlsbad, CA) to obtain labeled cDNA. Red and green labeled samples of biological replicas were then co-hybridized ("multiple yellow" strategy[22]) overnight at 50°C. After washing (0.1% SDS and 1% SSC) to remove the non-hybridized cDNA, each array was scanned at 630 V (635 nm) and 580 V (532 nm) with GenePix 4100B scanner (Axon Instruments, Union City, CA) and images were primarily analyzed with GenePixPro 6.0 (Molecular Devices, Sunnyvale, CA). Microarray data were processed as described previously in reference 6. A gene was considered as significantly up or downregulated when comparing four hearts from one condition to those from another if the absolute fold change was >1.5x and the p-vlaue of the Student's heteroscedastic t-test of equality of the means of the distributions with a Bonferroni-type adjustment for each redundancy group (set of spots probing the same gene) was <0.05. GenMapp[23] and MappFinder (www.genmapp.org) software and associated databases were used to identify the most affected GO (Gene Ontology) categories. In order to determine whether genes differentially expressed in untreated and treated infected hearts with respect to uninfected hearts were disproportionately affected in

specific pathways, we used GenMAPP and MappFinder software (Gladstone Institute; San Francisco: www.genmapp.org) to provide the statistics of affected GO categories. GO sets with fewer than 10 analyzed members were excluded from this analysis.

The novel parameter transcriptomic recovery efficacy (TRE) was computed as:

$$TRE = \frac{DX + UX - XD - XU}{DX + UX + XD + XU + DD + DU + UD + UU} \times 100\%$$

where: D, U, X indicate whether the gene was down, up or not regulated in the saline-treated (first position) or BMC-treated (second position) infected hearts. TRE is thus the percentage of up and downregulated genes in infected hearts whose expression level was restored to normal (UX & DX) penalized by the percentage of not regulated genes in infected hearts whose expression changed due to treatment alone (XD & XU).

Statistical analysis. Morphometric data were analyzed using Student's t test or ANOVA followed by Turkey. Differences were considered significant when p < 0.05.

References

1. Soares MBP, Santos RR. Current status and perspectives of cell therapy in Chagas disease. Mem Inst Oswaldo Cruz 2009; 104:325-32.
2. Köberle F. Chagas disease and Chagas syndromes: the pathology of American Trypanosomiasis. Adv Parasitol 1968; 6:63-116.
3. Soares MB, Lima RS, Rocha LL, Takyia CM, Pontes-de-Carvalho L, de Carvalho AC, et al. Transplanted bone marrow cells repair heart tissue and reduce myocarditis in chronic chagasic mice. Am J Pathol 2004; 164:441-7.
4. Goldenberg RC, Jelicks LA, Fortes FSA, Weiss LM, Rocha LL, Zhao D, et al. Bone Marrow Cell Therapy Ameliorates and Reverses chagasic cardiomyopathy in a mouse model. J Infec Dis 2008; 197:544-7.
5. Macambira SG, Vasconcelos JF, Costa C, Klein W, Lima RS, Guimarães P, et al. Granulocyte colony-stimulating factor treatment in chronic Chagas disease: Preservation and improvement of cardiac structure and function. FASEB J 2009; 23:3843-50.
6. Soares MBP, Lima RS, Rocha LL, Vasconcelos JF, Rogatto SR, Santos RR, et al. Gene expression changes associated with myocarditis and fibrosis in hearts of mice with chronic chagasic cardiomyopathy. J Infec Dis 2010; 202:416-26.
7. Andrade ZA. Immunopathology of Chagas disease. Mem Inst Oswaldo Cruz 1999; 94:71-80.
8. Rossi MA, Souza AC. Is apoptosis a mechanism of cell death of cardiomyocytes in chronic chagasic myocarditis? Int J Cardiol 1999; 68:325-31.
9. Sharma UC, Pokharel S, Brakel TJV, Berlo JHV, Cleutjens JPM, Schroen B, et al. Galectin-3 marks activated macrophages in failure-prone hypertrophied hearts and contributes to cardiac dysfunction. Circulation 2004; 110:3121-8.
10. Rabinovich GA, Ramhorst RE, Rubinstein N, Corigliano A, Daroqui MC, Kier-Joffé EB, et al. Induction of allogenic T-cell hyporesponsiveness by galectin-1-mediated apoptotic and non-apoptotic mechanisms. Cell Death Differ 2002; 9:661-70.
11. Reifenberg K, Lehr HA, Torzewski M, Steige G, Wiese E, Küpper I, et al. Interferon-gamma induces chronic active myocarditis and cardiomyopathy in transgenic mice. Am J Pathol 2007; 171:463-72.
12. Lok DJ, Van Der Meer P, de la Porte PW, Lipsic E, Van Wijngaarden J, Hillege HL, et al. Prognostic value of galectin-3, a novel marker of fibrosis, in patients with chronic heart failure: Data from the DEAL-HF study. Clin Res Cardiol 2010; 99:323-8.
13. Nikkari ST, Jarvelainen HT, Wight TN, Ferguson M, Clowes AW. Smooth muscle cell expression of extracellular matrix genes after arterial injury. Am J Pathol 1994; 144:1348-56.
14. Li J, Brown LF, Laham RJ, Volk R, Simons M. Macrophage-dependent regulation of syndecan gene expression. Circ Res 1997; 81:785-96.
15. Zhang Y, Pasparakis M, Kollias G, Simons M. Myocyte-dependent regulation of endothelial cell syndecan-4 expression. Role of TNFalpha. J Biol Chem 1999; 274:14786-90.
16. Zhao Y, Sui X, Ren H. From procaspase-8 to caspase-8: Revisiting structural functions of caspase-8. J Cell Physiol 2010; 225:316-20.
17. Pelus LM, Horowitzc D, Coopera SC, King AG. Peripheral blood stem cell mobilization: A role for CXC chemokines. Crit Rev Oncol Hematol 2002; 43:257-75.
18. Berg JS, Powell BC, Cheney RE. A Millennial Myosin Census. Mol Biol Cell 2001; 12:780-94.
19. Garg N, Popov VL, Papaconstantinou J. Profiling gene transcription reveals adeficiency of mitochondrial oxidative phosphorylation in *Trypanosoma cruzi*-infected murine hearts: Implications in chagasic myocarditis development. Biochim Biophys Acta 2003; 1638:106-20.
20. Gupta S, Wen JJ, Garg NJ. Oxidative Stress in Chagas Disease. Interdiscip Perspect Infect Dis 2009; 2009:1-8.
21. Wen JJ, Yachelini PC, Sembaj A, Manzur RE, Garg NJ. Increased oxidative stress is correlated with mitochondrial dysfunction in chagasic patients. Free Radic Biol Med 2006; 41:270-6.
22. Iacobas DA, Iacobas S, Urban-Maldonado M, Scemes E, Spray DC.. Similar transcriptomic alterations in Cx43 knock-down and knock-out astrocytes. Cell Commun Adhes 2008; 15:195-206.
23. Dahlquist KD, Salomonis N, Vranizan K, Lawlor SC, Conklin BR. GenMAPP, a new tool for viewing and analyzing microarray data on biological pathways. Nat Genet 2002; 31:19-20.

8.3 ANEXO III

Costa-Ferro Z. S., et al. Transplantation of bone marrow mononuclear cells decreases seizure incidence, mitigates neuronal loss and modulates pro-inflammatory cytokine production in epileptic rats. Neurobiol Dis, v. 46, n. 2, May, p. 302-313, 2012.
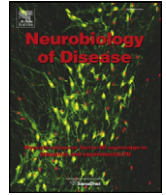
Transplantation of bone marrow mononuclear cells decreases seizure incidence, mitigates neuronal loss and modulates pro-inflammatory cytokine production in epileptic rats

Zaquer S.M. Costa-Ferro [a,b], Bruno S.F. Souza [b,c], Marcos M.T. Leal [b], Carla Martins Kaneto [b], Carine Machado Azevedo [b], Igor Campos da Silva [b,d], Milena B.P. Soares [b,c], Ricardo Ribeiro-dos-Santos [b], Jaderson C. DaCosta [a,*]

[a] Instituto de Pesquisas Biomédicas e Instituto do Cérebro, Pontifícia Universidade Católica do Rio Grande do Sul, Porto Alegre, RS, Brazil
[b] Centro de Biotecnologia e Terapia Celular, Hospital São Rafael, Salvador, BA, Brazil
[c] Centro de Pesquisas Gonçalo Moniz, Fundação Oswaldo Cruz, Salvador, BA, Brazil
[d] Serviço de Anatomia Patológica e Citopatologia, Hospital São Rafael, Salvador, BA, Brazil

ARTICLE INFO

ABSTRACT

Approximately 30% of patients with mesial temporal lobe epilepsy do not respond to treatment with antiepileptic drugs. We have previously shown that transplantation of mononuclear bone marrow cells (BMC) has an anticonvulsant effect in acute epilepsy. Here, we used pilocarpine to induce epilepsy in rats and studied the effects of BMC injected intravenously either at the onset of seizures or after 10 months of recurrent seizures. BMC effectively decreased seizure frequency and duration. In addition, decreased levels of proinflammatory cytokines (TNF-α, IL-1β and IL-6) and increased levels of anti-inflammatory cytokine (IL-10) were observed in the brain and serum of BMC-treated rats. Transplants performed at seizure-onset protected against pilocarpine-induced neuronal loss and gliosis and stimulated the proliferation of new neurons in epileptic rats. Our data demonstrate that BMC transplantation has potent therapeutic effects and could be a potential therapy for clinically intractable epilepsies.

© 2012 Elsevier Inc. All rights reserved.

Introduction

Temporal lobe epilepsy (TLE) is the most common type of epilepsy in adults (Engel, 1996). Mesial temporal epilepsy is a subtype of TLE associated with hippocampal sclerosis (Engel, 2001a; Wieser, 2004) and is one of the most frequent types of drug-resistant epilepsy (Engel, 2001a, 2001b). Clinical and neuropathological findings support the hypothesis that TLE with hippocampal sclerosis develops in 3 phases: a postnatal initial precipitating injury, a latent period corresponding to epileptogenesis, and the occurrence of spontaneous recurrent seizures (SRS; Mathern et al., 1996). In rats, status epilepticus (SE) induced by the systemic injection of the muscarinic receptor agonist pilocarpine is followed by a seizure-free period (latent phase) prior to the onset of SRS (Turski et al., 1987). SRS is accompanied by hippocampal cell loss, axon sprouting (Mello et al., 1993), and increased neurogenesis

(Parent et al., 1997). In recent years, reports have suggested that inflammatory processes in the brain contributes to epilepsy and seizure recurrence (Vezzani and Granata, 2005; Vezzani et al., 2008).

Due to its focal nature and associated tissue degeneration, TLE is an attractive target for cell therapy applications. The bone marrow mononuclear cell fraction (BMC) contains populations of mesenchymal and hematopoietic stem cells that secrete a host of cytokines and growth factors involved in natural repair processes (Takahashi et al., 2006). A contribution of BMC to the regeneration of brain injuries has been already demonstrated (Brazelton et al., 2000; Eglitis and Mezey, 1997). In a rodent brain ischemia model, BMC (Baker et al., 2007; Brenneman et al., 2010; de Vasconcelos dos Santos et al., 2010; Giraldi-Guimarães et al., 2009; Iihoshi et al., 2004; Kamiya et al., 2008) and/or mesenchymal stem cells (Bao et al., 2011; Chopp and Li, 2002; Hu et al., 2004; Liu et al., 2009; Zacharek et al., 2010) were highly effective in promoting functional neurological recovery. In the clinical trials of cell-based therapies already performed, the results were highly promising in stroke and spinal cord injury (see review by Walker et al., 2010). In epileptic models, we demonstrated that BMC transplantation immediately after SE prevents the chronic seizure development, reduces neuronal loss, and influences reorganization of the hippocampal neuronal network (Costa-Ferro et al., 2010).

* Corresponding author at: Instituto do Cérebro, Pontifícia Universidade Católica do Rio Grande do Sul (PUCRS), Av. Ipiranga 6690, 90610-000, Porto Alegre, RS, Brazil. Fax: +55 51 3320 3312.
  E-mail address: samuelgreggio@yahoo.com (J.C. DaCosta).
  Available online on ScienceDirect (www.sciencedirect.com).

The objective of the present study was to evaluate the therapeutic potential of BMC in rats during the chronic phase of pilocarpine-induced epilepsy and its possible mechanisms of action.

Materials and methods

Animals

Male Wistar rats (50–60 days old) were used. Food and drinking water were available ad libitum. Enhanced green fluorescent protein (GFP)-transgenic adult male C57BL/6 mice were used as BMC donors. All animal procedures were approved by the Animal Care and Ethics Committee of Pontifícia Universidade Católica do Rio Grande do Sul, RS, Brazil. All experiments were conducted in a blinded manner relative to the treatment condition of the animals. Every effort was made to minimize the animal's suffering and to reduce the number of animals used. The "Principles of laboratory animal care" (NIH publication No. 85–23, reviewed 1996) were strictly followed.

Induction of SE and epilepsy

All rats received intraperitoneal (i.p.) injections of lithium chloride (127 mg/kg, Sigma, St. Louis, MO, USA) and methylscopolamine-bromide (1 mg/kg, Sigma) 18–20 h and 30 min, respectively, prior to induction of SE. SE was induced by treatment with pilocarpine (50 mg/kg, i.p. Sigma) and was interrupted after 2 h by administering the anticonvulsant diazepam (20 mg/kg i.p.). Control animals were given saline (i.p.) (adapted from Clifford et al., 1987). The severity of seizures was rated using the Racine scale (Racine, 1972), and only those animals that displayed class V behavioral seizures were used in the study.

BMC and fibroblast preparation and transplantation

BMCs were harvested from male EGFP-transgenic mice. The animals were euthanized with 200 μl of 8% ketamine hydrochloride (Cristália, Brazil) and 2% chlorpromazine (União Química, Brazil) prior to dissection. Fresh bone marrow was extracted from the humerus, femur, and tibia by flushing with PBS. After centrifugation, the cell pellet was resuspended with RPMI medium and fractionated on a density gradient generated by centrifugation over a Ficoll–Hypaque solution (Histopaque 1119 and 1077, 1:1; Sigma) at $400 \times g$ for 30 min at room temperature. The mononuclear fraction over the Ficoll–Hypaque layer was collected and washed twice with PBS. After washing by centrifugation at $300 \times g$ for 10 min, the viable cells with trypan blue were counted in a Neubauer chamber.

We used fibroblasts from the L929 cell line as a control for BMC transplantation. Fibroblasts were maintained in DMEM with 10% FBS and 50 g/ml gentamicin (Sigma) in culture flasks incubated at 37 °C in 5% CO_2. After reaching 80–90% confluence, cells were treated with 0.05% trypsin solution (Sigma), washed in saline solution, resuspended in 1 ml of saline and counted in a hemacytometer.

BMC and L929 cell suspensions were adjusted to a concentration of 1×10^7 cells/ml in a volume of 100 μl. Cell suspensions or saline solution were administered by tail vein injection either 22 days or 10 months after SE.

Flow cytometric analysis

Mononuclear cells were washed with PBS and incubated at 4 °C for 30 min with conjugated antibodies against murine CD34 PE, CD90 PE, CD11b PE, CD44 PE, CD117 Cy5, CD45 APC and Sca-1 Cy5 (BD Pharmingen, San Diego, CA, USA). Labeled cells were analyzed using a FACScalibur cytometer (Becton Dickinson, San Diego, CA, USA) equipped with CellQuest software. At least 50,000 data points were collected. The means ± SD for the markers expressed by

mononuclear cells were CD34 (4.86 ± 0.43), CD45 (96.36 ± 1.80), CD117 (13.95 ± 0.88), CD11b (60.22 ± 3.30), CD44 (95.61 ± 1.78), CD90 (8.10 ± 1.28), Sca1 (36.06 ± 1.8) and GFP (96.52 ± 0.76).

Experimental groups

Rats were video-recorded from the third day after SE to identify the onset of SRS. The seizures were quantified from day 15 to day 22 after SE, to determine pre-treatment seizure frequencies. On day 22, the rats were randomly divided into three groups (Fig. 1): (A) epileptic rats transplanted 22 days after SE, which were further divided into the subgroups (1) epileptic (injected with saline solution), (2) mBMC (transplanted with mouse BMC) and (3) rBMC (transplanted with rat BMC); (B) epileptic rats transplanted with mBMC 10 months after SE, divided into the subgroups (1) epileptic (injected with saline solution) and (2) mBMC (transplanted with mouse BMC); and **(C)** L929 control cells, epileptic rats transplanted with L929 mouse fibroblasts. Each experiment also had a normal control group composed of non-epileptic rats that were injected with saline and were kept in the same housing conditions as the epileptic rats throughout the experiment.

Monitoring of spontaneous recurrent seizures

The frequency and duration of SRS were video-recorded for 8 h per day from 3 to 22 days post-SE. In all rats, the seizures were quantified between 15 and 22 days after SE. On day 22, randomly selected animals received mBMC, rBMC or saline solution and were recorded for the first week following transplant.

Eight epileptic rats that presented a similar frequency of SRS at the first time point were transplanted with L929 cells and video-recorded during the first week immediately after transplantation and for one week per month in the three subsequent months.

In addition, ten non-treated epileptic rats, in which seizures were assessed from day 15 to day 22 after SE, were also video-recorded for one week in months 8, 9, and 10 after SE. Half of these animals received mBMC transplantation, and half received saline solution. Both mBMC and saline groups were video-recorded for SRS assessment in the following eight weeks.

For statistical analysis, we used the frequency and average duration of individual SRS 1 week pre- and post-treatment. Cumulative pre- and post-transplantation seizure scores were then compared to determine the percentage difference.

Histological evaluation and analyses of neurogenesis and migration of transplanted cells

Epileptic rats transplanted with mBMC or saline and non-epileptic rats of groups A and B were anesthetized with thiopental (40 mg/kg i.p) and decapitated. Whole brains were removed and hemisected. One hemisphere was used for mRNA analysis, and the other was fixed in 4% paraformaldehyde for 24 h. After fixation, the brains were dehydrated and embedded in paraffin. Serial coronal sections of 5 μm were cut. Regions of interest were determined with the help of the rat brain atlas according to Franklin and Paxinos (1997), and points between the coordinates of the bregma ($-$1.58–3.64 mm) were analyzed.

Quantification of NeuN$^+$ cells

Neuronal counting was performed in coronal sections at approximately equidistant intervals localized between: $-$1.58 and 3.64 mm caudal from the bregma (Franklin and Paxinos, 1997). Nine sections were obtained from each animal per each region and time point. In each section, undamaged neurons of the hippocampal CA1, CA3 fields and hilus of DG were defined as follows (Fig. 4A). Hilus was defined as the inner border of the granule cell layer and the proximal end of the
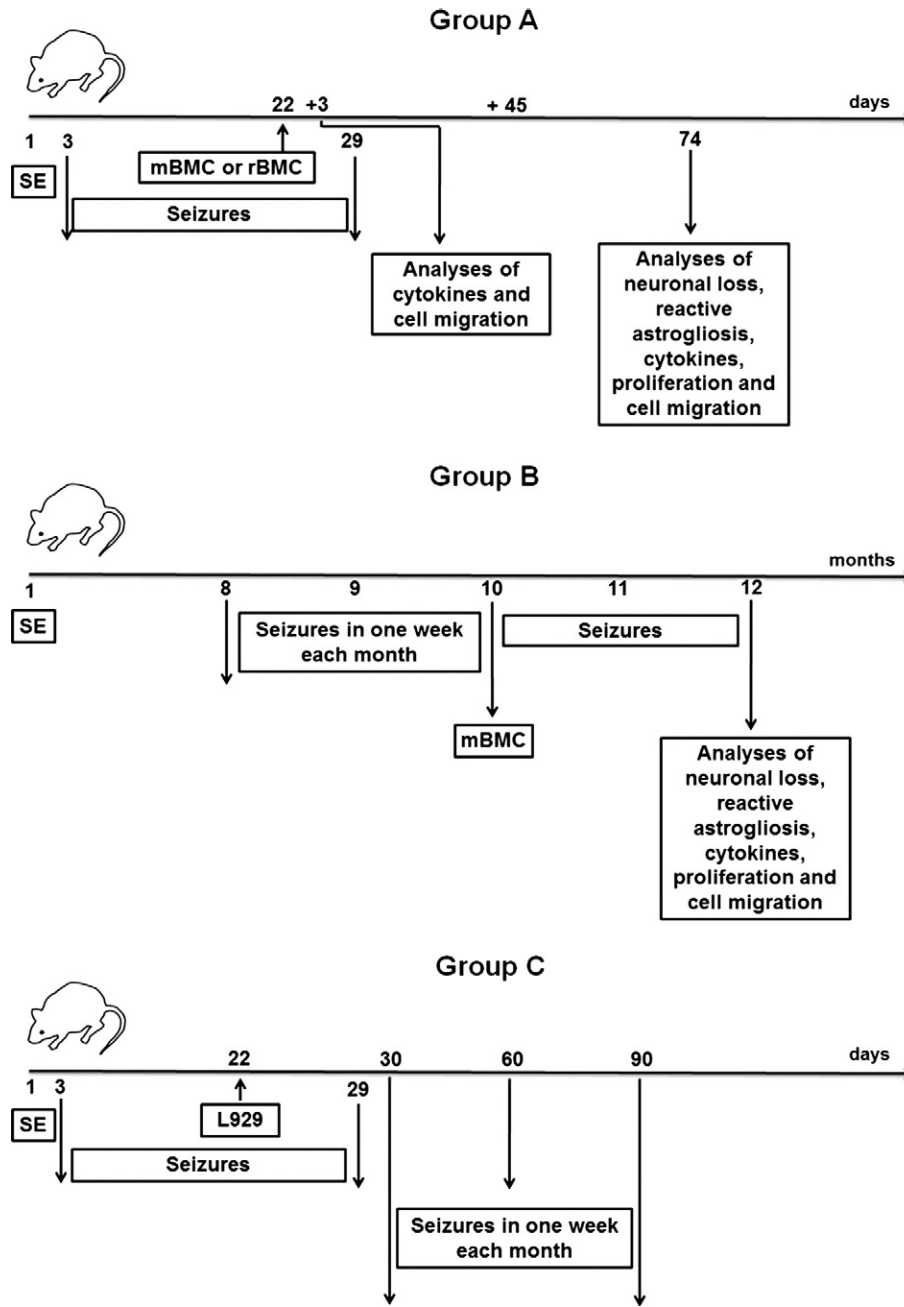
Fig. 1. Summary of experimental approach. SE experimental design, seizure monitoring, cell transplantation, neuronal loss, reactive astrogliosis, cell migration, and cytokine analyses. Group A: epileptic rats transplanted with BMC 22 days after SE; Group B: epileptic rats transplanted with BMC 10 months after SE; Group C: epileptic rats transplanted with L929 fibroblasts.

CA3c/CA4 region. The images were obtained with a $40\times$ lens, and neurons were counted within a frame with an area of $900\ \mu m^2$, using Image-Pro Plus analysis software v.7.0 (Media Cybernetics, Inc. USA). Neurons with visible DAPI-stained nuclei found overlaying the left and upper borders of the counting frame were counted together with the nuclei located within the analyzed square. The cell counts were corrected by Abercrombie's formula (Abercrombie, 1946).

Nissl and hematoxylin-eosin staining

Histological analysis of cells was performed in adjacent hippocampal sections stained by the Nissl method (1% cresyl violet) and hematoxylin-eosin (H&E) (-1.70, -2.46 and 3.40 mm from bregma). The slides were scanned with an Aperio Scanscope (Aperio Technologies, San Diego, USA) under 20 or $40\times$ magnification. Neuronal

loss, reactive gliosis, edema, and microvascular proliferation (if present) were graded as mild, moderate, or severe.

Quantification of GFAP$^+$ cells

Sections containing GFAP-labeled glial cells were examined using z-stacks obtained with a confocal microscope eighteen images per region (-1.70, -2.46 and -3.40 mm from the bregma) were examined for each time point. Images of the stratum radiata of CA1 and CA3 as well as the hilus were digitally captured and analyzed using Image Pro Plus v. 7.0 (Media Cybernetics), which automates the analysis by segmentation, converting all immunolabeled elements that fall within a threshold range into red pixels and the rest of the image into yellow pixels. The same threshold range that defined positivity was used in all images analyzed. The software then calculates the percentage of red and

yellow, allowing for the comparison of the pixel values between the groups, defined as the percentage of stained area.

Doublecortin (DCX) staining

The expression of the immature neuronal marker DCX (see below) was also analyzed (see antibodies section). Fluorescence signals from double-labeled sections were detected by confocal microscopy. For the CA1 and CA3, a single square with an area of 104.400 μm^2 was analyzed, and for the DG, 4 squares were analyzed. Mean values per each area per slice and per rat were used in the statistical analysis.

GFP staining

To investigate the migration of BMC to the brain in the group A, GFP$^+$ cells were visualized by confocal microscopy 3 days after transplantation. GFP expression was also evaluated by real time quantitative polymerase chain reaction in groups A and B 45 and 60 days after transplantation, respectively (see below).

Antibodies

The slices were deparaffinized and rehydrated. Antigen retrieval was performed using citrate buffer (pH = 6.0, at 95–98 °C) for 20 min. The sections were incubated overnight at 4 °C with one of the following primary antibodies: biotinylated anti-neuronal nuclei antibody (NeuN, 1:100, Chemicon International, Temecula, CA, USA), rabbit anti-doublecortin (DCX, 1:800, Abcam, San Francisco, CA, USA), rabbit anti-glial fibrillary acidic protein (GFAP, 1:200, Neomarkers, CA, USA) or chicken anti-green fluorescent protein (GFP, 1:400, Avés

Lab, Tigard, OR, USA). The next day, sections were incubated for 1 h at room temperature with streptavidin or secondary antibodies (Streptavidin-Alexa Fluor 488 conjugated, anti-rabbit IgG Alexa Fluor 488, anti-rabbit IgG Alexa Fluor 633, 1:200, Molecular Probes, Carlsbad, CA, USA). Sections were washed twice in PBS Tween 0.05% and then in PBS, dried and coverslipped using Vectashield mounting medium with 40,6-diamidino-2-phenylindole (DAPI; Vector Laboratories, CA, USA) or TO-PRO (1:200, Molecular Probes). Images were taken using the Fluoview 1000 confocal microscope with the F10-ASW v.2.1 software (Olympus).

Analysis of cytokine production

The transcription of cytokine genes was evaluated by real-time quantitative polymerase chain reaction (qPCR) in rats sacrificed 3 and 45 days after transplantation (group A) and 60 days after transplantation (group B). Total RNA was isolated from the whole brain with TRIzol reagent (Invitrogen), and the concentration was determined by photometric measurement. High Capacity cDNA Reverse Transcription Kit (Applied Biosystems) was used to synthesize cDNA from 1 μg of RNA following the manufacturer's recommendations. qRT-PCR assays were performed to detect the expression levels of *TNF-α* (tumor necrosis factor alpha), *IL-1β* (Interleukin 1 beta), *IL-6* (Interleukin 6) and *IL-10* (Interleukin 10) genes. Amplification mixtures for qRT-PCR contained 20 ng template cDNA, 10 μl Taqman Master Mix (Applied Biosystems) and probes and for *TNF-α* (Mm00443258_m1), *IL-1β* (Mm00434228_m1) *IL-6* (Mm00446190_m1) and *IL-10* (Mm00439616_m1) in a final volume of 20 μl. To detect transplanted mouse BMCs, GFP expression was also evaluated. All reactions were run in duplicate on an ABI7500 Sequence Detection
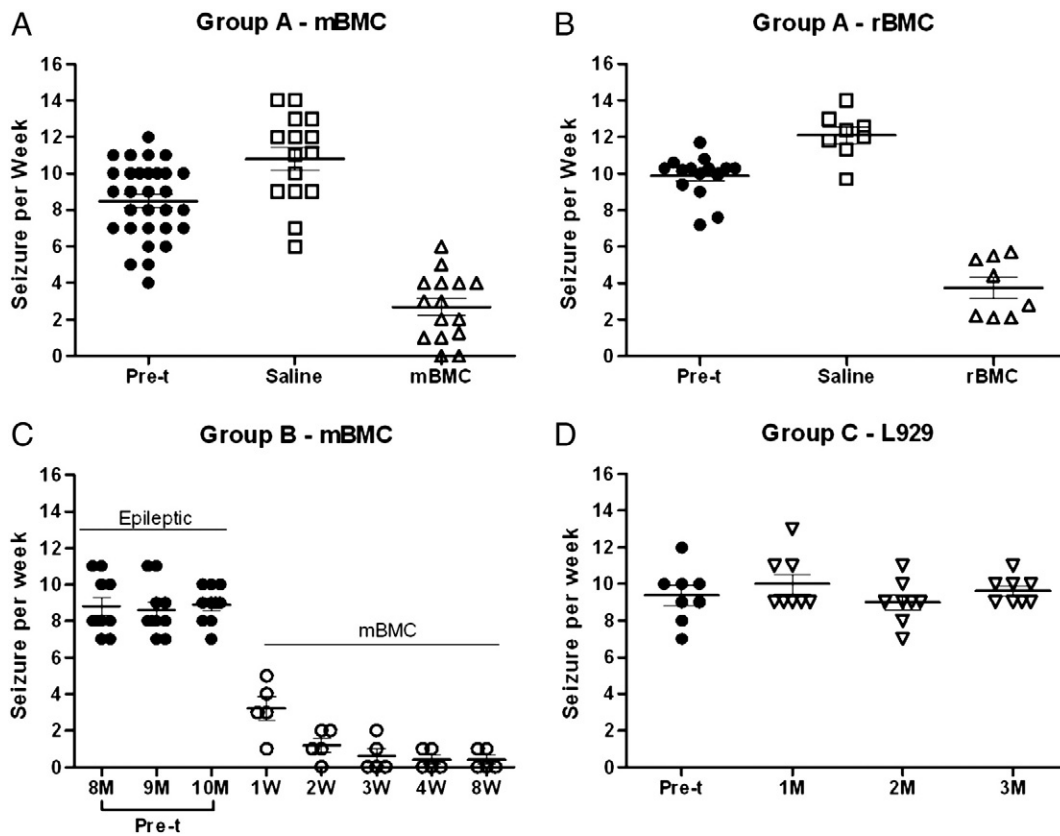

Fig. 2. Spontaneous recurrent seizures recorded in individual rats. (A and B) Epileptic seizures were recorded during one week pre- (Pre-t) and post-treatment in epileptic rats treated 22 days after SE. (A) Rats were treated with mouse BMC (mBMC; n = 15) or saline (n = 15). (B) Rats were treated with rat BMC (rBMC; n = 8) or saline (n = 7). (C) Epileptic seizures were recorded during one week in the 8th, 9th, and 10th months after the first seizure record (15–22 days after SE, n = 10). Group mBMC (n = 5) underwent transplantation 10 months after SE and seizures were recorded for all 8 weeks after the transplant. (D) Seizures recorded in epileptic rats transplanted with L929 fibroblasts 22 days after SE and recorded one week in each of the subsequent 3 months (n = 8).

System (Applied Biosystems, Foster City, CA, USA) under standard thermal cycling conditions. Experiments with coefficients of variation greater than 5% were excluded. A no-template control (NTC) and no-reverse transcription controls (No-RT) were also included. The results are presented as the fold-increase of expression of the individual mRNAs, with the target internal control *GADPH* using the cycle threshold method.

Serum concentrations of IL-1β, IL-6, IL-10, and TNF-α were determined by an enzyme-linked immunosorbent assay (ELISA) in group A and B rats (the same animals included in the brain cytokine qPCR analysis). All cytokines were measured in duplicate using specific antibody kits (R&D Systems, Minneapolis, MN, USA) according to manufacturer's instructions.

Data analysis

Statistical analyses were performed using Prism software (version 5.01, GraphPad Software, San Diego, CA, USA). Seizure frequency, neuronal loss, gliosis quantification and ELISA assays were analyzed with one-way analysis of variance (ANOVA) followed by Tukey's posttests or the Newman–Keuls multiple comparison test. GFP$^+$ cells and expression of mRNA was analyzed with two-way ANOVA followed by Bonferroni posttests or one-way analysis by Neuman–Keuls multiple comparison test. Differences in numbers of DCX-positive cells were analyzed with Student's *t*-tests. The data are presented as the mean ± SD or mean ± S.E.M., as indicated in the figure legends. Differences were considered significant if $p < 0.05$.

Results

Pilocarpine-induced spontaneous seizures and the effects of BMC

Systemic administration of lithium and pilocarpine rapidly induced a robust convulsive SE (latency: 28 ± 13 min). The rats that did not develop SE were excluded from the study. The mortality rate in the seven days after pilocarpine treatment was approximately
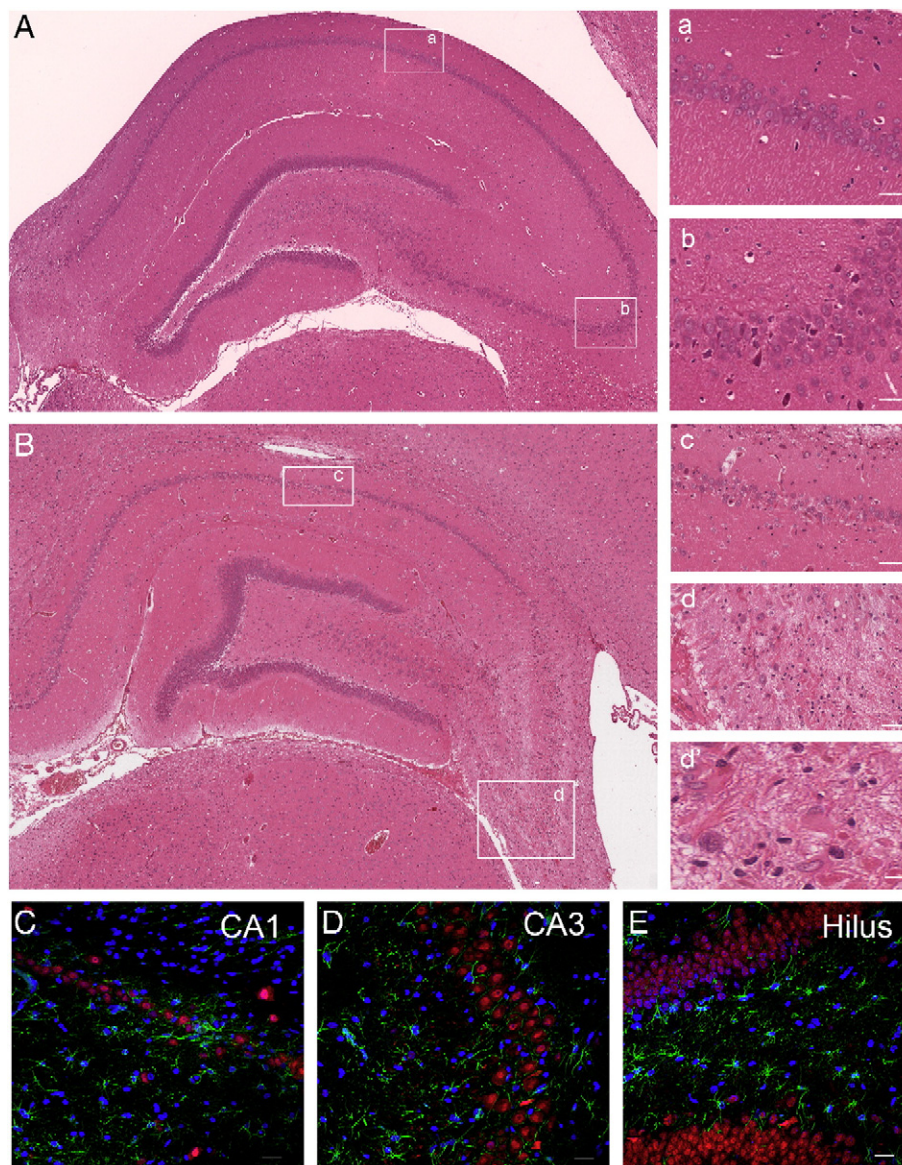

Fig. 3. Histological analysis of epileptic rat brain. (A–B) Representative H&E stained sections of hippocampal formations of a non-epileptic control rat (A, a, b) and epileptic rat (B), showing extensive neuronal loss in the CA1 (c) and CA3 (d) subfields, showing mild to moderate gliosis, gemistocystic astrocytes (d′; arrowheads), and edema and vascular proliferation. Gliosis in regions of neuronal loss was observed by confocal micrococy in hippocampus sections obtained from an mBMC-epileptic rat of Group B, stained with anti-GFAP (green), anti-NeuN (red) antibodies, and DAPI for nuclear visualization (C–E). Scale bars: 50 μm.

50%, but significant mortality was not observed after the first week. SRSs began 12 ± 5 days following SE.

In group A, which received transplants 22 days after SE, the epileptic rats that received an injection of saline solution exhibited approximately 27% increase in the number of seizures/week. Conversely, in rats transplanted with BMCs, the number of seizures/week decreased by 65% in mBMC (Fig. 2A; $p<0.001$; pre vs. mBMC-transplantation) and 62% in rBMC (Fig. 2B; $p<0.001$ pre vs. rBMC-transplantation).

For comparison, in group B, the occurrence of seizures was evaluated during the first week in months 8, 9 and 10 after the first recorded seizure and for 8 weeks following transplantation. A significant difference in the frequency of SRS was observed between the groups. Epileptic animals exhibiting a similar frequency of SRS 8–12 months after SE showed a marked decrease in the number of SRS 1–4 weeks after transplantation. These low levels of SRS remained during the four subsequent weeks. There was a decrease of approximately 62% in the first week, 86% in the second, and 97% in the fourth
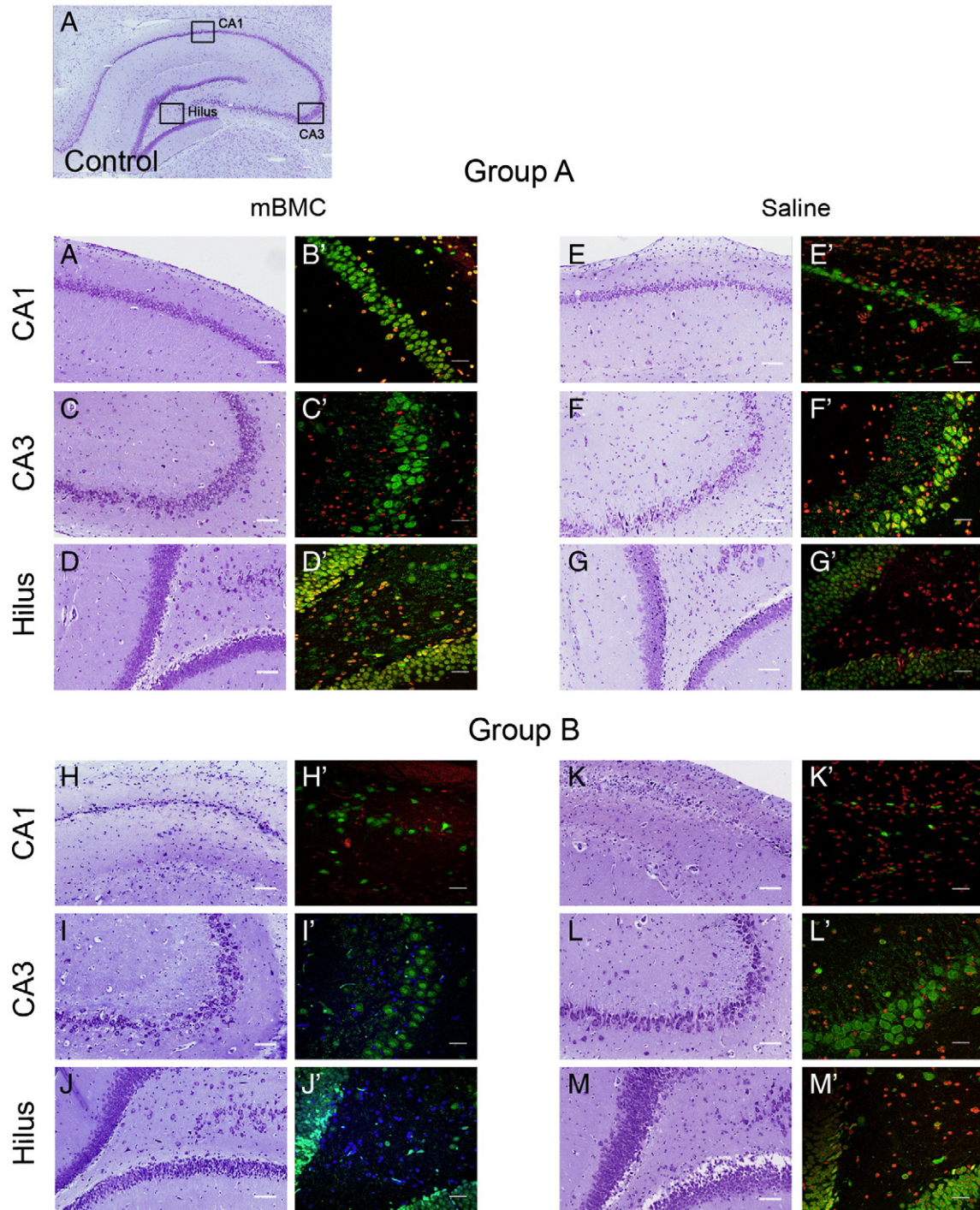

Fig. 4. Neuronal injury in the hippocampal formation. (A) Section from a control rat brain indicating the areas of analysis: CA1 and CA3 pyramidal cell layers and the hilus of DG. Group A: CA1, CA3 and hilar areas from mBMC-treated epileptic rats (B–D) and saline-treated epileptic rats (E–G). Group B: CA1, CA3 and hilar areas from mBMC-treated rats (H–J) and saline-treated epileptic rats (K–M). (A–M) Nissl-stained sections. (B′–M′) Confocal microscopy images of sections stained with anti-NeuN antibody (green) and DAPI (blue) or TO-PRO (red) for nuclei visualization. Scale bars: 50 μm, (n = 5/group).

and eighth weeks after transplantation (Fig. 2C, $p<0.001$; saline-epileptic vs. mBMC-epileptic rats for each time point).

A variable and significant difference was found in the mean duration of seizures: approximately 48% in the rBMC and mBMC-transplanted rats in the group A and 57% in the mBMC in the group B ($p<0.001$).

In group C, rats transplanted with L929 fibroblasts had no significant alteration in SRS frequency or duration during the entire observation period after transplantation compared to saline epileptic rats (Fig. 2D).

Histological evaluation of the hippocampus

Damage in the hippocampus was observed in both saline- and BMC-epileptic rats. In group A, two out of five animals from the saline-epileptic group showed evidence of active hippocampal inflammation, with few infiltrating leucocytes, moderate edema, vascular proliferation and reactive gliosis, with gemistocystic astrocytes, in areas of extensive neuronal loss. Most animals, however, presented variable degrees of neuronal loss and mild or moderate gliosis, with no edema or vascular proliferation in the evaluated areas. In group B, we observed extensive neuronal loss together with mild-to-moderate gliosis, but no edema or vascular proliferation (Fig. 3).

Cresyl violet staining and NeuN immunofluorescence in the hippocampal regions was typically found in the pyramidal cell layers of CA1 and CA3 and the hilus of the dentate in epileptic rats (Figs. 4A–M). The number of NeuN$^+$ cells in these areas dramatically decreased in saline-epileptics rats (Figs. 5A–F, $p<0.001$), but BMCs significantly ameliorated cell loss in group A. Neuronal counts in the CA1 and CA3 regions of the mBMC group showed a small difference (Figs. 5A and C, $p<0.01$), but the number of neurons increased in the hilus (Fig. 5E, $p>0.05$) compared to control rats. In addition, the number of NeuN$^+$ cells in the CA1 and hilus of DG was preserved in the mBMC group compared with the saline-epileptic rats ($p<0.001$, Figs. 5A and E). In group B, we observed greater neuronal cell loss in the CA1 and hilus of DG in mBMC group (Figs. 5B and F; $p<0.001$), whereas in the CA3, only moderate damage was found (Fig. 5D; $p<0.01$).

In addition to changes observed in neuron populations, we found reactive astrogliosis as shown in Fig. 6. Astrocytes from control rats had small cell bodies and thin processes, while epileptic rat astrocytes had enlarged cell bodies and elongated processes. These characteristics were even more pronounced in epileptic rats from group B. We observed that these morphological changes were partially reversed in BMC-epileptic rats (Figs. 6A–L). We did not observe differences in the intensity of GFAP$^+$ area between saline-epileptic rats in groups A and B, but we did observe differences in cell morphology. The quantification of GFAP-stained area in the same regions revealed increased GFAP expression in the epileptic rats compared to controls (Figs. 6M and N $p<0.001$). In group A, BMC-epileptic rats had lower expression of GFAP when compared to saline-epileptic rats (Fig. 6M, $p<0.001$).

Effects of BMC on hippocampal neurogenesis

Seizures upregulate a number of factors that increase endogenous neurogenesis in the DG (Parent et al., 1997). We investigated whether prior seizure experience affected the fates of transplanted mBMC. DCX is a protein expressed in immature neurons and is associated with neuronal differentiation (Ming and Song, 2005). Therefore, staining for DCX, NeuN and DAPI was performed. In group A, DCX$^+$ cells were present in the CA1 (Fig. 7A) and in the DG (Fig. 7B) of mBMC-epileptic rats 45 days after transplantation. They were also seen in the DG in saline-epileptic rats at the same time point (Fig. 7C). Moreover, the number of DCX$^+$ cells was increased in the saline-epileptic group compared to the mBMC-epileptic group (Fig. 7D, $p<0.01$). The brains of rats transplanted with mBMC 10 months after SE were examined 60 days after transplantation (group B). Most of
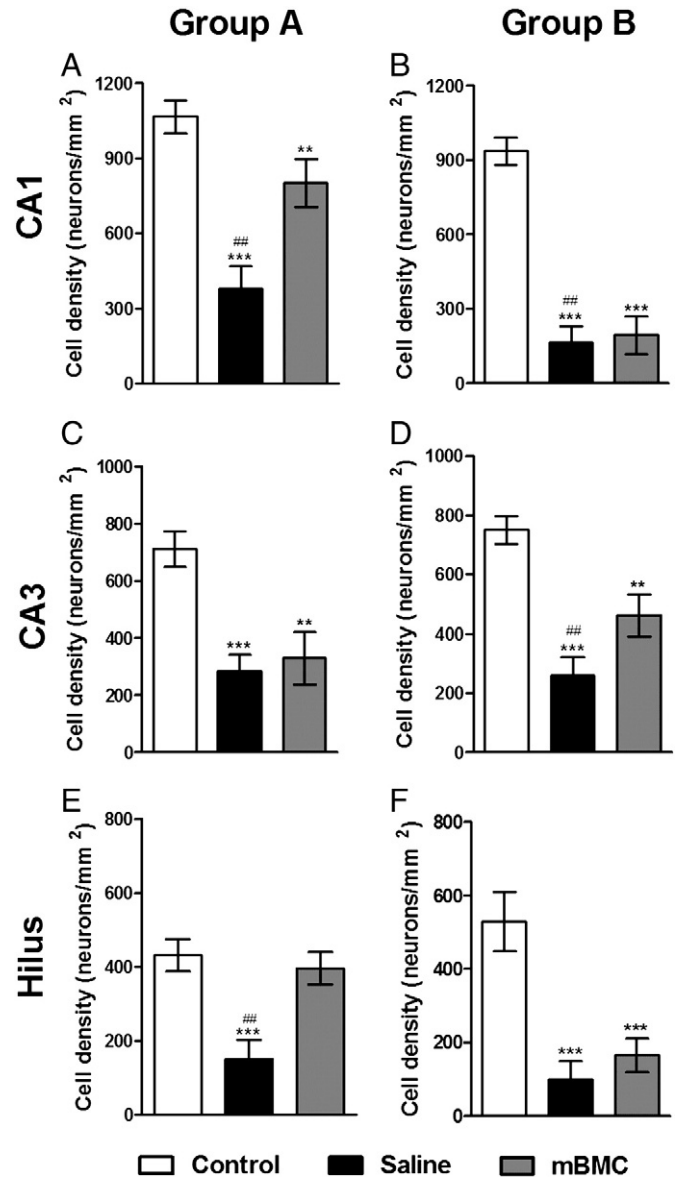

Fig. 5. Quantification of neuronal damage in the hippocampal formation. (A–F) Neuron counts from NeuN-stained brain sections in the area selected for quantification in CA1, CA3, and the hilus of the DG. Control (white), saline (black) and mBMC (gray) groups. Data are expressed as the mean ± SEM, n = 5 per group. Analyses of data by one-way ANOVA and Tukey's posttest indicated significant differences for all panels. Differences relative to the control group are indicated by * ($p<0.05$) and between saline-epileptic vs. mBMC-epileptic rats by # ($p<0.05$).

the double-labeled cells had relatively large somata with visible dendrite-like processes and co-localized with NeuN in the CA3/CA4 area (Fig. 7E) and in the DG (Fig. 7F). DCX$^+$ cells were rarely found in brain sections of saline-epileptic rats at this time point (Fig. 7G); however, the numbers of DCX$^+$ cells were increased in the mBMC group (Fig. 7H, $p<0.01$).

Presence of bone marrow-derived GFP$^+$ cells in the epileptic brain

The presence of transplanted GFP$^+$ cells in epileptic and controls rats was investigated. We found donor cells in the spleens of transplanted animals, indicating that the transplant was successful (data not shown). Rare GFP$^+$ cells were also found in the hippocampi of mBMC-epileptic rats. Most the double-labeled cells appeared in pairs or in clusters (Figs. 8A and B) in different areas of the hippocampus three days
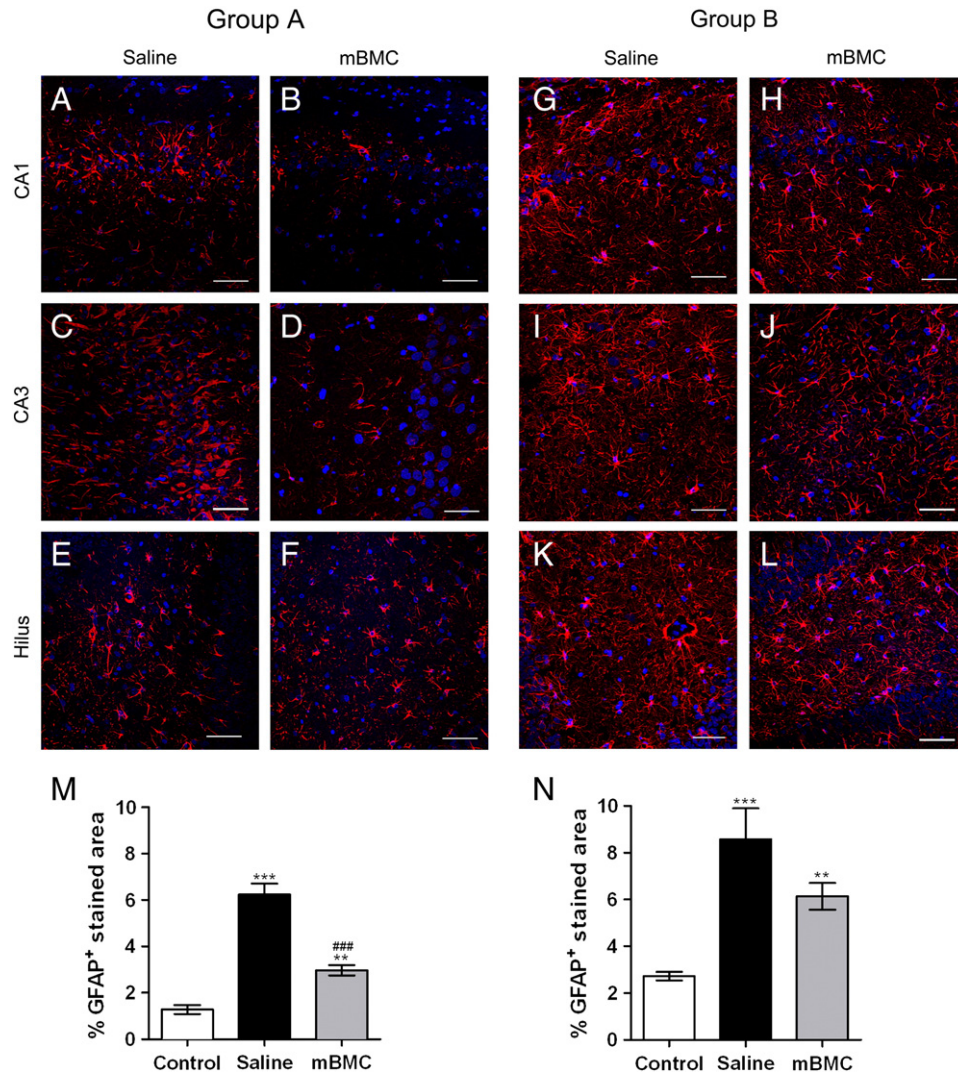
Fig. 6. Quantification of reactive astrocytes in the epileptic rat brain. (A–L) Representative confocal microscopy images of sections stained for GFAP (red) and DAPI (blue) for nuclei visualization. Scale bars: 50 μm. (M and N) Percentage of GFAP$^+$ cells in the hippocampus (CA1, CA3, and hilus) of control (white), saline (black) and mBMC (gray). Data are expressed as the mean ± SEM, n = 5 per group. One-way ANOVA and Tukey's posttest indicated significant differences for all panels. Differences relative to control group are indicated by * ($p < 0.05$) and between saline-epileptic vs. mBMC-epileptic rats by # ($p < 0.05$).

after transplantation. However, none of these GFP$^+$ cells expressed neuronal or glial cell markers. To confirm the presence of mouse BMCs in the brain, we investigated GFP expression by quantitative real-time PCR 45 and 60 days after transplantation in groups A and B, respectively. In the mBMC transplanted group, the GFP mRNA level was significantly higher, suggesting the presence of mouse BMCs in the brain (Fig. 8C).

Expression of cytokines

To investigate the mechanisms by which BMC therapy resulted in a reduction of seizures, we tested whether BMC transplantation modulates the transcription of TNF-α, IL-1β, IL-6, and IL-10. In group A, TNF-α, IL-1β and IL-6 mRNA levels in epileptic rats were strikingly elevated compared to those of normal controls. After 3 and 45 days of transplantation, the expression of TNF-α mRNA was 3-fold greater than control levels in the epileptic group (Fig. 9A, $p < 0.001$). IL-1β mRNA levels were increased in the brains of epileptic rats (Fig. 9B, $p < 0.05$ and $p < 0.001$, 3 and 45 days, respectively). IL-6 mRNA expression was increased in epileptic brains in both time points analyzed (Fig. 9C, $p < 0.01$). However, no differences in TNF-α, IL-1β mRNA and IL-6 mRNA expression were found between mBMC-epileptic and control rats (Figs. 9A, B and C, $p > 0.05$). In contrast to the pro-

inflammatory cytokines, the mRNA levels of the anti-inflammatory cytokine IL-10 gene increased in mBMC-treated epileptic rats in both time points analyzed (Fig. 9D, $p < 0.001$ and $p < 0.05$, 3 and 45 days after mBMC, respectively). In group B, TNF-α, IL-1β and IL-6 mRNA was not significantly increased by mBMC transplantation (Figs. 9E, F and G). However, IL-10 mRNA was increased 2.0-fold in the mBMC-treated epileptic rats (Fig. 9H, $p < 0.01$ mBMC vs. control, and $p < 0.05$ mBMC vs. epileptic-saline).

Three days after transplantation, serum levels of TNF-α and IL-1β were increased in the saline-epileptic rats (Figs. 9I and J, $p < 0.05$ and $p < 0.01$, respectively). In contrast, the levels of TNF-α and IL-1β were normal in rats transplanted with mBMC levels (Figs. 9I and J). The levels of IL-10 increased 1.6-fold in epileptic rats and 2.5-fold in mBMC-treated rats when compared to normal controls (Fig. 9K, $p < 0.05$ control vs. epileptic, $p < 0.001$ control vs. mBMC). IL-6 was not detected in the sera of any group (data not shown).

Discussion

Epilepsy is a debilitating neurological disorder characterized by recurrent seizures triggered by excessive neuronal excitability. In our study, BMCs were transplanted in epileptic rats either 22 days
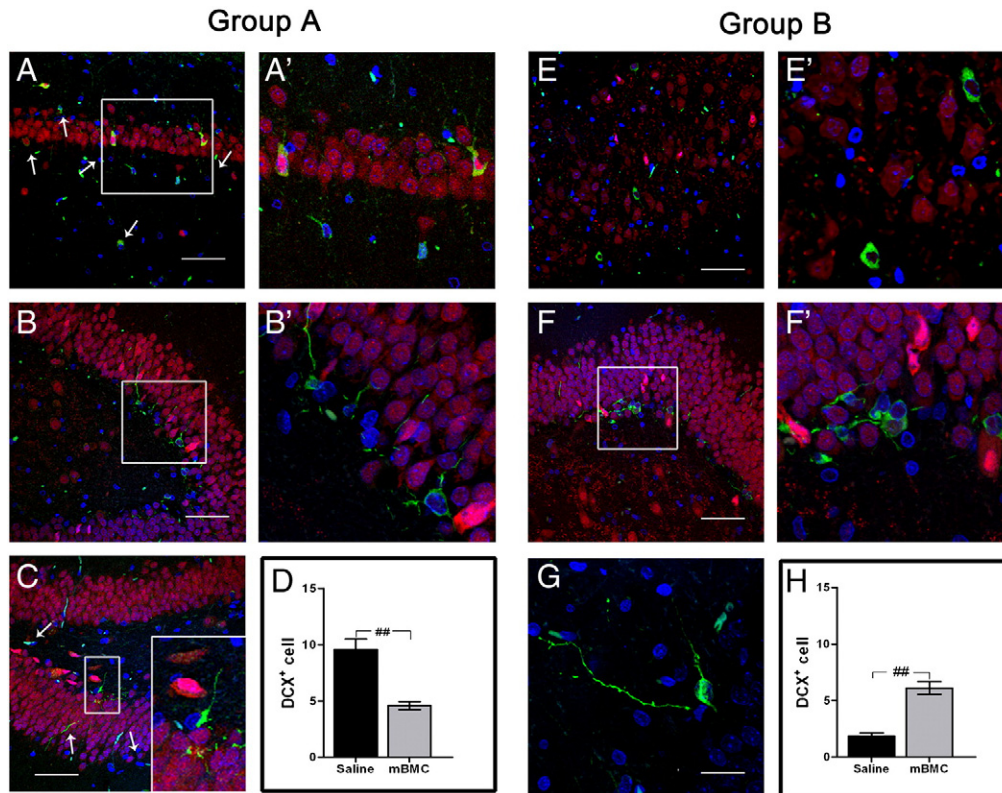
Group A   Group B

Fig. 7. Doublecortin expression in epileptic brain sections. DCX staining 45 days after transplantation reveals young neurons in the dentate gyrus (A) and the CA1 (B) of the mBMC-epileptic rats, (C) and in saline-epileptic rats. (D) Quantification of DCX + cells in saline (dark) and mBMC (gray). Staining 60 days after transplantation in the CA3/CA4 areas (E), in the DG (F), and in epileptic rats (G). (H) comparison of the DCX + cell in saline (dark) and mBMC (gray). DCX (green), NeuN (red), and DAPI (blue). Data are shown as mean ± S.E.M., n = 5 per group, statistically significant differences indicated by (##, $p < 0.001$) as determined by Mann–Whitney tests. Scale bar: 50 μm.

(group A) or 10 months after SE (group B). The data clearly show that, irrespective of the donor (syngeneic or xenogeneic), BMC-treated rats had a marked reduction in the frequency and duration of seizures compared with saline-treated epileptic rats. This reduction correlated with the downregulation of pro-inflammatory cytokine mRNA expression and upregulation of the anti-inflammatory cytokine IL-10 in the brain.

Several studies demonstrated that adult rats with SE have a number of morphologic changes, such as extensive neuronal loss in various temporal or extratemporal structures (for review, see Cavalheiro et al., 2006). Correlating with the decrease in SRS, we observed that the striking neuronal loss in CA1, CA3, and hilus of saline-treated epileptic rats did not occur in epileptic rats treated with BMC 22 days after SE. In fact, these animals showed a substantial preservation of the hippocampal neurons and maintenance of a functional neural network. In a previous study, we showed that BMC transplantation 22 days after SE ameliorated learning and spatial memory impairments in chronic epilepsy (Venturin et al., 2011).

Preservation of hippocampal neuron populations by the BMC therapy did not occur in rats transplanted after a longer period of SRS (10 months after SE, group B), since, by the time of transplantation, there was already an extensive established neuronal loss compared to normal controls. However, BMC-epileptic rats had an increase in the number of neurons when compared to saline-epileptic rats, and many of those expressed DCX, a marker of immature neurons. This result suggests an induction of endogenous neurogenesis by BMC therapy. We did not find any differences between non-epileptic controls and saline-epileptic rats regarding the number of DCX⁺ cells in the

hippocampus. In contrast, we found increased numbers of DCX⁺ cells in the hippocampus of both BMC-epileptic and saline-epileptic rats in the initial period of SRS (22 days after SE, group A). Saline-epileptic rats had increased cell proliferation compared to BMC-epileptic rats at this time point; therefore, the result may be explained by the increased frequency of seizures in the saline-epileptic group. It has been previously shown that seizures induce the proliferation, migration, and differentiation of neuronal progenitors in the hippocampus (Ming and Song, 2005). Furthermore, it was demonstrated that transplanted bone marrow cells pre-labeled with BrdU or retrovirus co-localize with mature neuronal markers, such as MAP-2 and NeuN, in ischemic injured brains (Crain et al., 2005; Hess et al., 2002; Kawada et al., 2006). We did not find donor cells in the brain expressing DCX, suggesting that transplanted bone marrow cells have a paracrine effect in our model of epilepsy.

Pathological factors induce immediate morphological and functional changes in the cells, a compensatory response to changes in the extracellular environment. For example, reactive astrocytes become hypertrophic, with swollen cell bodies and processes. Long-term morphological changes in astrocytes may induce the proliferation (i.e., astrogliosis) and migration of these cells to nearby damaged neurons (Janeczko, 1994). Like neuronal damage, hippocampal glial activation is a common feature observed in experimental SE and in patients with mesial TLE (Aronica et al., 2000; Eid et al., 2008). Astrocytes can also synthesize and release proinflammatory cytokines (Vezzani et al., 2008). In this study, the reactive gliosis in mBMC-treated epileptic rat was less intense than that observed in saline-epileptic rats, where glial cells seem to surround neurons in damaged areas.
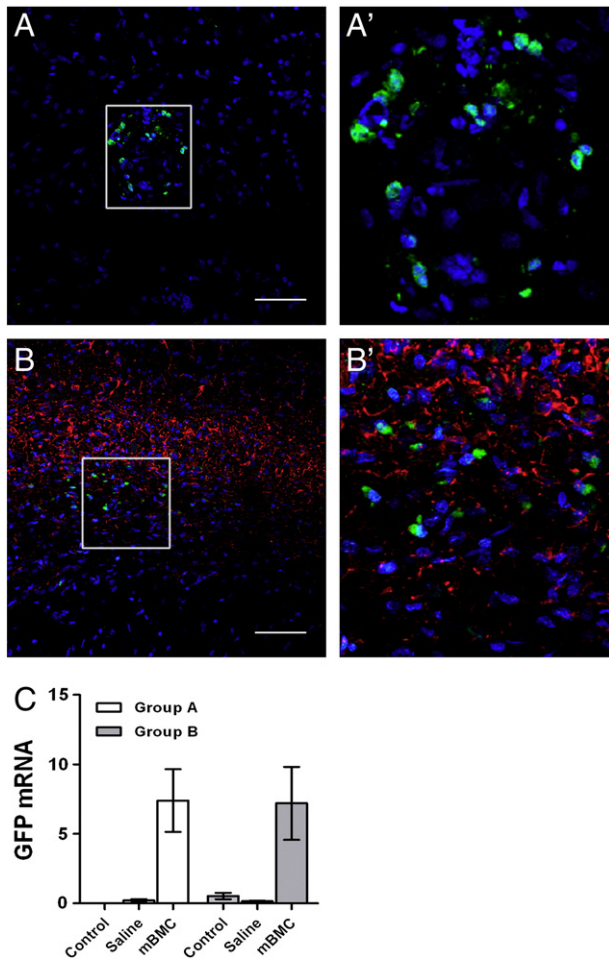
Fig. 8. Migration of transplanted GFP⁺ cells to brains of mBMC-treated epileptic rats. Brain sections from mBMC-epileptic rat stained with anti-GFP antibody (green), and counterstained with DAPI (blue) for nuclear visualization (A and B). (B) Sections were co-stained with anti-GFAP antibody (red). (A′ and B′) Selected regions of A and B at higher magnification. Scale bars: 50 μm. (C) GFP mRNA levels in the brains of control and epileptic rats were normalized to *GAPDH* mRNA, demonstrating the presence of transplanted GFP expressing cells in the mBMC-epileptic brain (n = 4 per group). **, $p < 0.01$ compared to control and saline-epileptic groups, analysis of data by two-way ANOVA and Bonferroni posttest.

The reduction of SRS in BMC-epileptic rats may be related to the low levels of inflammatory cytokines detected in the brain and in the serum of animals treated with mBMC. Cytokines mediate cell communication and are released for autocrine and paracrine signaling (Vilcek, 1998). Excessive or sustained production of pro-inflammatory cytokines can contribute to neuronal hyperactivity and neurodegeneration in acute and chronic epilepsy (reviewed by Vezzani et al., 2011).

Several reports have reported increased production and secretion of pro-inflammatory cytokines (e.g., TNF-α, IL-1β, and IL-6) in the hippocampus after tonic-clonic seizures, which affect seizure severity and recurrence (see review by Li et al., 2011). For example, high levels of the pro-inflammatory cytokine TNF-α can cause severe damage via its action on p55 receptors by regulating the cellular trafficking of amino-3-hydroxy-5-methylisoxazole-4-propionic acid (AMPA) receptors and amplifying the glutamate responses from astrocytes (Bezzi et al., 2001). IL-1β induces the synthesis of IL-6 and TNF-α in astrocytes and microglia (Schobitz et al., 1994), and mice overexpressing IL-6 and TNF-α in glia develop both seizures and neurodegeneration (Akassoglou et al., 1997; Campbell et al.,

1993). This cytokine can increase neuronal excitability by markedly inhibiting astrocytic glutamate uptake (Ye and Sontheimer, 1996), lowering gamma-aminobutyric acid (GABA) levels in the hippocampus, enhancing NMDA receptor function and Ca^{2+} influx, and inhibiting K^+ efflux (see by Rijkers et al., 2009).

Here, we have concentrated our analysis on classical pro- (TNF-α, IL-1β, and IL-6) and anti-inflammatory cytokines (IL-10). We observed a marked reduction in the expression of the pro-inflammatory cytokines in the epileptic brains of rats treated with mBMC compared to saline-treated epileptic rats. We also demonstrated that BMC increased the expression of IL-10 transcripts in the brain and protein in the serum. BMC or bone marrow-derived mesenchymal stem cells have been shown to have immunomodulatory effects through their effect on IL-10 expression in a rat model of cerebral infarction (Brenneman et al., 2010; Liu et al., 2009) and by providing a favorable microenvironment for neurogenesis after ischemic stroke (Morita et al., 2007). In addition to cytokine modulation, the combination of other mechanisms, such as increased neuroprotection and neurogenesis promoted by neurotrophic and growth factors, could be responsible for the observed effects. In this regard, it has been shown that in the hippocampus of epileptic rats, glial-cell-derived neurotrophic factor (GDNF) attenuates epileptogenesis (Kanter-Schlifke et al., 2007), while brain-derived neurotrophic factor (BDNF) increases neurogenesis, reduces neuronal loss, and decreases the occurrence of spontaneous seizures (Bovolenta et al., 2010). Increased expression of BDNF and neural growth factor (NGF) was reported in a stroke model after mesenchymal stem cell transplantation (reviewed by Dharmasaroja, 2008). It is possible that BMC treatment modulated neurotrophin expression, a possibility we intend to explore in future studies.

Our BMC treatment consisted of different cell types present in the mononuclear cell fraction, including monocytes and mesenchymal and endothelial precursors, which may have different and additive therapeutic potentials. Recently, we demonstrated that despite a significant functional recovery of rats transplanted with BMC immediately after SE (Costa-Ferro et al., 2010), or 22 days after SE (Venturin et al., 2011), only a few transplanted cells were found in the brain. This result was corroborated in the current study; only a small number of donor cells were found in the epileptic brain, confirming the low rate of migration of BMC to the brain.

In conclusion, this study shows that BMC transplantation in epileptic rats has potent therapeutic actions. Most importantly, the frequency and duration of seizures were reduced regardless of whether the transplant was performed in the initial phase or after a protracted period of SRS. BMC preserved neurons, reduced astrocyte activation, and induced the proliferation of new neurons in the DG. Activation and proliferation of progenitor cells was also found in other hippocampal subregions, including CA1 and CA3, possibly due to a modulation of the inflammatory response following treatment with BMC. Our results indicate that BMC, which are easily obtainable for autologous application, may be a safe and effective therapy for treating chronic epilepsy.
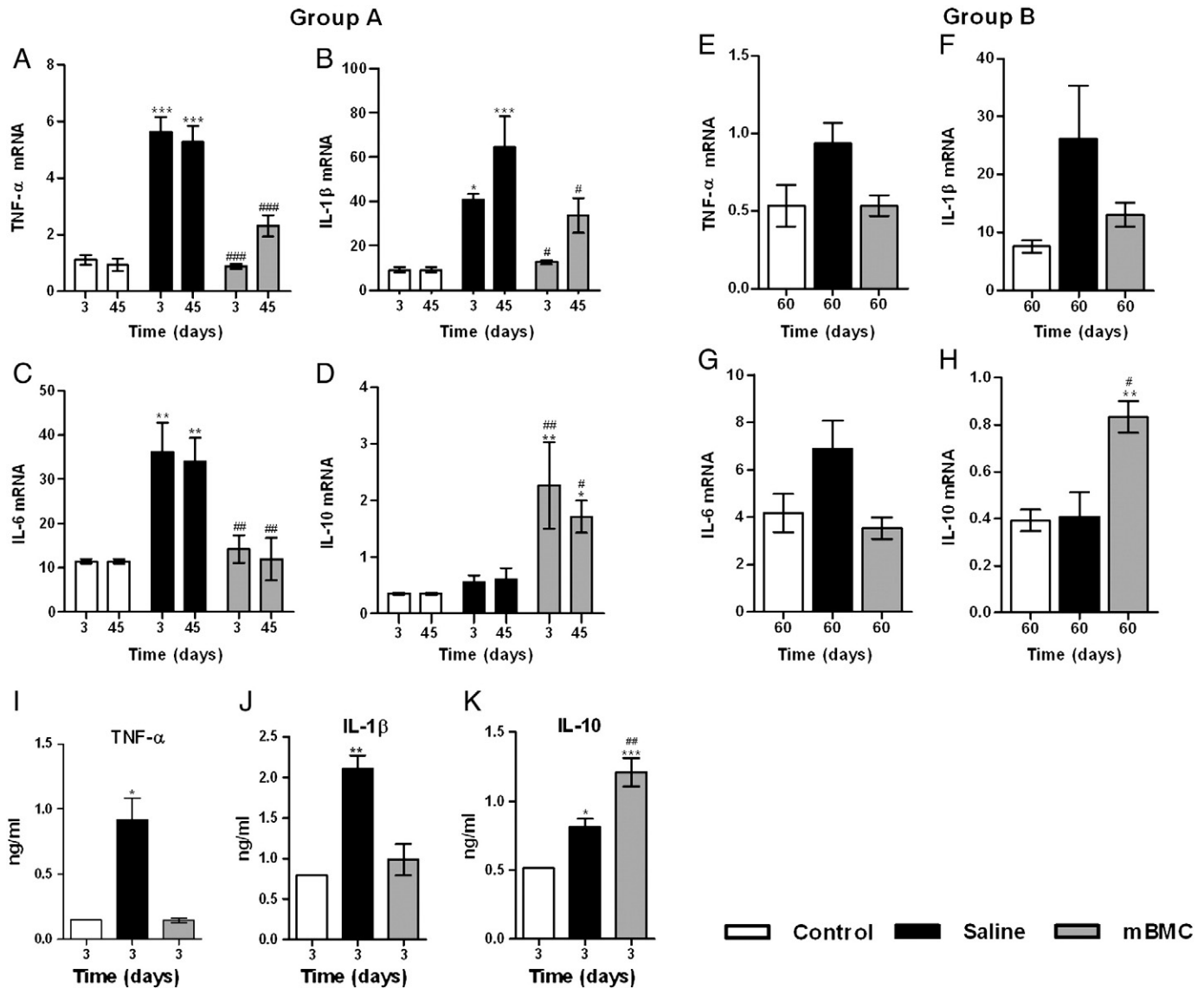
Disclosure

Acknowledgments

Fig. 9. Induction of epilepsy and BMC treatment affects the production of inflammatory cytokines. (A–H) Total RNA from the brains of control, saline-epileptic and mBMC animals was extracted, and levels of TNF-α, IL-1β, IL-6 and IL-10 mRNA were measured quantitatively by qRT-PCR (Taqman hydrolysis probes). (A–D) Group A, 3 and 45 days after transplantation. (E–H) Group B, 60 days after transplantation (n = 5 per group). The results are presented as the fold-increase of expression of the individual mRNAs normalized to GAPDH. *$p < 0.05$ for the control vs. the epileptic groups and #, $p < 0.05$ compared to saline vs. BMC-epileptic groups in the two-way ANOVA followed by Bonferroni posttest. (I–K) Serum cytokine concentrations in Group A 3 days after transplantation. Data are expressed as the mean ± SEM, n = 5 per group.*$p < 0.05$ compared to control and saline-epileptic groups and #, $p < 0.05$ compared to epileptic and BMC-epileptic groups in the one-way ANOVA and followed by Newman–Keuls multiple comparison test.

References

Abercrombie, M., 1946. The density of neurones in the human hippocampus. Anat. Rec. 94, 239–247.

Akassoglou, K., Probert, L., Kontogeorgos, G., Kollias, G., 1997. Astrocyte-specific but not neuron-specific transmembrane TNF triggers inflammation and degeneration in the central nervous system of transgenic mice. J. Immunol. 58, 438–445.

Aronica, E., van Vliet, E.A., Mayboroda, O.A., Troost, D., da Silva, F.H., Goiter, J.A., 2000. Upregulation of metabotropic glutamate receptor subtype mGluR3 and mGluR5 in reactive astrocytes in a rat model of mesial temporal lobe epilepsy. EJN 12, 2333–2344.

Baker, A.H., Sica, V., Work, L.M., Williams-Ignarro, S., de Nigris, F., Lerman, L.O., Casamassimi, A., Lanza, A., Schiano, C., Rienzo, M., Ignarro, L.J., Napoli, C., 2007. Brain protection using autologous bone marrow cell, metalloproteinase inhibitors, and metabolic treatment in cerebral ischemia. Proc. Natl. Acad. Sci. U. S. A. 104, 3597–3602.

Bao, X., Wei, J., Feng, M., Lu, S., Li, G., Dou, W., Ma, W., Ma, S., Na, Y., Qin, C., Zhao, R.C., Wang, R., 2011. Transplantation of human bone marrow-derived mesenchymal stem cells promotes behavioral recovery and endogenous neurogenesis after cerebral ischemia in rats. Brain Res. 7, 103–113.

Bezzi, P., Domercq, M., Brambilla, L., Galli, R., Schols, D., De Clercq, E., Vescovi, A., Bagetta, G., Kollias, G., Meldolesi, J., Volterra, A., 2001. CXCR4-activated astrocyte glutamate release via TNFalpha: Amplification by microglia triggers neurotoxicity. Nat. Neurosci. 4, 702–710.

Bovolenta, R., Zucchini, S., Paradiso, B., Rodi, D., Merigo, F., Navarro Mora, G., Osculati, F., Berto, E., Marconi, P., Marzola, A., Fabene, P.F., Simonato, M., 2010. Hippocampal FGF-2 and BDNF overexpression attenuates epileptogenesis-associated neuroinflammation and reduces spontaneous recurrent seizures. J. Neuroinflammation 18, 7:81.

Brazelton, T.R., Rossi, F.M.V., Keshet, G.I., Blau, H.M., 2000. From marrow to brain: expression of neuronal phenotypes in adult mice. Science 290, 1775–1779.

Brenneman, M., Sharma, S., Harting, M., Strong, R., Cox Jr., C.S., Aronowski, J., Grotta, J.C., Savitz, S.I., 2010. Autologous bone marrow mononuclear cells enhance recovery after acute ischemic stroke in young and middle-aged rats. J. Cereb. Blood Flow Metab. 30, 140–149.

Campbell, I.L., Abraham, C.R., Masliah, E., Kemper, P., Inglis, J.D., Oldstone, M.B., Mucke, L., 1993. Neurologic disease induced in transgenic mice by cerebral overexpression of interleukin 6. Proc. Natl. Acad. Sci. U. S. A. 90, 10061–10065.

Cavalheiro, E.A., Naffah-Mazacoratti, M.G., Mello, L.E., Leite, J.P., 2006. The pilocarpine modelo of seizures. In: Pitkanen, A., Schwartzkroin, P.A., Moshé, S.L. (Eds.), Models of Seizures and Epilepsy. Elsevier, Amsterdam, pp. 433–448.

Chopp, M., Li, Y., 2002. Treatment of neural injury with marrow stromal cells. Lancet Neurol. 1, 92–100.

Clifford, D.B., Olney, J.W., Maniotis, A., Collins, R.C., Zorumski, C.F., 1987. The functional anatomy and pathology of lithium-pilocarpine and high-dose pilocarpine seizures. Neuroscience 23, 953–968.

Costa-Ferro, Z.S., Vitola, A.S., Pedroso, M.F., Cunha, F.B., Xavier, L.L., Machado, D.C., Soares, M.B., Ribeiro-dos-Santos, R., DaCosta, J.C., 2010. Prevention of seizures

and reorganization of hippocampal functions by transplantation of bone marrow cells in the acute phase of experimental epilepsy. Seizure 19, 84–92.

Crain, B.J., Tran, S.D., Mezey, E., 2005. Transplanted human bone marrow cells generate new brain cells. J. Neurol. Sci. 233, 121–123.

de Vasconcelos dos Santos, A., da Costa Reis, J., Diaz, 2010. Therapeutic window for treatment of cortical ischemia with bone marrow-derived cells in rats. Brain Res. 1306, 149–158.

Dharmasaroja, P., 2008. Bone marrow-derived mesenchymal stem cells for the treatment of ischemic stroke. J. Clin. Neurosci. 1, 12–20.

Eglitis, M.A., Mezey, E., 1997. Hematopoietic cells differentiate into both microglia and macroglia in the brains of adult mice. Proc. Natl. Acad. Sci. 94, 4080–4085.

Eid, T., Williamson, A., Lee, T.S., Petroff, O.A., de Lanerolle, N.C., 2008. Glutamate and astrocytes–key players in human mesial temporal lobe epilepsy? Epilepsia 49, 42–52.

Engel Jr., J., 1996. Introduction to temporal lobe epilepsy. Epilepsy Res. 26, 141–150.

Engel Jr., J., 2001a. Mesial temporal lobe epilepsy: what have we learned? Neuroscientist 7, 340–352.

Engel Jr., J., 2001b. A proposed diagnostic scheme for people with epileptic seizures and with epilepsy: report of the ILAE Task Force on Classification and Terminology. Epilepsia 42, 796–803.

Franklin, K.B.J., Paxinos, G., 1997. The Mouse Brain in Stereotaxic Coordinates. Academic, San Diego.

Giraldi-Guimarães, A., Rezende-Lima, M., Bruno, F.P., Mendez-Otero, R., 2009. Treatment with bone marrow mononuclear cells induces functional recovery and decreases neurodegeneration after sensorimotor cortical ischemia in rats. Brain Res. 1266, 108–120.

Hess, D.C., Hill, W.D., Martin-Studdard, A., Carroll, J., Brailer, J., Carothers, J., 2002. Bone marrow as a source of endothelial cells and NeuN-expressing cells After stroke. Stroke 33, 1362–1368.

Hu, D.Z., Zhou, L.F., Zhu, J.H., 2004. Marrow stromal cells administrated intracisternally to rats after traumatic brain injury migrate into the brain and improve neurological function. Chin. Med. J. 117, 1576–1578.

Iihoshi, S., Honmou, O., Houkin, K., Hashi, K., Kocsis, J.D., 2004. A therapeutic window for intravenous administration of autologous bone marrow after cerebral ischemia in adult rats. Brain Res. 1007, 1–9.

Janeczko, K., 1994. The proliferative activity of astrocytes after immunoglobulin uptake in the injured mouse cerebral hemisphere. Folia Histochem. Cytobiol. 32, 239–241.

Kamiya, N., Ueda, M., Igarashi, H., Nishiyama, Y., Suda, S., Inaba, T., Katayama, Y., 2008. Intra-arterial transplantation of bone marrow mononuclear cells immediately after reperfusion decreases brain injury after focal ischemia in rats. Life Sci. 83, 433–437.

Kanter-Schlifke, I., Georgievska, B., Kirik, D., Kokaia, M., 2007. Seizure suppression by GDNF gene therapy in animal models of epilepsy. Mol. Ther. 15, 1106–1113.

Kawada, H., Takizawa, S., Takanashi, T., Morita, Y., Fujita, J., Fukuda, K., Takagi, S., Okano, H., Ando, K., Hotta, T., 2006. Administration of hematopoietic cytokines in the subacute phase after cerebral infarction is effective for functional recovery facilitating proliferation of intrinsic neural stem/progenitor cells and transition of bone marrow-derived neuronal cells. Circulation 113, 701–710.

Li, G., Bauer, S., Nowak, M., Norwood, B., Tackenberg, B., Rosenow, F., Knake, S., Oertel, W.H., Hamer, H.M., 2011. Cytokines and epilepsy. Seizure 20, 249–256.

Liu, N., Chen, R., Du, H., Wang, J., Zhang, Y., Wen, J., 2009. Expression of IL-10 and TNF-alpha in rats with cerebral infarction after transplantation with mesenchymal stem cells. Cell. Mol. Immunol. 6, 207–213.

Mathern, G.W., Babb, T.L., Leite, J.P., Pretorius, K., Yeoman, K.M., Kuhlman, P.A., 1996. The pathogenic and progressive features of chronic human hippocampal epilepsy. Epilepsy Res. 26, 151–161.

Mello, L.E., Cavalheiro, E.A., Tan, A.M., Kupfer, W.R., Pretorius, J.K., Babb, T.L., Finch, D.M., 1993. Circuit mechanisms of seizures in the pilocarpine model of chronic epilepsy: cell loss and mossy fiber sprouting. Epilepsia 34, 985–995.

Ming, G.L., Song, H., 2005. Adult neurogenesis in the mammalian central nervous system. Annu. Rev. Neurosci. 28, 223–250.

Morita, Y.S., Takizawa, H., Kamiguchi, T., Uesugi, H., Kawada, Takagi, S., 2007. Administration of hematopoietic cytokines increases the expression of anti-inflammatory cytokine (IL-10) mRNA in the subacute phase after stroke. Neurosci. Res. 58, 356–360.

Parent, J.M., Yu, T.W., Leibowitz, R.T., Geschwind, D.H., Sloviter, R.S., Lowenstein, D.H., 1997. Dentate granule cell neurogenesis is increased by seizures and contributes to aberrant network reorganization in the adult rat hippocampus. J. Neurosci. 17, 3727–3738.

Racine, R.J., 1972. Modification of seizure activity by electrical stimulation. I: afterdischarge threshold. Electroencephalogr. Clin. Neurophysiol. 32, 269–279.

Rijkers, K., Majoie, H.J., Hoogland, G., Kenis, G., De Baets, M., Vles, J.S., 2009. The role of interleukin-1 in seizures and epilepsy: a critical review. Exp. Neurol. 216 (2), 258–271.

Schobitz, B., De Kloet, E.R., Holsboer, F., 1994. Gene expression and function of interleukin 1, interleukin 6 and tumor necrosis factor in the brain. Prog. Neurobiol. 44, 397–432.

Takahashi, M., Li, T.S., Suzuki, R., Kobayashi, T., Ito, H., Ikeda, Y., Matsuzaki, M., Hamano, K., 2006. Cytokines produced by bone marrow cells can contribute to functional improvement of the infarcted heart by protecting cardiomyocytes from ischemic injury. Am. J. Physiol. Heart Circ. Physiol. 291, 886–893.

Turski, L., Cavalheiro, E.A., Czuczwar, S.J., Turski, W.A., Kleinrok, Z., 1987. The seizures induced by pilocarpine: behavioral, electroencephalographic and neuropathological studies in rodents. Pol. J. Pharmacol. Pharm. 39, 545–555.

Venturin, G.T., Greggio, S., Marinowic, D.R., Zanirati, G., Cammarota, M., Machado, D.C., DaCosta, J.C., 2011. Bone marrow mononuclear cells reduce seizure frequency and improve cognitive outcome in chronic epileptic rats. Life Sci. 15, 229–234.

Vezzani, A., Granata, T., 2005. Brain inflammation in epilepsy: experimental and clinical evidence. Epilepsia 46, 1724–1743.

Vezzani, A., Bolosso, S., Ravizza, T., 2008. The role of cytokines in the pathophysiology of epilepsy. Brain Behav. Immun. 22, 797–803.

Vezzani, A., French, J., Bartfai, T., Baram, T.Z., 2011. The role of inflammation in epilepsy. Nat. Rev. Neurol. 7, 31–40.

Vilcek, J., 1998. The cytokines: an overview. In: Thomson, A. (Ed.), The Cytokine Handbook. Academic Press, San Diego, pp. 1–20.

Walker, P.A., Harting, M.T., Shah, S.K., Day, M.C., El Khoury, R., Savitz, S.I., Baumgartner, J., Cox, C.S., 2010. Progenitor cell therapy for the treatment of central nervous system injury: a review of the state of current clinical trials. Stem Cells 20, 369578.

Wieser, H.G., 2004. Mesial temporal epilepsy with hippocampal sclerosis. ILAE Commission report. Epilepsia 45, 695–714.

Ye, C., Sontheimer, H., 1996. Cytokine modulation of glial glutamate uptake: a possible involvement of nitric oxide. Neuroreport 7, 2181–2185.

Zacharek, A., Shehadah, A., Chen, J., Cui, X., Roberts, C., Lu, M., Chopp, M., 2010. Comparison of bone marrow stromal cells derived from stroke and normal rats for stroke treatment. Stroke 41, 524–530.